1-1-2010

Theoretical analysis of acoustic emission signal propagation in fluid-filled pipes

M.N. Mahabubul Alam Chowdhury
Ryerson University

THEORETICAL ANALYSIS OF ACOUSTIC EMISSION SIGNAL PROPAGATION IN FLUID-FILLED PIPES

by

M N Mahabubul Alam Chowdhury
BSc in Electrical & Electronic Engg., Dhaka University of Engineering and Technology (DUET), Gazipur, Bangladesh, 1992
MSc in Electrical & Electronic Engg., Bangladesh University of Engineering and Technology (BUET), Dhaka, Bangladesh, 1997

A thesis
presented to Ryerson University
in partial fulfillment of the
requirement for the degree of
Master of Applied Science

in

Electrical and Computer Engineering.

Toronto, Ontario, Canada, 2009

Author's Declaration

I hereby declare that I am the sole author of this thesis.

I authorize Ryerson University to lend this thesis to other institutions or individuals for the purpose of scholarly research.

Signature

I further authorize Ryerson University to reproduce this thesis by photocopying or by other means, in total or in part, at the request of other institutions or individuals for the purpose of scholarly research.

Signature

Theoretical Analysis of Acoustic Emission Signal Propagation in Fluid-filled Pipes, a thesis by M N Mahabubul Alam Chowdhury, presented to Electrical and Computer Engineering, Ryerson University, in partial fulfillment of the requirement for the degree of Master of Applied Science, 2009.

Abstract

The theoretical investigation of acoustical wave propagation in cylindrical layered media is the main interest of our research. The propagation of wire break or slip related acoustical signal in the buried water-filled Prestressed Concrete Cylinder Pipe (PCCP) is taken as a specific application.

The PCCPs are widely used for potable- and waste-water distribution and transmission systems, which are generally located below the surface ground. Therefore, it is difficult to inspect or detect the damage caused by the wire-break or slip related events in the pipeline. In current practice, the acoustic emission (AE) monitoring system is used for random examination of prestressing wires by excavating or internal inspecting of the pipe walls, which is based on field data analysis. This gives only the localized knowledge of wire break or slip, which can be misleading, underestimated of the extent of corroded areas, deterioration or wire failure, due to the system resonance, acoustoelastic effect, loading effect, etc. There is no systematic theoretical analysis from the acoustic signal generation to propagation related to these effects, and hence, a common problem in AE technology is to extract the physical features of the ideal events, so as to detect the similar signals.

The theoretical analysis is important to understand how the AE signal is generated by the leak, wire break or slip related events and how the path characteristics, excitation frequency, and modes of propagation physically affect the signal propagation. For this purpose, an acoustical model is developed from the Navier's equation of motion. This can simulate vibrating AE signal propagation through the fluid-filled PCCP. The interaction of this propagation with the pipe structure is modeled by using Newton's law of motion in equilibrium. The principle of virtual work is used to develop the fluid-structure interaction.

In this work, the impact of the path on the spectral profiles of the vibrating AE signals in different locations throughout the pipes were investigated for low and high frequency excitation signals. At low frequency, there is only plane wave propagation, therefore the stoneley or tube mode analysis is used for this purpose. The tube wave effects on the acoustical wave propagation were observed from this analysis. At high frequencies, there also exist rayleigh or shear modes which exhibit oscillatory amplitudes in the fluid and a decaying amplitude in the pipe and the surrounding medium. The eigenfrequency and the modal analysis is used in this case. From the analyses, the phase velocity, group velocity, tube wave velocity, system resonance frequencies, cut-off frequencies were observed.

The high frequency analysis has some special advantages over low frequency signal. This can provide an earlier indication of incipient faults, which is important to detect the AE event in early stage of pipe deterioration. Moreover, it was established that the frequency of propagating AE signal in the pressurizing fluid medium ranges up to 30 kHz. Therefore, it is important to investigate the wave propagation of AE signal at these frequencies. This work examines the spectral characteristics of AE signal propagation through the fluid column inside the pipe within the range of sonic/ultrasonic frequency.

The acoustic wave propagation in fluid-filled PCCP of various radius, stiffness and thickness of the pipe as well as different types of surrounding medium, is obtained by applying a numerical Finite Element Method (FEM). Finally, the results are compared with available analytical solutions.

The proposed model is independent of sources, dimensions and medium characteristics. Therefore, it can be used for the analysis of acoustic wave propagation through any type of cylindrical shells immersed or surrounded by different types of medium. The current analysis, therefore, has fundamental importance in many applications.

Acknowledgments

The completion of this thesis involves contributions and assistance from many individuals.

First of all, I would like to express my invaluable profound gratitude to my supervisors, Professor Dr. Lian Zhao from Dept of Electrical and Computer Engineering and Professor Dr. Zaiyi Liao from Dept of Architectural Science of Ryerson University, for their professional directions, helpful comments, kind support and constant encouragement throughout the research period.

I am greatly grateful to Professor Dr. Ramani Ramakrishnan of Architectural Science Department for his precious instruction. His dynamic thinks, broad and profound knowledge and patient instruction have given me a great help.

This work is partially supported by the Ontario Centres of Excellence (OCE) under Grant no. EE50196, National Sciences and Engineering Research Council (NSERC) of Canada under Grant no. DG 293237-04 and 313375-07, and Ryerson University research grant. I'm also grateful to these institutions for their financial support.

The members of our lab supported me in my research work. I want to thank them for all their help, support, interest and valuable hints. Especially, I am obliged to Ran Wu, Thomas Behan for their assistance and valuable suggestions to complete my work. I am also grateful to Surinder Jassar, Meharoon Shaik, Lavanya Rajagopalan, Samuel Huang, and Ringo for their help during the preparation of my thesis and final presentation.

I am very grateful for the love and support of my family and friends. Especially, I appreciate the patience of my son Sharear and my daughter Shareen during the time I was involved in carrying out this project. The morale support given by my wife Nazma is also greatly regarded.

Above all, words cannot express my sincere thanks to the almighty God for showering countless blessings to me.

Contents

List of Tables

List of Figures

Chapter 1

General Introduction

1.1 Introduction

Liquid carrying structure, said as a pipe, should be impervious against leakage of liquid from the inside to the outside and also against the ingression of external materials inside. Earlier, steel or cast iron pipes were used for this purpose. In the first half of the 20th century, concrete was introduced as a structural material for large diameter pipes. In 1942, the first prestressed concrete Lined Cylinder Pipe (LCP) was introduced, where a concrete lined steel cylinder was wrapped with a helix of highly stressed steel wire and coated with a dense cement mortar to protect the wire. They are found suitable up to 1,520 mm dia [1]. Later in 1950, a second type of prestressed concrete Embedded Cylinder Pipe (ECP) was developed, where the steel cylinder is embedded in the concrete core after that stressed steel wire helix is wounded, so that the wire is in contact with concrete rather than with the steel cylinder. These are found suitable for the pipe diameter up to 9,000 mm [1]. Both types of Prestressed Concrete Cylinder Pipes (PCCP) are used for potable water supply and sewage systems. These pipes are ideally suited for pressure range of 0.4 to 2 MPa, where the cast iron or mild steel pipes are not economical and the Reinforced Concrete Cylinder Pipes (RCCP) are not suitable [2].

The PCCP has been widely used for the large-scale transmission of potable or waste water for more than half a century. These pipelines have generally been very reliable. However, there have been occasional failures caused by corrosion, consequently, breakage of the high-

strength prestressed wires that reinforce these pipes. This breakage causes sudden release of elastic energy stored in the prestressed wire in the form of acoustic waves. If enough wires fail, the structural capacity of the PCCP will be compromised and the pipe is in danger of catastrophic rupture. And hence, condition assessment has become essential to ensure the continued safe operations.

Non-destructive testing (NDT) has been a useful tool for continuous condition monitoring of concrete pipe systems. The testing involves capturing the wire break or slip related signals by the sensors, which are then analyzed to indicate the level of active distress in the observed pipeline. This condition assessment has become a necessary risk management strategy for municipalities or companies that own the infrastructure.

Acoustic Emission Testing (AET) is one of the main technologies used in related industry for non-destructive pipe detection. This technology is mainly based on random examination of prestressing wires by excavating or internal inspecting of the pipe walls. It establishes the level of active distress in individual PCCP by measuring the frequency and number of wire related events that occur over a specified range in a defined period of time. Wire-break or slip related events (WRE) are defined as breakage or slippage in the prestressing wires, which are currently captured using hydrophones or accelerometers. After the data from these units is retrieved and analyzed, a client is presented with a report that indicates the level of active distress in the observed pipeline.

Current practise of acoustic emission (AE) detection and recognition using AET is widely used in many physical and engineering fields such as leak detection and pipeline inspection. The conventional method is based on field data analysis, which gives only the localized knowledge of wire break or slip. This can be misleading and underestimated of the extent of the corroded areas, deterioration or wire failure [3]. This fact is due to the system noise, acoustoelastic effect and loading effect. The evaluation criteria of AE signal does not exist in form of actual data related to that test. For example, the threshold of AE signal is set firmly to the knowledge and experience of the service provider. The speed of acoustical wave in the propagating medium is considered as a constant value to locate the AE source position [4].

Moreover, due to the background noise, both continuous and impulsive, actual AE signal can not be detected properly [5]. High level of continuous noise such as fluid flow, system noise may obscure some weak AE signals. Some impulsive noise may also produce acoustic signals similar to the genuine AE signals [6]. Therefore, theoretical analysis and knowledge is important for the evaluation of AE signal.

The theoretical investigation of the acoustical wave propagation of AE signal in fluid-filled PCCP is the main interest of this research. The impact of the path on the spectral profiles of the vibrating acoustic signals in different locations throughout the pipe were investigated for low and high frequency excitation signals. At these frequencies, the tube mode and rayleigh mode are the main propagating modes in the fluid medium inside the pipe. The tube wave, eigenfrequency and modal analysis were performed for this purpose. The phase velocity, group velocity, tube wave velocity, system resonance frequency, cut-off frequency were determined from these analyses.

The theoretical analysis of the high frequency AE signal propagation through the fluid-column inside the pipe were observed under different pipe and surrounding medium conditions. The high frequency analysis has superior sensitivity over the low frequency vibration signal. This can provide earlier indication of the incipient faults, such as frictional rubbing of WRE in the pipeline inspection. The time response of the spectral characteristics of high frequency AE signal at different locations throughout the pipe were determined.

The acoustic wave propagation in fluid-filled pipe of various radius, stiffness and thickness of the pipe as well as different types of surrounding medium were performed by applying a commercial numerical Finite Element (FE) analysis, and the results are compared with available analytical solutions.

1.2 Review of Earlier Studies

The PCCP that are used for the potable or waste water distribution or transmission are difficult to inspect for damage due to their location below the earth surface. Most of the damage occurs in the pipe wall due to the corrosion that causes breakage of prestressed wire.

The difficulty has led the water utilities to rely on continuous condition assessment to ensure the continued safe operations.

Many methods were developed to detect the energy released from the wire failure and to locate the corroded areas. These methods can be classified as, top-down approach and bottom-up approach. The flow diagram of these approaches are shown in Fig. (1.1).

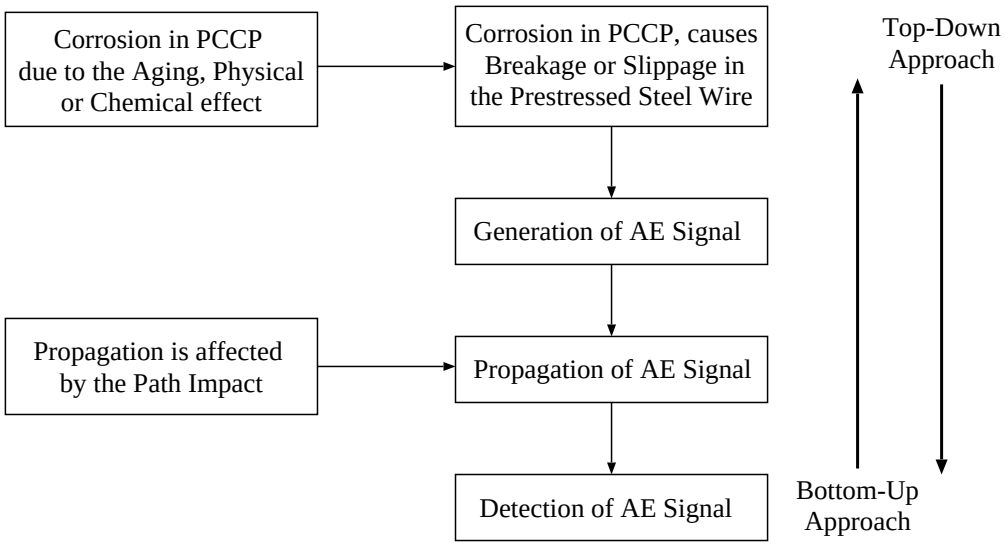

Figure 1.1: Flow diagaram of AE signal generation to propagation and detection.

The bottom-up approach is generally used in the related industry for the AE monitoring of pipeline system. The methods or techniques that are developed on this approach is mainly based on field or test data analysis. As shown in Fig. (1.1), these methods first measure or detect the AE signal from the system and then locate the corroded areas. These methods include half cell potential measurement, visual inspection and tapping, acoustic emission monitoring, soil resistivity measurements, infrared thermography, remote field inspection, impact echo/spectral analysis of surface waves, ground penetrating radar, etc. [7]- [18]. These methods are usually ineffective [19] in case of long length (range) of pipe inspection from a single probe position and where the pipes are under insulation, soil, or tar, embedded in concrete or hidden from sight. Theoretical knowledge on the guided wave propagation and the impact of surrounding medium on the propagating wave is important to overcome this

problem.

On the other hand, the top-down approach is based on the theoretical analysis, which can be used to understand and to interpret the testing data. As shown in Fig. (1.1), the method related to this approach deals with the acoustic wave generation to propagation under different conditions, which is important to analyze and to detect the AE events properly. An enormous earlier studies [20]- [33] on theoretical analysis of acoustical waves focused on the guided wave (e.g. harmonic wave, axisymmetric and non-axisymmetric waves, multimode wave, lamb and love wave, ultrasonic wave, leaky wave, etc.) propagation through empty or fluid-filled elastic, non-elastic, coated, non-coated, cylindrical pipe. These work mainly dealt with the idealize situations and gives generalized solutions of the problem. Some of these work dealt with the specific applications, such as, borehole, impedance tube, HVAC system, thermodynamic and chemical engineering process. As far as our knowledge, there is no systematic theoretical analysis in the open literature form the AE signal generation to propagation through the fluid-filled PCCP.

Therefore, the current study goes beyond the earlier studies by considering the fluid-filled pipes as a medium for the transmission of AE signals and by emphasizing the low to high frequency as the excitation signal frequency. The acoustic signal, generated by the leak, wire break or slip in pipeline usually creates high and low frequency signals. It was established that at low frequency (wavelength is much larger than pipe radius), there is only stoneley or tube modes propagating with plane wavefronts [34]- [40]. While at high frequencies (wavelength is equal or lesser than the pipe radius), there also exists rayleigh or shear normal modes which exhibits oscillatory amplitudes in the fluid and decaying amplitude in the pipe and the surrounding media [41]- [46]. The rate of information transmission grows in proportion to the frequency of the excitation. Consequently, there is a need to investigate number of modes generated in each excitation frequency. It is known that, higher the excitation frequency, the more modes propagate and stronger the dispersion characteristics become. For the high frequency excitation signal, therefore, it is very difficult to retrieving the actual AE signal. However, the detailed theoretical analysis is performed in this work, to get the information

about the AE signal generation to propagate in fluid-filled pipe, under different situation.

1.3 Non-destructive Testing

The NDT is a noninvasive techniques aiming to determine the integrity, component or structure of a material or quantitatively measure some characteristic of an object. In contrast to destructive testing, NDT does no harm of the test object [47]. NDT plays an important role, which is necessary to assure safety and reliability. This testing method also acts as a quality assurance management tool for the materials, products, and equipment, which fail to achieve their design requirements or projected life due to undetected defects, and which may require expensive repair or replacement. Such defects may also be the cause of unsafe conditions or catastrophic failure. Therefore, NDT can be used to examine, or to monitor the integrity of a structure throughout its service life.

The method that can be used for NDT depends on the physical properties of the materials. Among all the NDT methods such as magnetic testing, penetrant testing, ultrasonic testing and radiographic testing, AE testing plays a distinctive role which is usually applied during loading of a structure, while most others are applied before or after loading. The NDT technique that involves the AE monitoring of reinforced concrete structure, is a passive way of damage monitoring.

1.4 Acoustic Emission Monitoring

It is well known that AE monitoring is a non-destructive means of evaluation which listens to sound waves generated by the stresses within a material. The scientific application of AE monitoring first emerged in the 1950s, but appeared to fall out of fashion from the late 1970s and onward. With the increased focus on cost-effective ways of optimizing machine, equipment and device reliability and availability, AE is now experiencing an important renaissance as a valuable Condition Based Monitoring (CBM) and predictive maintenance tool. This technology is also widely used in different industries to a NDT and technical diagnostic

of industrial objects, such as, pipelines, pressure vessels, pneumotest, etc. including in an operation mode.

The AE monitoring is one of the popular and widely used NDT methods for detection and recognition of AE signal in many physical and engineering fields. Several researchers have used the AE techniques for monitoring cracks in concrete [48]- [66] and for monitoring of debonding and corrosion of prestressed wire in concrete [67]- [69].

AE monitoring can be deployed in a wide range of usable applications of NDT such as [70]:

- metal pressure vessels for cracks and corrosion;
- piping systems for splits and leakage;
- flat bottomed storage tanks for leakage and corrosion;
- civil engineering structures for process monitoring and global or local long-term monitoring.

The types of AE analysis that is normally used in NDT are [71]:

- analysis of signal amplitude as a function of stress and time;
- analysis of the number of signals which exceed a reference threshold;
- computation of the energy of the detected signals;
- analysis of the frequency content of the signals;
- localization of the signal source;
- correlation analysis, where each detected signal is compared with previously recorded signals.

It should be noted that the test conditions for all the applications must be similar to normal service conditions. Otherwise, AE will not obtain veritable and reliable results.

1.5 Acoustic Emission Testing

Among the other NDT methods, the AET technique is popular in the related industry due to its important advantages. One major advantage of AET is that it can be performed at the interference in-service without any disturbance [70]. In addition, the localization ability gives another major advantage of AET. Therefore, a suspected area can be reported to the client. This early warning advantage opens the way for performing following tests economically to verify the defect. This technique also provides a real-time monitoring method to the specimen [6].

In the pipeline, when a present defect expands, tension energy is released, and an acoustic signal is generated [72]. AE techniques are used to observe and monitor these invisible events. Although some of the events occur before monitoring, or are too weak to be detected during inspection, various events occur due to temperature, pressure, physical defect development and environmental conditions so that they become detectable.

AET is a dynamic technique that works when solid materials lose their elasticity and just begin to split, while other NDT methods are static. For example the ultrasound method, which is a typical NDT technique, is able to detect the geometric shape of a defect in a specimen using an artificially generated source signal and a receiver, whereas the AET detects the elastic waves radiated by a growing fracture [73].

When other NDT techniques probe the structure, AET listens for emissions from active defects and splits. It is the class of phenomena whereby an elastic wave is generated by the rapid release of energy from the source in a material. The elastic wave, normally between 10 kHz and 1 MHz, propagates through the solid material to the surface where it can be detected by one or more sensors [74]. This signal is then processed and localized to extract the source of the AE events. Consequently, AET is a very sensitive NDT technique to observe damage processes during the entire observation without any disturbance to the specimen.

1.6 Acoustic Emission Signal

All solid materials, both rigid and elastic, have certain elasticity. They become strained under external forces, and spring back when released [75]. Higher force makes heavier deformation, thus the elastic energy is greater. Also corrosion decreases the sustainable limit of the material. When the energy is large enough and the elastic limit is exceeded, a fracture happens immediately if it is a brittle material, or occurs after a certain plastic deformation if it is a long suffering material. The occurred fracture rapidly relaxes the material by a fast dislocation. This kind of rapid release of elastic energy is defined as an AE event. It generates an elastic wave that propagates and can be detected by sensors.

The frequency of released elastic wave has a very wide range depending on the material. For example, the frequency of AE signal of metallic objects is in the range of ultrasound above 100 kHz [6]. The frequency of sound of glasses crack is inside sound wave range. On the other hand, when the tiny crack occurred to metal or some other solid materials, it is not hearable as the emitted burst is ultrasound. This type of pulses and bursts are one of the sources that AE technique is hunting for.

Another type comes from the plastic deformation. During the deformation, dislocations move through the crystal lattice. AE signals are generated from these movements, but most of them only have very small amplitudes. Thus they can be detected reliably only at a short distance and with less noise background. Fortunately, this type of movements produces continuous signals rather than short bursts. The splitting of material contains both these two types. It makes pulses when defects are produced. It also generates continuous waves when the defect is extending. In a word, AET is a receptive technique that analyzes the pluses and waves emitted by a defect right at the moment of its occurrence [75].

The frequency characteristics of an AE signal has certain relationship with the external pressure and defect size of its releasing source. Previous studies show that the amplitude of AE signal is proportional to the released energy [76], and the frequency distribution is related with the size of the defect [77]. For instance, in leak detection of a pipeline, the AE signal detected from larger leak hole contains more low frequency components. An explanation of

this phenomenon is that larger hole creates smaller pressure, which results in lower frequency components. Similarly, smaller hole or defect creates higher pressure that produces higher frequency components. However, such characteristics are still not enough to classify certain AE signals. This is because AE signals are non-stationary signals.

1.6.1 AE Signal Propagation

The AE signal generated by the wire break or slip in PCCP, passes through a number of media, such as the pipe, fluid and the surrounding medium (outer formation), before being picked up by the sensors. Initially, this signal propagates as a spherical wave, later on, when the wave dominates all the cross-sectional area of the pipe, it travels as a wavefront as shown in Fig. (1.2), which can be detected by one or more sensors. This wave propagation can be modeled as the convolution of the AE signal and the impulse response of the pipe. As a result, the acoustic signal received by the sensors can be considered as the superposition of the different delayed version of AE signal due to the multipath propagation. This is due to the reflection, refraction and diffraction of the acoustic signal during its propagation.

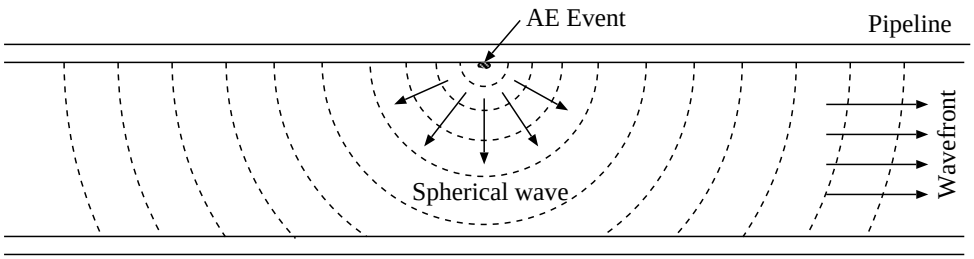

Figure 1.2: Typical AE signal propagation.

The AE events that occur in pipeline usually create two types of signals: one is a mechanical wave which propagates along the steel wire in the pipe at high frequency (above 100 kHz), another is a low frequency wave (about 30 kHz) that propagates through the medium (gas or liquid) inside the pipe [72]. The attenuation of these waves has a square relationship with their frequency, and the coefficient of this relationship is distinguished by the particular medium. Observed values for attenuation (in $\mathrm{dB\,ft^{-1}}$) in several gases and water are 4.9 x

$10^{-11}f^2$ and 7.8 x $10^{-14}f^2$, respectively where f is the frequency of AE signal [78]. Therefore, AE signals propagating through the steel wire attenuate very quickly, because the frequency is high. Generally speaking, the high frequency wave attenuates faster than the low frequency wave. This attenuation also depends on different material and even medium inside and outside the material. Sometimes frequency components are absorbed by distinguished materials. However, those low frequency waves that propagate in the medium can be detected even at sites hundreds of meters away from the original signals. In addition, this kind of wave interacts with the pipe wall so that it can be detected by sensors mounted outside of the pipe.

In linear location case such as pipeline, the wave propagation is more complex due to wave reflection and absorption by the inner wall of the material. In addition, the medium inside and outside the pipe is an essential effect to the propagation of the elastic waves. For example, in the pipeline inspection, generated waves propagate through both the solid wall and the medium inside the pipe. The propagation through the wall has greater attenuation such that it can not be detected at a distance farther than several meters. While the waves propagating through the medium inside the pipe are much more reliable to be recorded hundreds of meters away [72]. In addition, this propagation is varied in different conditions such as the characteristics of medium, the speed of the medium, the temperature, and the landscape.

1.6.2 AE Signal Parameters

The AE signals that have been recorded by the sensors are analyzed in AE techniques. It uses statistical parameters for feature extraction and signal classification. The statistical parameters of a typical AE signal are shown in Fig. (1.3).

The meanings of the parameters are as follows:

- Amplitude is the highest peak voltage attained by an AE waveform.
- Counts are the threshold-crossing pulses that counted.

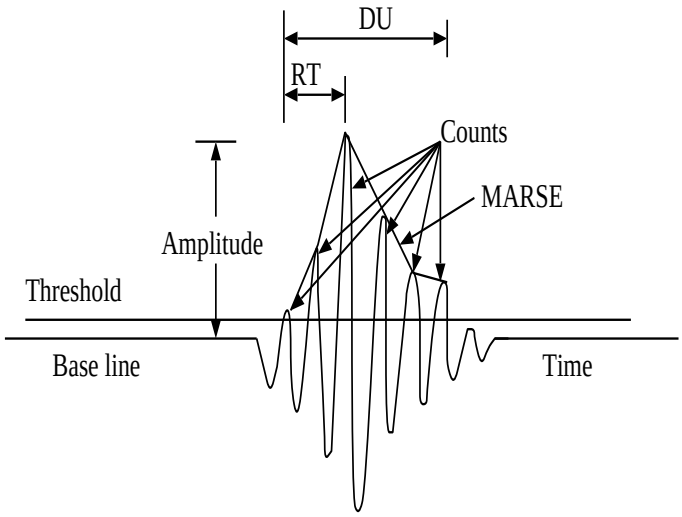

Figure 1.3: Typical parameters of an AE signal.

- MARSE (measured area under the rectified signal envelope) is the measured area under the rectified signal envelope.
- Duration (DU) is the elapsed time from the first threshold crossing to the last.
- Rise time (RT) is the elapsed time from the first threshold crossing to the signal peak.

AE Source Location

Usually there are two methods of the source localization of a signal recorded by the two sensors:

1. from the difference of the amplitude, and
2. from the difference of the arrival time.

The first method is hard to apply because it is affected by many aspects, which makes the attenuation function for different cases hard to define [77].

In the pipeline inspection, usually the second method is used to locate the AE source position in the pipe. It is assumed that acoustic waves travel at a constant velocity in the same material. Once the AE event is recorded by two or more sensors, the difference of

arrival time and sound velocity in the material is used to determine the location of the source. The detailed description of this method is given in Section 2.4.1.

In this method, the arrival time is defined as the start of the duration (DU), as shown in Fig. (1.3). It is the first threshold crossing of AE signal. However, up to the certain distance, the real AE signal is concealed by the background noise. Therefore, the uncertainty of arrival time causes certain error of the localization work. This uncertainty also affects the traveling speed of the acoustic signal, which is not constant due the elastic effect of the surrounding mediums.

1.7 Motivation, Objectives and Scope of the Research

As described in Section 1.2, the bottom-up approach is used in the related industry for the detection and recognition of AE signal and to locate the corroded areas. The current technology is mainly based on field data analysis. This gives only the localized knowledge of the wire break or slip, which can be misleading and underestimated of the extent of corroded areas, deterioration or wire failure [3]. This fact is due to the system noise, acoustoelastic and loading effect. AE signals are generally recognized and identified according to the knowledge and experience of the service provider. To identify the AE signal, they used a fixed set of threshold and consider only the background noise [6]. Moreover, the speed of the acoustical wave is considered as a constant to locate the AE source position [4]. But in the real scenario, during the propagation, the main AE signal is convoluted with the impulse responses of the pipe, which is known as system noise. This impulse response varies depending upon fluid-flow, radius, thickness and stiffness of surrounding layers. As a result, the characteristics of AE signal (e.g. amplitude, velocity, shape, etc.) changes due to the path impact. These make detected AE signals less accurate. Moreover, at the high frequency the impulse response of the pipe becomes more complicated due to the multi-mode and mode conversion. Therefore, it is difficult to de-reverberate and decipher the original AE signal at the receiving end (sensor) without any theoretical knowledge. To approach this problem, we are motivated to introduce a top-down approach for the AE signal generation to propagation.

In this approach, the theoretical analysis of AE signal in buried water-filled PCCP is taken as a specific application.

To fulfill our target, the following objectives are envisaged.

Understanding the Characteristics of Vibration from AE Signal

The physical mechanism of AE signal generation from wire deterioration within PCCP is investigated. A mathematical model is developed for the AE signal in the form of acoustic pressure generated from the wire deterioration within the PCCP and use it throughout the work to simulate the wire deterioration for further research activities.

Understanding the Impact of Path on the Vibration Signal from the AE Source to Sensors

The vibration signal generated by AE events relate to deterioration that passes through a number of media, such as pipes, fluid and earth, before the signal is picked up by the sensors. This wave propagation can be modeled as the convolution of the AE signal and the impulse response of the pipe. The impulse response of the pipe may vary depending upon fluid flow, diameter, thickness and elastic properties of the pipe and surrounding medium. Since the PCCP has a cylindrical shape, therefore, the acoustic wave received by the sensor can be considered as the superposition of the different delayed version of AE signal due to multipath propagation which may either add destructively or constructively. Therefore, it is important to understand how the path physically affects the signal. The effect of the path is researched and developed a mathematical method to appropriately model the impacts of the path on the spectral profiles of the vibration signals in different locations throughout the pipes.

Tube Wave Analysis of AE Signal

At low frequency AE signal, when the wavelengths are much larger than the pipe radius, there is only the stoneley or tube mode that exists as a propagating mode with plane wave-

fronts. This plane wave propagation of acoustic signal in the fluid inside the pipe is affected by the characteristics of the pipe. The tube wave analysis is used to observe the effect of path at different pipe profile. The characteristics of the low frequency acoustic signal in the rigid and the elastic pipes are observed from the analysis. This theoretical study can produce the fundamental concepts of low profile acoustic signal in the AE monitoring system.

Eigenfrequency Analysis of Acoustical Waves

The eigenfrequency is the system's natural frequency of vibration. At these frequencies, small or even zero driving force can produce large amplitude vibration because of the stored vibrational energy. In the PCCP, the acoustic signals are generated through the breakage or sliding of prestressed wires. These signals feature certain frequency spectral characteristics that are close to the eigenfrequency of the piping system. Therefore, in AE monitoring system, it is important to know about these eigenfrequencies, which generates the additional vibrating signal and changes the characteristics of the original AE signal. This may cause a false or wrong detection of AE signal in the sensors. In some cases, these reverberations are very strong, which may causes malfunction in the sensitive measurement system. The eigenfrequency analysis is used to determine the spectra of system resonance frequency, and to observe the effect of system resonance on the AE signal in the water-filled PCCP.

Modal Analysis of Guided Wave

In the pipeline, AE signal propagates as a guided wave. This wave can propagate over long distances with proper excitation. At low frequencies, the wave propagates as an evanescent mode, but at high frequencies, it has also propagating mode. The number of propagating modes grow proportional to the excitation frequency. Consequently, more modes cause complicated dispersion characteristics. In the elastic pipe, such waves have strong dispersive phenomena. Therefore, the modal analysis is important to determine the dynamic characteristics of the system. In this research, the modal analysis is performed to determine the PCCP structures dynamic characteristics; such as cut-off frequency, propagation constant,

and the number of propagating modes.

High Frequency Analysis of Acoustic Signal

In the condition monitoring system, the high frequency AE signal measurement technique provides special advantages in many applications. This analysis can provide earlier indication of developing faults such as frictional rubbing, which can not be detected by the low frequency analysis. In the pipeline inspection, wire break or slip related events occurs due to the impairment of passivating quality of the high pH mortar of the PCCP. Early indication of this event can save the time and the money, as well as ensure the continued safe operation. Moreover, the frequency of propagating AE signal in the pressurizing fluid medium ranges up to 30 kHz. Therefore, the high frequency analysis is important to observe the WRE in the pipeline inspection. In this study, the spectral characteristics of the high frequency AE signal through the fluid-column inside the pipe is observed under different pipe and surrounding medium condition. The theoretical results are discussed and compared with the available analytical solutions.

1.8 Overview of the Proposed Work

There are many methods developed for the AE monitoring of piping system. These are mainly, top-down approach, which is related to the theoretical analysis and bottom-up approach, which is related to the field-data analysis (see Fig. (1.1)). Among the other bottom-up approach, the AET method is widely used in the related industry, due to its important advantages. In spite of the advantages, it has some limitations to detect and locate the AE events. To approach this problem, first study the AET method in brief, and figure out the limitations. Later, the detailed theoretical analysis of AE signal generation to propagation are performed.

The theoretical study proposed in this work is related to the top-down approach, and beyond the earlier studies that found in the open literature. For the theoretical analysis, an acoustical model is developed based on Navier's equation of motion and use the Newton's law

of motion and the principle of virtual work for the fluid-structure and -surrounding medium interaction. The AE source is modeled using Hook's law based on energy dissipation from WRE. The theoretical investigation of the low frequency AE signal is performed using the tube wave analysis. The eigenfrequencies, modes of propagation, cut-off frequency of the system and the phase speed of the acoustic wave are observed by the eigenfrequency and the modal analysis. The behaviour of the high frequency AE signal propagation throughout the PCCP is observed by the sonic/ultrasonic analysis.

Finally, the information obtained from the theoretical analysis of this work is discussed in detail. The importance of the theoretical knowledge for the evaluation of AE signal and to overcome the limitations of current AE monitoring technology are also discussed.

1.9 Organization of the Thesis

The thesis is organized as follows:

The brief description of current technology, such as, PCCP construction and dimensions, generation of AE signal, current technique of AE signal measurement and AE event localization, etc. are discussed in Chapter 2. The advantages and limitations of current technology are also discussed in this chapter.

The time- and frequency-domain acoustical pressure model and source model is developed in Chapter 3. The interaction and the boundary condition between different layers are discussed and modeled here.

Chapter 4 describes the low frequency tube wave analysis of AE signal propagation through fluid-filled PCCP under different pipe and surrounding formations. The results are compared with available analytical solution.

In Chapter 5, the eigenfrequency and the modal analysis of AE signal is described. The numerical results are obtained under different situations and compared with analytical solution.

The importance of high frequency analysis of AE event and the numerical analysis of the signal generated from these events through different pipes and surrounding medium are

discussed in Chapter 6. The results are compared with the available analytical solutions.

Finally in Chapter 7, conclusion, recommendations for future works are described. The study presented in this work produced the fundamentals on which better non-destructive pipe performance testing technologies can be designed. Detailed discussion and recommendations on this matter are presented in the chapter.

Chapter 2

Current Technology

2.1 Introduction

In the NDT industry, AET method is currently used to detect the AE event in the pipeline due to its technological advantages. This method is related to the bottom-up approach (see Fig.1.1), and based on field-data analysis. The brief description of this method is described in this chapter, where WRE detection and localization of PCCP is taken as a specific application. Despite the advantages, AET method has some limitations, which are also described here. The causes of corrosion and the generation of AE signal in the PCCP and its constructional details are described to get an idea about the current technologies.

The physical characteristics of prestressed pipe, joint between the pipe sections, corrosion and AE signal generation, are described in Section 2.2. The sensors that are used for AE signal detection and recording purpose is also described in Section 2.3. Section 2.4 describes the AET method, which is used in related industry for NDT of pipeline inspection and leak detection. The basic methodology of AET technique, AE signal localization, some typical AE signals recorded by the sensors are also presented in this section. The application of AET method and some advantages and limitations of this technique is presented in Sections 2.5 and 2.6, respectively. Finally, the summary of this Chapter is described in Section 2.7.

2.2 Prestressed Pipe Design

The Prestressed Concrete Cylinder Pipe (PCCP) is a rigid pipe designed to take optimum advantage of the tensile strength of steel and the compressive strength and corrosion inhibiting properties of concrete. It is widely used throughout the world. In the U.S. and Canada there is an estimated 30,000 miles of this product installed [79]. There are no known estimates for the remainder of the world, but it is used in every continent. It has been used for over 40 years for such applications as water transmission and distribution pipelines in municipal, industrial and irrigation systems, cooling water systems in the plant, sewer force mains and gravity sewers, inverted siphons, subaqueous pipelines and lines for pressure tunnels.

2.2.1 Pipe Structure

The American Water Works Association (AWWA) maintains the standard for PCCP in its Standard C 301 (manufacture) and Standard C 304 (design). The designed procedures of this standard is applicable to lined-cylinder pipe and to embedded-cylinder pipe. In the construction, high-strength concrete core is used as the principal structural component, which provides a smooth inner surface for fluid flow. This core includes a steel cylinder that works as a watertight membrane and provides longitudinal tensile strength, and increases circumferential and beam strength. In LCP, the steel cylinder forms the outer element of the core and in ECP, it contained within the core. The core is then helically wrapped by the high-tensile steel wire under controlled tension. This high strength wire is designed to produce uniform compressive prestress in the core and enabling it to withstand high internal pressure (300 $\mathrm{lbs\,in^{-2}}$) and large external loads [3]. Finally, the pipe is coated with dense cement-mortar, so as to protect the pipe from physical damage and external corrosion [80]. The cross-sections and elements of both types of pipes are shown in Fig. (2.1).

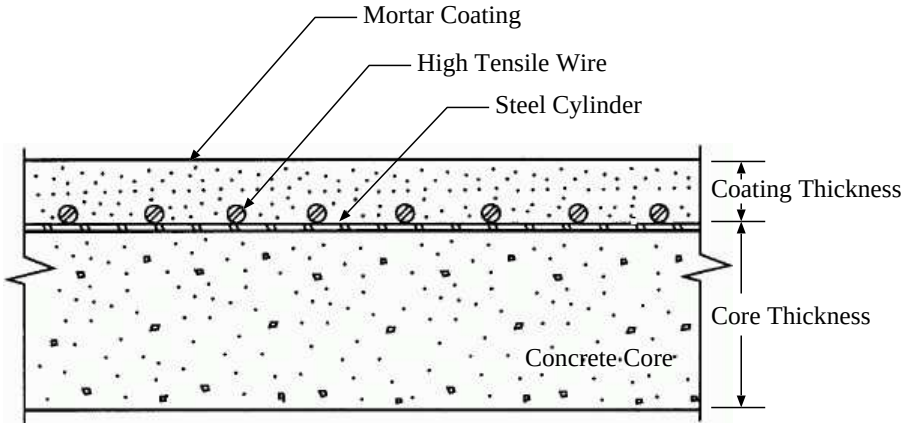

(a) Lined cylinder pipe.

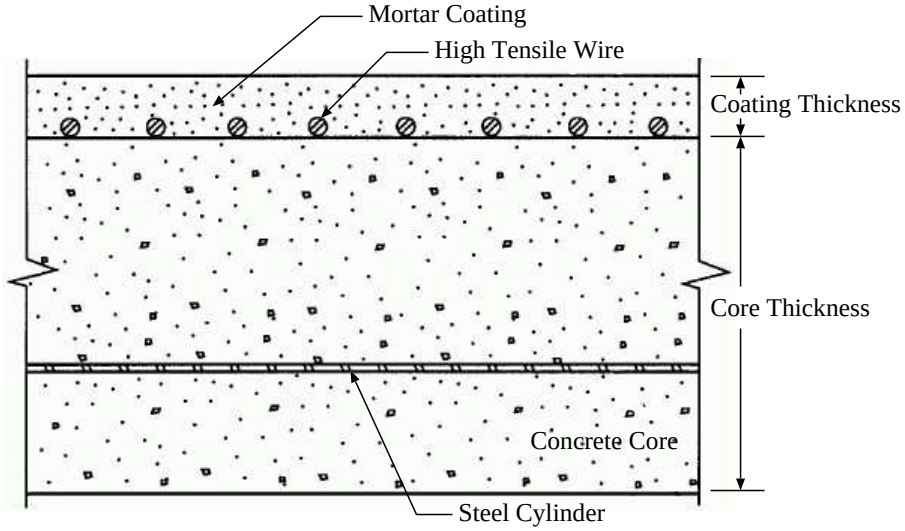

(b) Embedded cylinder pipe.

Figure 2.1: Schematic cross-sections of lined and embedded cylinder pipe

2.2.2 Pipe Dimensions

The dimensions of the pipe mainly depends on the type of pipes and the working condition. According to the standard, the LCP is suitable with inside diameter of 410 mm through 1,520 mm (16 in. through 60 in.) and ECP is suitable with inside diameter of 610 mm (24 in) and larger [1].

The pipe is manufactured in standard laying length of 16 to 24 feet (5 m to 7 m), and the standard core thickness is approximately 7 to 8 percent of nominal inside pipe diameter [81]. Table (2.1) shows the typical core thickness of PCCP.

Table 2.1: Typical core thickness of PCCP.

Nominal inside pipe diameter (in)	Typical core thickness (in)
42	3.50
45	3.75
48	4.00
51	4.25
54	4.50
57	4.74
60	5.00
66	5.25
72	5.25
78	5.75
84	6.25
90	6.75
96	7.25
102	7.75
108	8.25
114	8.75
120	9.25
132	9.25
144	10.25
156	11.25
168	12.25
180	13.25

2.2.3 Pipe Joint

According to AWWA standard, each section of the pipe is connected to the next using a bell and spigot joint, which uses a rubber gasket to seal the joint and a grout cap to fill the remaining gap. The spigot ring is the protruding end of a PCCP joint, which contains a shaped groove to retain the O-ring rubber gasket. The rubber gasket is incorporated at each joint for water tightness and flexibility.

Figures (2.2) and (2.3) show a LCP and ECP section pipe joint according to AWWA standard C-301 (L) and C-301 (E), respectively.

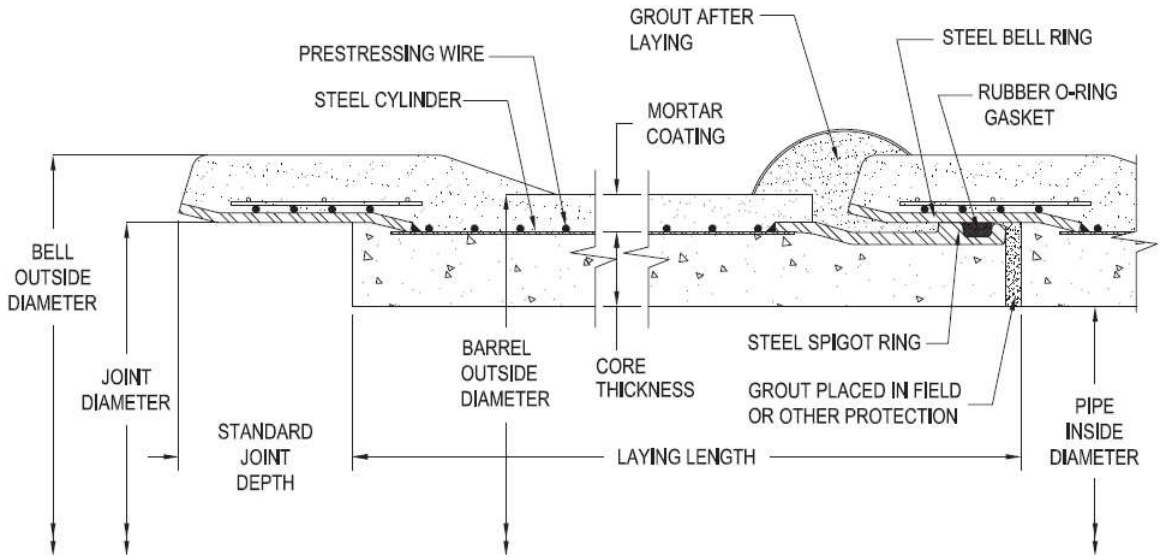

Figure 2.2: Schematic of LCP section joint according to AWWA standard.

2.2.4 Corrosion in PCCP

The PCCP generally consists of a thin steel cylinder lined or embedded with cement-concrete mortar. The cured steel-concrete core is subsequently helically wrapped with a high tensile wire and coated with high pH cement-rich mortar. In the mortar, the prestressed wires are protected from galvanic corrosion. However, when the protective mortar is chemically or physically compromised, the passivating quality of the high pH mortar breaks down. This causes corrosion to start on prestressed wire. The wire normally breaks when the corrosion

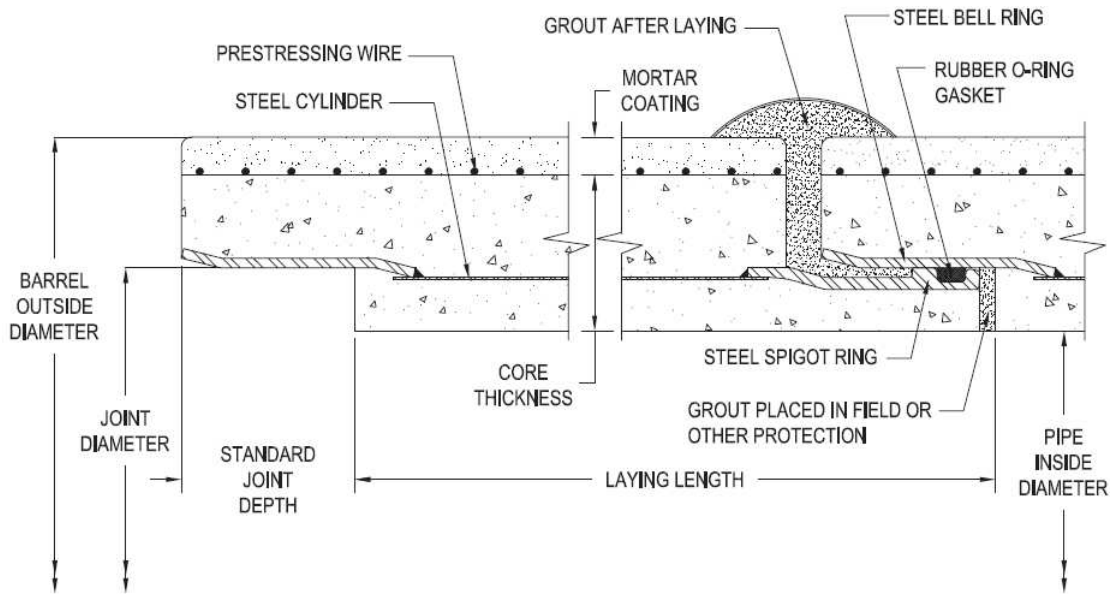

Figure 2.3: Schematic of ECP section joint according to AWWA standard.

activity has reduced their diameter to the point where the stress applied to them exceeds their yield point. This process may also cause further damage to the mortar around the wires or the steel-concrete inside the pipe. If enough wires fail, the structural capacity of the PCCP will be compromised and the pipe is in danger of a catastrophic rupture.

2.2.5 Generation of AE Signal

The stress embedded on the wires during the manufacturing process of PCCP is grater than 70% of ultimate breaking strength of the wire. Therefore, a strand of 1/4 inch Class III wire will possess more than 7,000 lbs of tension when wrapped on the core [3]. Hence, a relatively small amount of corrosion, due to the reduction of modulus and compression of concrete because of aging and/or physical and chemical effects, will result breakage or slippage of reinforce wire [82]- [84]. This causes sudden release of elastic energy stored in the prestressed wire in the form of acoustical (sound) waves [85], which is known as AE signal. The release of acoustic energy would continue as a defect extends and as plastic strain occurs in the presence of a defect.

2.3 Acoustic Monitoring Devices

In pipeline inspection, specially designed acoustical sensors are used as AE monitoring devices. Two types of sensors have been used to detect the acoustical waves are:

- hydrophone, and
- accelerometer.

A hydrophone is a microphone designed to be used underwater for recording or listening to underwater sound. Most hydrophones are based on a piezoelectric transducer that generates electricity when subjected to a pressure change. Such piezoelectric materials can convert a sound signal into an electrical signal since sound is a pressure wave in fluids. A typical hydrophone is shown in Fig. (2.4)(a).

Hydrophones are constructed of ceramic materials. It can detect acoustic signals by sensing the vibration that is transmitted through the pipe wall into the water column. Hydrophones are installed through valves into the flow stream of the active pipeline, as shown in Fig. (2.4)(b). The installed hydrophones are then continuously monitor the pipe for AE events, which propagates through fluid column.

(a) (b)

Figure 2.4: (a) A typical hydrophone and (b) a hydrophone installed in pipeline.

An accelerometer is a device that measures non-gravitational accelerations. These accelerations are produced by mechanically accelerating the accelerometer via its casing. Single- and multi-axis models are vertical to detect magnitude and direction of the acceleration as a vector quantity and can be used to sense orientation, vibration and shocks. Modern accelerometers are often small Micro Electro-Mechanical Systems (MEMS), and are indeed the simplest MEMS devices possible, consisting of little more than a cantilever beam with a proof mass (also known as seismic mass). Mechanically the accelerometer behaves as a mass-damper-spring system; the damping results from the residual gas sealed in the device. A typical accelerometer is shown in Fig. (2.5)(a).

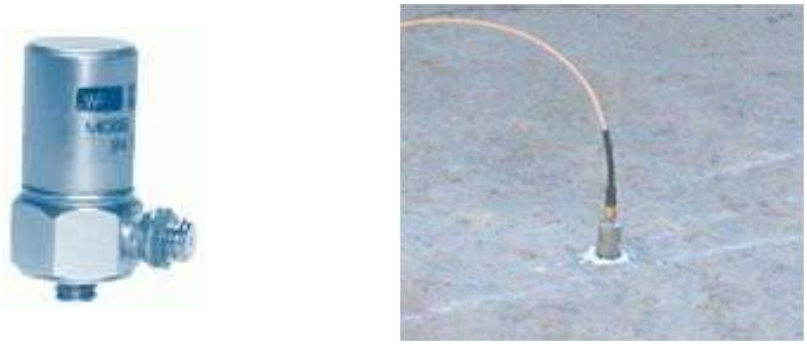

(a) (b)

Figure 2.5: (a) A typical accelerometer and (b) an accelerometer installed in pipeline.

Accelerometers are installed on the surface of the pipeline, as shown in Fig. (2.5)(b). Incentive to use accelerometers in AE testing is to assist hydrophones, as hydrophones are more sensitive than accelerometers. Accelerometers are also used in empty pipelines, where hydrophones do not work.

Once the AE event occurs, the signal will propagate both ways along the pipeline, and may be detected by the closest pair of sensors. Sometimes if the amplitude is large enough, the signal might be detected by the third or the fourth sensor. As studied in [72], the detected result is reliable with sensor spacing at 262 meters distance, and this can vary according to landscape, temperature, pipe structure, etc. Therefore, an ideal AE signal should be detected by two sensors closest to it, and the arrival time difference can be used to localize the position

of the defect.

2.4 Current Applied Technology

2.4.1 Acoustic Emission Testing

Among the other AE monitoring system, AET is widely used in the related industry. The AET method in PCCP monitoring is used to detect the acoustic events, being transmitted through a pipeline. It identifies the AE signal associated with corrosion related events, or more specifically a WRE in the prestressing wire or a delamination in the mortar coating of the pipeline. Two or more acoustic sensors are installed on an existing pipeline to record the AE data from a specific area in the pipeline. Acoustic systems then monitor the pipe for the AE signals of wire break or slip and alert the observer of the system, when an AE signal has been detected.

This AE signal received by the sensors are recorded by the Data Acquisition System (DAS), which filters out ambient noise in the pipeline and identifies the acoustic events with the properties of wire break or delamination. When an event has been determined to have all the acoustic characteristics of a prestressed wire failure, the analytical software further evaluates the signal to locate the origin of the event. For this purpose, the time of arrival of the AE signals is recorded. The known speed of the sound in water is used as well as the spacing between the sensors. By comparing the arrival time between two adjacent sensors, the signal processor determines the location of the WRE. The number of WRE that are recorded over the monitoring period can indicate the severity of the problem. Once the locations of the corroded areas are known, the owner of the pipeline can then decided whether the damage pipe sections should be exposed to check their overall condition.

In current practice, AE signals are recognized and identified according to the knowledge and the experience of the service provider. A fixed set of threshold level is used to identify the AE signal, and consider only the background noise. The velocity of acoustical waves inside the medium is considered as constant. The usable frequency ranges of these sensors can go up to 40 kHz, and spacing ranges from 150 m up to 750 m (500 feet up to 2500 feet) [4]

on pipelines ranging in diameter from 0.75 m to 2 m (30 inches to 78 inches). There is no standard sensor spacing for any given PCCP pipeline [61]. The optimum sensor spacing is determined by the service provider based on location, configuration, diameter, and type of pipe, along with various other conditions. The field data collected from the sensor is used to localize the acoustic events.

2.4.2 Localization

In AET method, the source of AE signal is determined by the recorded acoustic signal. It is known as localization of pipe distress. The distance of AE source from one of the two sensors is calculated by the arrival times of the event at each sensor, as shown in Fig. (2.6).

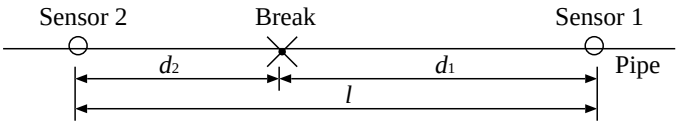

Figure 2.6: Schematic of WRE source localization.

Mathematically, the location of a localized event is determined as [4],

$$d_1 = \left[\frac{v(t_1 - t_2) + l}{2}\right], \tag{2.1}$$

where d_1 is the distance of AE source from sensor 1, v is acoustical wave speed in water, t_1 and t_2 are the arrival time of AE signal at sensor 1 and 2, respectively, and l is the distance between the two sensors.

The accuracy of the AE source location calculated with the Eq. (2.1), depends on accurate distances between the two sensors and the speed of sound in water [4]. There are also minor changes in accuracy due to the flow velocity and the change of temperature of the water [4,9].

2.4.3 Testing Process

A typical test setup of AET is shown in Fig. (2.7) [4]. In the measurement, the occurrence of WREs (AE signal) are detected by the two sensors (hydrophone and/or accelerometer) located at position 1 and 2, respectively. The time required by the AE signal to arrive

at the sensors is directly related to the distance it travels. This time and the AE signals are recorded in the testing process by the system connected with the sensors (as shown in Fig. (2.7)).

The recorded signals are then analyzed by the set of rules based on knowledge and experience of the service provider. If the signal satisfies the specific criteria of AE signal parameters, it is detected as a WRE signal. After that, the difference of arrival time and the sound velocity in the medium is used to determine the location of the source. Equation. (2.1) is used to calculate this position.

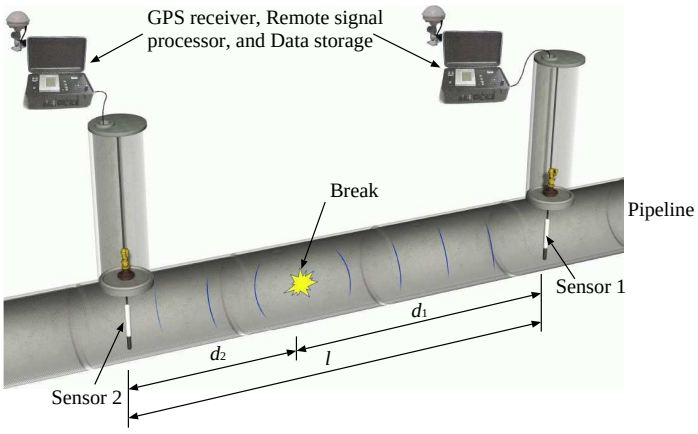

Figure 2.7: Typical test setup AET method.

2.4.4 Typical AE Signals

As an example, consider a test site of water-filled PCCP where AE signal is detected by the two sensors. Sensor-1 at site 1 is a hydrophone placed inside the pipe in the water medium. Sensor-2 at site 2 is an accelerometer placed on the pipe surface. Two sensors are separated by 160 m. The schematic of this example is shown in Fig. (2.8).

An event (break or slide) occurs at 85 m away from the Sensor-1 and 75 m away from the Sensor-2. Therefore, Sensor-2 (accelerometer) received the signal earlier than the Sensor-1 (hydrophone). Hydrophone received the signal from the water column and accelerometer from the pipe surface. Figure (2.9) shows the resulted WRE signal recorded by the hy-

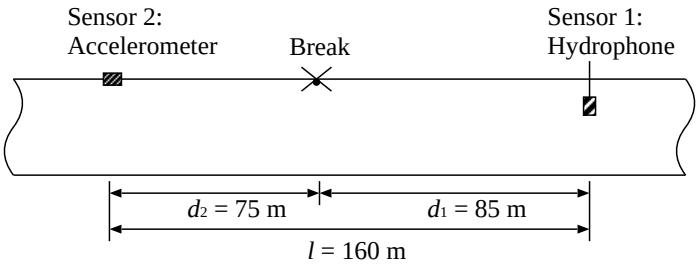

Figure 2.8: Schematic of an AET example.

drophone and accelerometer.

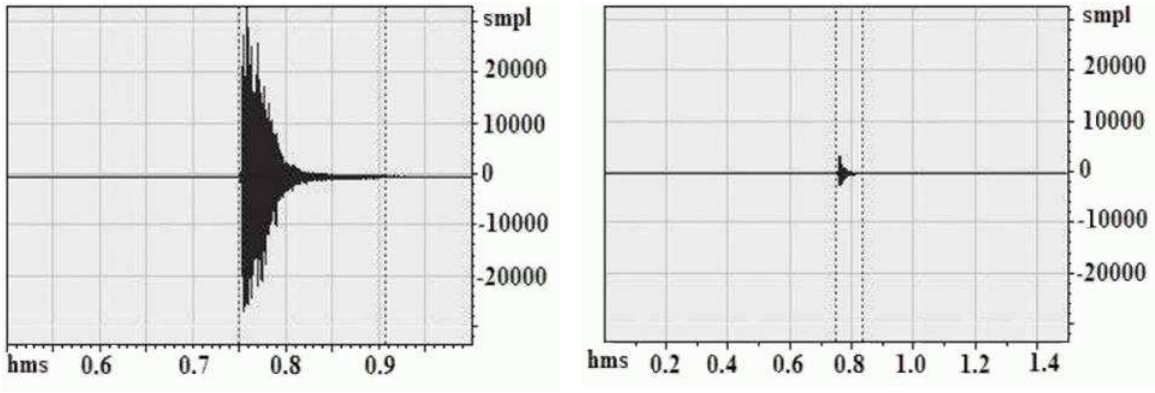

(a) (b)

Figure 2.9: Recorded AE signal by the (a) Hydrophone and (b) Accelerometer.

Figures (2.9)(a) and (b) clearly show that the signal amplitude recorded by the hydrophone is much stronger than the signal recorded by the accelerometer. For the best result, the duration of the signal should not be less than 0.05 seconds and it should be much larger than the background noise [6].

2.5 Applications of AET

AET is a powerful tool for materials testing and inspection, with entire series of advantages when compared to other NDT techniques. It has multiple applications for many diverse

purposes, such as [86]:

- Crack detection;
- Vessel inspection;
- Leak detection;
- Nuclear lift rig inspection;
- Pulp and paper machinery;
- Laboratory and field testing;
- Insulated and high temperature processes;
- Online and in-service testing.

2.6 Advantages and Limitations of AET

Among the other NDT based on AE monitoring technique, industry people are interested to use AET method due to its some important advantages. One major advantage of AET is that it can be performed at the interference in-service without any disturbance [70]. It also makes this technique more advanced than other NDT, since it is not necessary to place the sensor right at the defect position. In addition, the localization ability gives another major advantage of AET. Therefore, a suspected area can be reported to the client. This early warning advantage opens the way for performing following tests economically to verify the defect. This technique also provides a real-time monitoring method to the specimen, which minimize the system downtime for inspection. AET does not require access to the entire examination area.

As like as other methods, the AET method also has some disadvantages or limitations. This research focuses on some of these limitations, which are related with AE signal propagation through the pipe inside the fluid medium. These limitations can be summarized as follows [4, 6, 74, 75, 87]:

- Identification of wire breaks as opposed to other events must be demonstrably correct. This identification becomes more and more difficult and complicated with increasing distance to the sensors and with increasing the AE signal frequency. Because, the dispersion of the frequencies generated by the event grows with the increase of frequency, which will distort and disguise its character.

- The evaluation criterion does not exist in form of commonly accessible data. For example, the threshold of AE is set firmly to the knowledge and experience of the service provider. This is not correct in some case, because the level of AE signal is not fixed. It depends on released elastic energy of the AE events.

- In the source localization, the speed of acoustical wave inside the fluid column consider as constant. This is not true for all cases, due to the acoustoelastic effect.

- The background noise, both continuous and impulsive, makes the detected AE signals less accurate. In current practice, the system resonance are also considered as a background or ambient noise. But in some cases, the system resonance signal becomes more dominant than the original AE signal, which may mislead the recorded data.

- Some impulsive noise may produce acoustic signals similar to the genuine AE signal. This may causes false or incorrect signals at the sensors.

- As a pipeline decreases in diameter, the sensor spacing becomes more critical. In this case, AE signal traveling through a pipeline will bounce off the pipe wall as it travels up and down the pipeline. Consequently, the signal attenuates more quickly in a small diameter pipe than a large diameter pipeline. Theoretical analysis is important for this knowledge.

2.7 Summary

The characteristics of PCCP, including dimensions, materials, joints, etc. are described. The causes of corrosion, and hence, prestressed wire failure and the generation of WRE signal

are described. The basic characteristics of commonly used acoustic sensors for the pipeline inspection, are also described. The AE event localization technique of AET method and its advantages and limitations are described in detail.

The information about the PCCP is required to simplify the mathematical model and to simulate the numerical result. The knowledge about the sensors and the AET method is important to understand the current technology of AE monitoring system. The limitations of this technique, prevents the system to get the actual AE signal. The proper theoretical analysis and knowledge can help to overcome this problem.

Chapter 3

Mathematical Modeling

3.1 Introduction

The theoretical study performed in this work is related to the top-down approach (see Fig.1.1). The mathematical model is developed for this purpose based on Navier's equation of motion to simulate the acoustic wave propagation through fluid-filled pipe. In case of elastic pipe, the propagating acoustic wave of fluid medium has an interaction with the surrounding formation. This interaction has been modeled by using Newton's law of motion in equilibrium. The principle of virtual work is used to develop the fluid-structure and structure-fluid and -outer formation interaction. The AE source is modeled using Hook's law based on energy dissipation from WRE.

The basic mathematical model based on Navier's equation of motion is presented in Section 3.2. The simple physical model, using some acceptable assumptions is described in Section 3.3. The acoustic pressure model without the source can be obtained directly from the Navier's equation of motion. This homogeneous model is presented in Section 3.4. In Section 3.5, different types of acoustic sources that are generated from the wire-break or slip related events are described. The complete acoustic pressure model with AE source is presented in Section 3.6. The time domain and the frequency domain model is developed in this section. In Section 3.7, the fluid versus surrounding medium interaction is modeled using Newton's law of motion and the principle of virtual work. Finally, the summary of this Chapter is described in Section 3.8.

3.2 Model Formulation

The wire break or slip generated acoustic signal propagates through the pipe structure and the fluid in the pipe. In the complete solution of signal propagation, the signal's travel through different media should be considered. The complex coupled problem can be modeled easily through Navier's equation of motion.

For a homogeneous isotropic elastic medium, the Navier's equation of motion is [88]

$$\mu\nabla^2\mathbf{u} + (\lambda+\mu)\,\nabla(\nabla\cdot\mathbf{u}) = \rho\frac{\partial^2\mathbf{u}}{\partial t^2}, \tag{3.1}$$

where $\mathbf{u}$ is the time harmonic displacement field vector, μ and λ are the Lame's constants and ρ is the mass density of the medium.

The vector $\mathbf{u}$ can be decomposed into scalar ϕ and vector $\mathbf{\Psi}$ velocity potential as

$$\mathbf{u} = \nabla\phi + \nabla\times\mathbf{\Psi}, \tag{3.2}$$

with the constraint [89, 90]

$$\nabla\cdot\mathbf{\Psi} = 0. \tag{3.3}$$

Substituting Eq. (3.2) into (3.1) yields

$$\mu\nabla^2\left[\nabla\phi + \nabla\times\mathbf{\Psi}\right] + (\lambda+\mu)\,\nabla\nabla\cdot\left[\nabla\phi + \nabla\times\mathbf{\Psi}\right] = \rho\frac{\partial^2}{\partial t^2}\left[\nabla\phi + \nabla\times\mathbf{\Psi}\right]. \tag{3.4}$$

Using vector identity $\nabla\cdot\nabla\phi = \nabla^2\phi$ and $\nabla\cdot\nabla\times\mathbf{\Psi} = 0$, Eq. (3.4) can be written as

$$\nabla\left[(\lambda+2\mu)\,\nabla^2\phi - \rho\frac{\partial^2}{\partial t^2}\right] + \nabla\times\left[\mu\nabla^2\mathbf{\Psi} - \rho\frac{\partial^2\mathbf{\Psi}}{\partial t^2}\right] = 0. \tag{3.5}$$

The displacement Eq. (3.2) satisfies the equation of motion if the potentials ϕ and $\mathbf{\Psi}$ satisfy the following wave equations [20, 91]

$$\nabla^2\phi - \frac{1}{v_L^2}\frac{\partial^2\phi}{\partial t^2} = 0, \tag{3.6}$$

$$\nabla^2\mathbf{\Psi} - \frac{1}{v_S^2}\frac{\partial^2\mathbf{\Psi}}{\partial t^2} = 0, \tag{3.7}$$

where

$$v_L = \left[\frac{\lambda + 2\mu}{\rho}\right]^{1/2} = \left[\frac{E\,(1-\nu)}{\rho\,(1+\nu)\,(1-2\nu)}\right]^{1/2},$$

$$v_S = \left[\frac{\mu}{\rho}\right]^{1/2} = \left[\frac{E}{2\rho\,(1+\nu)}\right]^{1/2}, \tag{3.8}$$

E is the elastic modulus and ν is the poisson's ratio.

Eqs. (3.6) and (3.7) represent the longitudinal and shear wave equations with v_L and v_S being the longitudinal and shear wave velocities of the medium, respectively.

In the fluid medium, the acoustic signal has only longitudinal wave component, therefore, Eq. (3.6) is sufficient to describe the wave propagation inside the pipe. However, in the pipe structure the acoustic signal has both longitudinal and shear wave components that consists of axially symmetric and tortional modes, and hence, Eqs. (3.6) and (3.7) must be solved entirely [20, 21].

Analytical solutions of these equations for idealized situations have already been obtained [34]- [40]. The current study goes beyond the earlier studies by emphasizing the numerical analysis of acoustic wave propagation through the fluid column inside the pipe using commercial FE code. For this purpose, Eq. (3.6) is used to simulate the acoustic wave propagation through the fluid column and Newton's law of motion in equilibrium with principle of virtual work are used to introduce the effect of surrounding layered medium (e.g. pipe structure and outer medium) on the acoustic propagation through the complex geometry.

3.3 Simple Physical Model

The acoustic signal generated by a wire break or slip creates oscillation in the complex geometry. There are two types of AE signal generates in the pipe. One is the high-frequency mechanical wave (above 100 kHz), that propagate along the pipe structure, another is the low frequency wave (about 30 kHz), that readily propagates into the pressurized fluid in the pipe [72]. The PCCP structure mainly consists of concrete and steel components, which are highly attenuative compared to the fluid. The attenuation of both shear and longitudinal

vibrations in concrete and steel on the order of 100 kHz is high at about 30 dB ft^{-1} and 0.1 dB ft^{-1}, respectively [62, 92]. Moreover, each pipe section is generally 22 feet long [9] and according to the AWWA standard, each section of pipe is connected to the next using a bell and spigot joint, which uses a rubber gasket to seal the joint and a grout cap to fill the remaining gap (as shown in Fig. (2.2) and (2.3)), therefore the joints could be highly attenuative. In contrast, the attenuation of fluid is significantly less than the pipe structure (around 1 dB per 3000 feet for water) at the frequencies of interest [93].

For typical AE levels, the signal in the pipe structure attenuate very quickly (less than 100 feet). On the contrary, the signal that transmitted to the fluid column inside the pipe can be detected for several hundreds, perhaps thousands of feet [72]. Again in the non-destructive pipe testing, long length of pipe inspection was performed from a single probe position at a distance of about 500 feet or more [9]. Therefore, it can be assumed that the acoustic signals start to propagate from fluid column only, which then interact with the pipe wall.

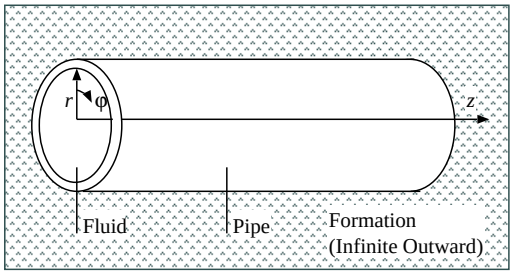

Figure 3.1: Schematic of a fluid-filled PCCP.

The schematic diagram of one section of the fluid-filled pipe submerged in the outer formation (medium) is shown in Fig. (3.1). Usually, the PCCP is submerged in earth (soil) and the pipe sections are generally 22 feet long [9]. The pipe sections are connected in series for the long distance transmission of water. In this study, other types of outer mediums such as, air, water are also used to observe the surrounding formation (medium) effects on the acoustic wave propagation.

3.4 Homogeneous Acoustic Pressure Model

The pressure (P) distribution of acoustic signal for uniform flow in a lossless fluid can be expressed by using pressure-velocity relation $P = -\rho\frac{\partial\phi}{\partial t}$, in Eq. (3.6) alone as [94]

$$\nabla^2\left(-\frac{1}{\rho_F}\right)P + \frac{1}{\rho_F v_F^2}\frac{\partial^2 P}{\partial t^2} = 0, \tag{3.9}$$

where ρ_F is the fluid density, v_F is the speed of the signal in the fluid medium.

The Eq. (3.9) represents the homogeneous equation for pressure flow in the fluid medium inside the pipe, which does not contain any source term.

3.5 Acoustic Source Model

The source can be modeled as the elastic energy that is reserved in the prestressed wire of PCCP structure and released due to the breakage or slippage of the wire. The energy of these mechanical disturbances appear as an acoustic signal with low and high frequency components.

These acoustic sources can be classified into two types [95]:

1. constant volume velocity sources, and
2. constant pressure sources.

3.5.1 Constant Volume Velocity Source

This type of source maintains a constant volume velocity, i.e., constant amount of fluid displacement per second, in the medium in which it is present. According to the impedance analogy, this volume velocity is considered as a flow variable which is similar to a current source in an electrical circuit. The analogous circuit of constant volume velocity source is shown in Fig. (3.2)(a).

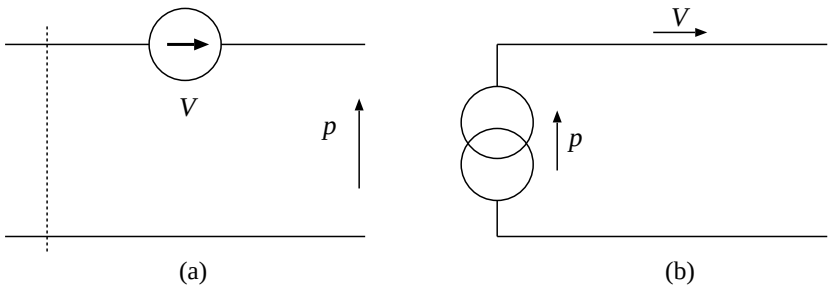

Figure 3.2: (a) Constant volume velocity and (b) Constant pressure sources.

3.5.2 Constant Pressure Source

A constant pressure source maintains a constant pressure drop across its terminals. Usually, this pressure can be measured without disturbing the acoustical setup in which it is present. Therefore, according to the impedance analogy, this can be considered to be analogous to a voltage source in an electrical circuit. The analogous circuit of constant pressure source is shown in Fig. (3.2)(b).

3.5.3 Source Strength

The amount of energy dissipation (which is the source strength of the AE events) from the wire-break or slip can be obtained from the Hook's law. According to this law, the force exerted by the prestressed wire when stressed by $\triangle l$ (which describes the stiffness of the wire) can be written as

$$F_e = kx, \tag{3.10}$$

where

$$k = \frac{EA}{l}, \quad \text{and} \quad x = \triangle l. \tag{3.11}$$

Here E is the Young's modulus or modulus of elasticity, which is the ratio of tensile stress $\left(\sigma = \frac{F_e}{A}\right)$ and strain $\left(\varepsilon = \frac{\triangle l}{l}\right)$, A is the original cross-sectional area of the wire through which the force is applied, $\triangle l$ is the amount by which the length of the wire changes and l is the original length of the wire.

Therefore, the elastic energy (U_e) released by the AE event can be expressed as [96]

$$U_e = \int F_e dl = \frac{EA}{l} \int \triangle l dl = \frac{1}{2} \frac{EA}{l} \triangle l^2, \tag{3.12}$$

and the elastic energy per unit volume is

$$\frac{U_e}{Al} = \frac{1}{2} E \left(\frac{\triangle l}{l} \right)^2 = \frac{1}{2} E \varepsilon^2. \tag{3.13}$$

Equation (3.13) is used to estimate the elastic energy density that released due to the AE events [96]- [104].

3.5.4 Modeling the Source

In the acoustic source model, constant volume velocity is used as a flow variable. The strength of AE source is the flow strength, which is obtained from the amount of elastic energy dissipation from the AE events.

For the sake of mathematical brevity, the source of AE signal (G) is modeled as [105,106]

$$G = \frac{\partial S}{\partial t} \delta^{(3)}(\mathbf{x} - \mathbf{x}'), \tag{3.14}$$

where S is the source flow strength of the signal that obtained from released elastic energy density, $\delta^{(3)}$ is the 3D Dirac delta function and $\mathbf{x}$ and $\mathbf{x}'$ are the 3D space vector of the observation and the source point, respectively.

3.6 Inhomogeneous Acoustic Pressure Model

To obtain the complete acoustic pressure model with source, introduce the source term from Eq. (3.14) into Eq. (3.9). Therefore, the pressure distribution of AE signal in the fluid medium inside the pipe can be written as

$$\nabla^2 \left(-\frac{1}{\rho_F} \right) P + \frac{1}{\rho_F v_F^2} \frac{\partial^2 P}{\partial t^2} = G, \tag{3.15}$$

Eq. (3.15) represents the transient equation (in time domain) of acoustic pressure distribution of AE signal through fluid-filled PCCP.

Let us assume that, the pressure varies harmonically in time as

$$P(\mathbf{x}, t) = p(\mathbf{x})\, e^{i\omega t}, \tag{3.16}$$

where $\mathbf{x}$ is a 3D space vector, p is the time harmonic pressure, $\omega\,(= 2\pi f)$ is the angular frequency, f is the frequency of the propagating signal.

By considering the same harmonic time dependence for the source term, Eq. (3.14) can be written as

$$g = i\omega S \delta^{(3)}(\mathbf{x} - \mathbf{x}'). \tag{3.17}$$

Using Eq. (3.16) and (3.17) into Eq. (3.15), the time harmonic equation (in frequency domain) of the acoustic pressure can be obtained as

$$\nabla^2 \left(-\frac{1}{\rho_F}\right) p - \frac{\omega^2 p}{\rho_F v_F^2} = g. \tag{3.18}$$

Equation (3.18) represents the inhomogeneous Helmholtz equation for acoustic pressure in the fluid medium.

3.7 Fluid vs Surrounding Medium Interaction

Two types of surrounding layered medium interaction, such as, fluid-structure and structure-fluid and -outer medium, and its effects on the acoustic pressure are considered during the modeling of wave propagation through the fluid column inside the pipe. Newton's law of motion in equilibrium and principle of virtual work are used to model this interaction.

3.7.1 Fluid-Structure Interaction

Initially, the acoustic signal that propagates through fluid column appears as an acoustic wave pressure on the pipe wall and generates only small displacements. Since the pipe structure is much stiffer than the fluid, it will interact without causing separation or voids, which means that the radial displacements and pressure at the fluid-structure interfaces must be compatible and in equilibrium.

The acoustic pressure forces that acts on the pipe structure can be written for transient case as

$$F_j^P = n_j P, \tag{3.19}$$

and for time harmonic case as

$$F_j^P = n_j p, \tag{3.20}$$

where n_j is the outward-pointing unit normal vector and F_j^P is the external acoustic pressure forces in three principal directions.

According to Newton's law of motion in equilibrium, the total work done in the pipe structure due to the displacements is equal to the external pressure forces. This force causes undergo unrelated but consistent displacements and deformations inside the pipe structure, which can be explained by the principle of virtual work (see Appendix-A).

According to the principle of virtual work, this force can be expressed in terms of stresses as

$$F_j^P = -\frac{\partial \sigma_{ij}}{\partial x_i}, \tag{3.21}$$

where σ_{ij} is the symmetric stress tensor consisting of normal and shear stresses.

The Navier's equation of equilibrium in the pipe structure in terms of displacement vector $\mathbf{u}$ can be obtained using stress-strain and strain-displacement relationships. For static case, using these relationships (see Eq. (B.1) and (B.2) in Appendix-B) into Eq. (3.21), the displacement equation in the structure can be rewritten as

$$\mathbf{F}^P = -\nabla \cdot (\mathbf{C} \nabla \mathbf{u}) \,. \tag{3.22}$$

where $\mathbf{C}$ is the elastic matrix consisting of Lame's constants.

In case of transient analysis, Eq. (3.22) can be expressed as [107]

$$\mathbf{F}^P = \rho \frac{\partial \mathbf{u}}{\partial t^2} - \nabla \cdot (\mathbf{C} \nabla \mathbf{u}) \,. \tag{3.23}$$

In time domain, Eqs. (3.19) and (3.23) are used to calculate the displacement in the pipe structure due to the acoustic pressure forces.

For time harmonic analysis, Eq. (3.23) becomes

$$\mathbf{F}^P = -\omega^2 \rho \mathbf{u} - \nabla \cdot (\mathbf{C} \nabla \mathbf{u}) \,. \tag{3.24}$$

Eqs. (3.20) and (3.24) are used in frequency domain, to calculate the displacement in the pipe structure due to the acoustic pressure forces.

3.7.2 Structure-Fluid Interaction

In equilibrium, the displacement in the structure generates the same but opposite amount of traction forces on the pipe wall.

In time domain, this forces can be written as

$$F_j^T = -n_j \frac{\partial u_{ij}^{'}}{\partial x_i} = -i n_j \omega \frac{\partial u_{ij}}{\partial x_i}, \tag{3.25}$$

and in frequency domain, it can be expressed as

$$F_j^T = -n_j \frac{\partial u_{ij}^{''}}{\partial x_i} = n_j \omega^2 \frac{\partial u_{ij}}{\partial x_i}, \tag{3.26}$$

Here ($'$) represents the time derivative of displacement vector and F_j^T represents the time harmonic traction forces acting in three principal directions.

The traction forces that act on the pipe wall interact with the acoustic pressure forces as a elastic waves. To couple the response of structure to the fluid column, Eq. (3.26) can be written in terms of acoustic pressure in time domain as [107]

$$\mathbf{F}^T = -\mathbf{n} \cdot \left(-\frac{1}{\rho_F} \nabla P \right). \tag{3.27}$$

and in frequency domain as

$$\mathbf{F}^T = -\mathbf{n} \cdot \left(-\frac{1}{\rho_F} \nabla p \right). \tag{3.28}$$

Eqs. (3.25) and (3.27) are used to calculate the acoustic pressure variation in time domain and Eqs. (3.26) and (3.28) are used to calculate the acoustic pressure variation in frequency domain, in the fluid column due to the traction forces on the pipe wall.

Similarly, the interaction between the pipe structure and the outer medium can be obtained by using the similar relationships. However, the elastic waves that are generated in

the surrounding layered medium (e.g. pipe structure and outer medium) due to the acoustic signal, are obtained by using the equations above. These elastic waves are then transmitted back into the fluid inside the pipe and thereby, affecting the characteristics of the propagation of acoustic signals.

3.8 Summary

The derivation of acoustical model based on Navier's equation of motion for the acoustic wave propagation through fluid-filled pipe is described. By using Newton's law of motion in equilibrium and the principle of virtual work, the derivation of fluid-structure and structure-fluid and -outer medium interaction is described. The acoustic source model is described by using Hook's law for the released elastic energy of the AE events.

The model that developed in this chapter is the basic mathematical model of the acoustic wave propagation through fluid-filled pipe. Using the same model the analysis of acoustic wave propagation through any type of cylindrical shells immersed or surrounded by different types of medium can be possible.

Chapter 4

Tube Wave Analysis

4.1 Introduction

At low frequencies AE signal, there is only Stoneley or tube mode that exists as a propagating mode with the plane wavefronts, which is affected by the characteristics of the pipe and the surrounding medium. The time response of the system is suitable to explore this tube wave effect on the propagating AE signal. The time domain acoustic model is used for this purpose. To understand the characteristics of WRE vibration and the impact of path on the vibration AE signal, the dispersion behaviour of wave propagation is analyzed for various pipe profiles surrounded by different soil medium. The low frequency transient analysis of the pipe system is taken at different points inside the pipe to investigate the result.

The significance of the tube wave analysis is described in Section 4.2. The analytical model of the tube wave is given in Section 4.3. The theoretical results obtained from this model are used for comparison. In Section 4.4, the acoustical model, which is used for numerical simulation is described in brief. The solution methodology, such as, model description, boundary conditions, and discretization are described in Section 4.5. The results and discussions are presented in Section 4.6. Finally, the summary of this Chapter is described in Section 4.7.

4.2 Significance of Tube Wave Analysis

The tube wave analysis of plane wave propagation in the fluid-filled pipe is used in the measurement of acoustic properties of substance [41]- [44]. Another common use is the impedance tube [108]- [113], in which the acoustic properties of an elastic material terminating the waveguide are measured. The seismic monitoring of underground fluid reservoirs, borehole coupling of dam site investigation, groundwater aquifers, etc. are the examples of real-time application of this analysis [114]- [122]. In seismic monitoring of underground fluid reservoirs, this type of analysis provides an update of the changes between wells, which will enable field operators to detect changes in the reservoirs as oil is pumped out of reservoirs and water is pumped in. Such monitoring will enable users to obtain information about the water front propagation in the reservoirs to prevent the premature water flooding, reservoir disintegration, and well-blocking. In dam site investigation, the scope of this analysis is to observe the sediment rigidity, shear wave velocity, and consolidation history of the clays. Many researches were performed on this matter for its technological importance.

In the PCCP, the plane wave propagation is used to measure the impact of path on the vibrating signal generated by the acoustic emission of WRE. This was established that at low frequencies when the wavelengths are much larger than the pipe radius, where the stoneley or tube mode is the only propagating mode with plane wavefronts in the fluid [41]- [44], [123, 124]. However at high frequencies, there also exist Rayleigh or shear modes which exhibit oscillatory amplitudes in the fluid and a decaying amplitude in the pipe and the surrounding medium. Therefore, care should be taken during the simulations to avoid the excitation of higher-order modes for meaningful results.

As far as our knowledge, there is no systematic theoretical analysis of tube wave effect on AE signal propagation through water-filled PCCP. In this work, the time domain acoustical model is carried out for the numerical analysis of the PCCP with a range of radii, thickness, and stiffness of the pipe and surrounded by different soil medium.

4.3 Tube Wave Analysis

The effect of path on low frequency AE signal propagation can be illustrated by the tube wave analysis at different pipe profile. The characteristics of pipe profile mainly depend on dimensions and elastic properties of the pipe materials and the surrounding medium. The elastic waves that are generated in the pipe structure due to the AE signal depends on these characteristics. However, during the propagation this elastic wave is transmitted into the fluid and decreases the velocity of acoustic wave of AE signal. This reduced wave is known as a 'Tube Wave'.

The phase velocity of the plane wavefront acoustic wave inside the pipe can be obtained from tube wave analysis. Mathematically, this this tube wave (v_T) can be expressed as [125]

$$v_T = \left[\frac{1}{v_F^2} + \frac{\rho_F}{M_L}\right]^{1/2}, \tag{4.1}$$

where

$$M_L = E_L \left[2(1+\nu_L) + \frac{D^2}{t(D+t)}\right]^{-1}, \tag{4.2}$$

and D is the diameter of the pipe, E_L, ν_L and t are the elastic (Young's) modulus, poisson's ratio and thickness of the surrounding layered medium, respectively.

In this work, the expression given in Eq. (4.1) is used to calculate the theoretical values of tube waves (v_T) of low frequency AE signal, that propagate into the fluid-filled PCCP.

4.4 Acoustical Model

In this analysis, the time domain inhomogeneous acoustical pressure equation is used as a mathematical model. From Eq. (3.15) it can be written as

$$\nabla^2\left(-\frac{1}{\rho_F}\right)P + \frac{1}{\rho_F v_F^2}\frac{\partial^2 P}{\partial t^2} = G, \tag{4.3}$$

where P is the transient pressure, ρ_F is the fluid density, v_F is the speed of signal in the fluid medium, and G is the source of AE signal in time domain.

Eq. (4.3) is used throughout the analysis for the low frequency AE signal propagation in the fluid inside the pipe.

In case of elastic pipe, there is an interaction between the fluid pressure, the pipe and the surrounding medium, which causes tube wave effect on the original acoustical signal. In this work, Eqs. (3.19) and (3.23) are used to calculate the displacement effect in the pipe structure due to the acoustic pressure and Eqs. (3.25) and (3.27) are used to calculate the acoustic pressure variation in the fluid column due to the traction forces on the pipe wall.

4.5 Solution Methodology

In this chapter, the numerical problem is solved for the acoustic pressure (P) distribution of AE signals through fluid-column only. During the solution, the fluid-structure and the structure-fluid and -outer medium coupling equations are used to simulate the effects of the surrounding medium into the acoustic pressure of the fluid.

This section contains a general description of the numerical implementation steps, which are required for the simulation of any type of fluid-filled elastic pipe (PCCP) model. Section 4.6 describes the specific model with necessary requirements.

4.5.1 Model Description

Consider a uniform and smooth circular shape pipe structure surrounded by a soil formation and aligned along the x-direction. The base dimensions and the cross-sectional view of the model geometry are shown in Fig. (4.1).

For simplicity, consider a pipe structure which consists of high-strength concrete only and does not account for fluid flow velocity. The simplification does not significantly impact the results of the analysis, but does result in a significant reduction in the computational resources [9]. Damping is absent in all media. The physical properties of the fluid (water) and surrounding solid materials are given in Table (4.1).

4.5.2 Boundary Conditions

The boundary conditions that are applied to this model are as follows:

- continuity of pressure in the fluid to pipe structure,

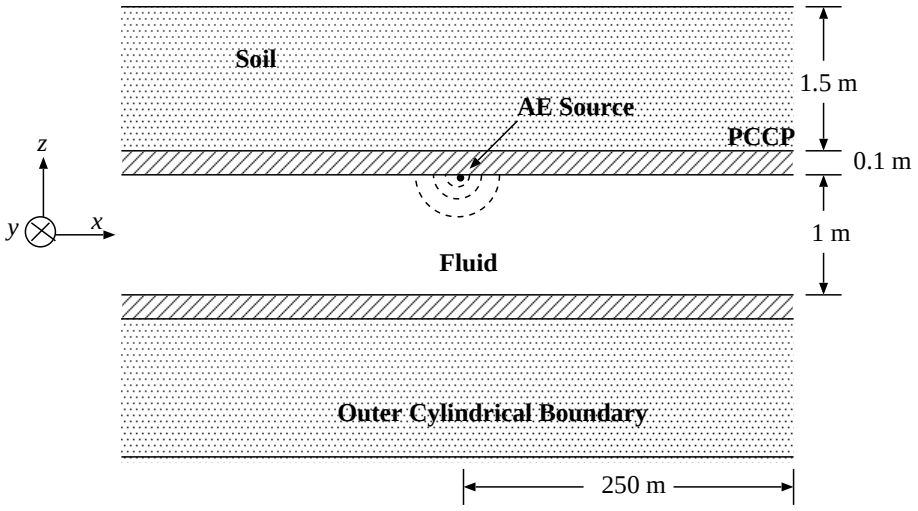

Figure 4.1: Cross-sectional view of model geometry with dimensions.

Table 4.1: Properties of the medium.

Properties	Fluid (Water)	Concrete	Soil
Density of medium (ρ), $\mathrm{kg\,m^{-3}}$	997	2400	1270
Speed of acoustic wave (v), $\mathrm{m\,s^{-1}}$	1500	–	463
Elastic (Young's) modulus (E), Pa	–	40^9	–
Poisson's ratio (ν)	–	0.33	–

- continuity of acceleration in the pipe to fluid/soil medium, and
- radiation condition in the outer model boundary.

The acoustic pressure (in the fluid domain) of AE signal acts as a boundary load on the 3D solid pipe structure to ensure the continuity of pressure. Mathematically this boundary condition can be expressed as [107]

$$\mathbf{F}^P = \mathbf{n}P. \tag{4.4}$$

This boundary load acts as an external force on the fluid-pipe surface which causes consistent displacements and deformations inside the pipe structure. According to the principle of virtual work (see Appendix-A), the total work from stress-strains of the structure is equal

to the work from the external forces. To satisfy the Newton's second law of motion, these stresses and strains are calculated using the normal acceleration of the pipe surface at the fluid boundary which ensures the continuity of acceleration.

The mathematical expression for the acceleration is

$$\mathbf{F}^T = -\mathbf{n}\nabla\mathbf{u}^{'}. \tag{4.5}$$

Finally, the radiation boundary condition is used on the outer perimeter of the model. For the outward traveling wave, this boundary condition provides minimal or no reflections from the model boundary.

Along the pipe axis, the radiation boundary condition is used with the plane wave propagation as [126]

$$\mathbf{n} \cdot \left(\frac{1}{\rho}\nabla P\right) + \frac{1}{\rho v}P + \frac{\partial P}{\partial t} = 0. \tag{4.6}$$

At the outer cylindrical surface, the radiation condition with the cylindrical wave propagation is used as [127]

$$\mathbf{n} \cdot \left(\frac{1}{\rho}\nabla P\right) + \frac{1}{\rho}\left(\frac{1}{v}\frac{\partial P}{\partial t} + \frac{1}{2r}P\right) = 0, \tag{4.7}$$

where r is the shortest distance between the sources to the point of interest.

4.5.3 Model Discretization

For the numerical solution, it is necessary to discretize the model into small segments with a fixed wavelength that must be resolved. In addition, small features in the geometry and/or near the interface boundary or source vicinity model have high local pressure gradients that must be resolved appropriately to obtain a consistent global solution.

The FEM based analysis is used to handle this mathematical integrity and coupling equation between different physical layers. The commercial FEM based software COMSOL Multiphysics is used to handle these complex issues. This software can handle the coupling effect of acoustic pressure from the fluid to the structure and the displacement from the structure to the fluid and the outer medium, efficiently. In this particular model, the second

order polynomial basis functions are used to derive the discretized model. The maximum element size of $0.2\,\lambda$ (where wavelength $\lambda = v/f$) is used with the second-order element to satisfy the rule-of-thumb minimum of ten degrees of freedom per wavelength for a reliable solution [107].

4.6 Results and Discussion

The transient analysis of mathematical model outlined above is applied in two scenarios, namely water-filled elastic pipe in the air and in the soil media. During the simulation, different dimensions and stiffness of the layered media were investigated. This illustrates the effect of pipe profiling on the tube mode propagation of AE signal through water-filled elastic pipe (PCCP). All simulations are done for the 0.2 kHz excitation frequency as this frequency is below the first cut-off frequency of the pipe used here and wavelength greater than the diameter of the pipe for tube wave analysis [36]. The constant volume velocity source [95] is used with the source flow strength 10^{-2} $\mathrm{m^3\,s^{-1}}$, to optimize the result. In order to verify the simulation results with the calculated theoretical values from Eq. (4.1), the time response of the system is taken at selected points in the pipe (at 0 m, 25 m, 50 m, 75 m, 100 m, 125 m, 150 m, 175 m, 200 m from source).

4.6.1 Effect of Pipe Elasticity

In this case we considered the water-filled elastic pipe in the air medium. The pipe with radius $R = 0.5$ m and thickness $t_p = 0.1$ m is used for this purpose. The elastic (Young's) modulus (E_p) of the pipe materials varies as 20 GPa, 30 GPa and 40 GPa with densities (ρ_p), $2200\,\mathrm{kg\,m^{-3}}$, $2300\,\mathrm{kg\,m^{-3}}$ and $2400\,\mathrm{kg\,m^{-3}}$, respectively. Other properties of the pipe and the fluid are kept constant as in Table (4.1).

From the Fig. (4.2) it is seen that, the calculated theoretical tube wave velocities which is given below in each graph, is matched with the wave speed as seen in the simulation results. As for example in Fig. (4.2)(a), the calculated v_T is $985\,\mathrm{m\,s^{-1}}$, therefore, the time required to travel the AE signal from the source to 50 m distance is 0.051 sec, which is same as seen

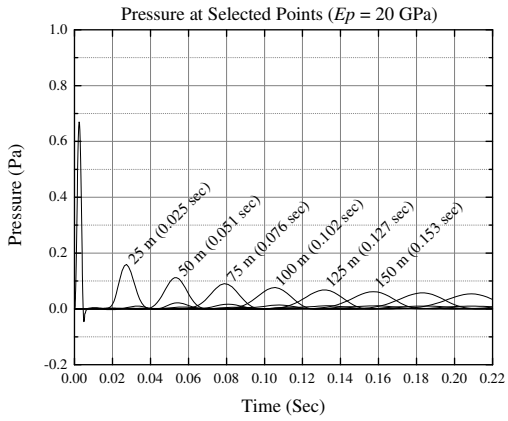

(a) $E_p = 20\,\mathrm{GPa}$ (Analytical $v_T = 985.12\,\mathrm{m\,s^{-1}}$).

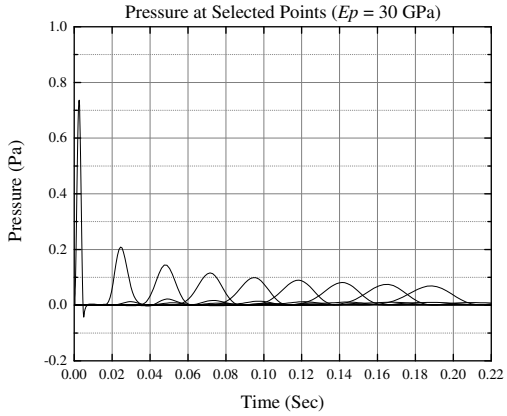

(b) $E_p = 30\,\mathrm{GPa}$ (Analytical $v_T = 1094.72\,\mathrm{m\,s^{-1}}$).

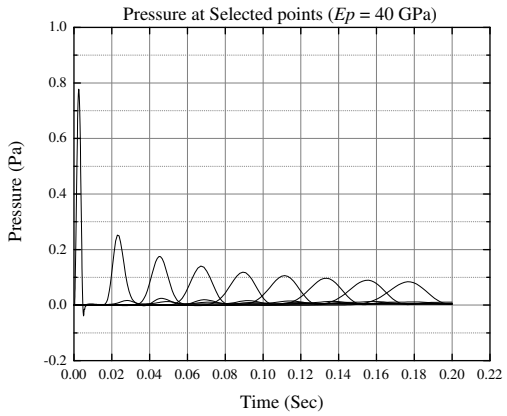

(c) $E_p = 40\,\mathrm{GPa}$ (Analytical $v_T = 1164.30\,\mathrm{m\,s^{-1}}$).

Figure 4.2: Tube wave response of water-filled elastic pipe at (a) $E_p = 20\,\mathrm{GPa}$, (b) $E_p = 30\,\mathrm{GPa}$, and (c) $E_p = 40\,\mathrm{GPa}$.

in the graph. Similarly, we can verify the simulation results for other distances.

From the results shown in Fig. (4.2) we can also observe that, the propagation speed is reduced to a lower speed due to the tube wave effect [36], compared to the speed of the acoustic wave in the water (approximately $1500\,\mathrm{m\,s^{-1}}$). The pipe stiffness increases with the increasing pipe elastic properties, which increases the wave's signal strength. This is the case because, the amount of signal energy penetration throughout the pipe structure decreases with the increasing pipe stiffness. Therefore, in all of the graphs above, it is clear that the AE signal propagation in water-filled elastic pipe is affected significantly by the pipe properties.

4.6.2 Effect of Pipe Dimensions

To observe the effect of pipe dimensions, the variable dimensioned water-filled elastic pipe in an air medium with fixed pipe properties ($E_p = 40\,\mathrm{GPa}$, $\rho_p = 2400\,\mathrm{kg\,m^{-3}}$) is used. In this case pipe thicknesses of $t_p = 0.1\,\mathrm{m}$, $0.15\,\mathrm{m}$ and $0.2\,\mathrm{m}$ with a fixed pipe radius ($R = 0.5\,\mathrm{m}$) is used. Next the pipe radius is varied as ($R = 0.5\,\mathrm{m}$, $1.0\,\mathrm{m}$ and $1.5\,\mathrm{m}$) with a fixed pipe thickness of $t_p = 0.1\,\mathrm{m}$. The other properties of the pipe and the fluid medium are taken from Table (4.1). The results for the $R = 0.5\,\mathrm{m}$ and $t_p = 0.1\,\mathrm{m}$ pipe are same as the results shown in Fig. (4.2)(c) and for other dimensions results are shown in Fig. (4.3) and (4.4), respectively.

From the graphs it is seen that, the simulation results of wave speed are in agreement with the theoretical calculated value given below in each graph. Moreover, from Fig. (4.2)(c) and (4.3) it is seen that increasing the pipe thickness increases the stiffness, which increases the tube wave speed. On the contrary in Fig. (4.2)(c) and (4.4), increasing the pipe radius decreases the system stiffness, which decreases the tube wave speed. In both cases, the signal strength decreases with the decreasing pipe stiffness. The important conclusion from this section is that the AE signal propagation in the water-filled elastic pipe is affected by the pipe dimensions.

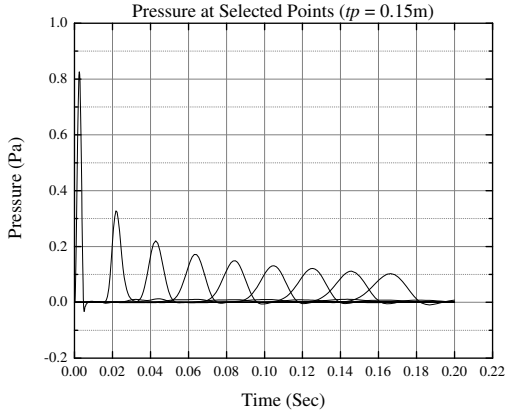

(a) $R = 0.5\,\mathrm{m}$, $t_p = 0.15\,\mathrm{m}$ (Analytical $v_T = 1235.39\,\mathrm{m\,s^{-1}}$).

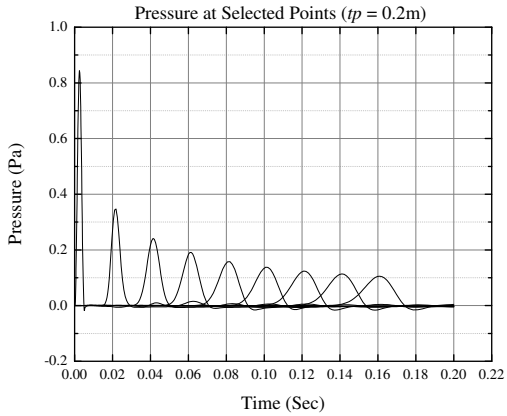

(b) $R = 0.5\,\mathrm{m}$, $t_p = 0.2\,\mathrm{m}$ (Analytical $v_T = 1275.58\,\mathrm{m\,s^{-1}}$).

Figure 4.3: Tube wave response of water-filled elastic pipe at (a) $t_p = 0.15\,\mathrm{m}$, (b) $t_p = 0.2\,\mathrm{m}$.

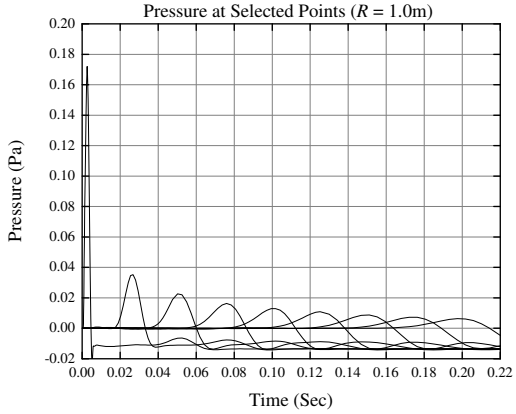

(a) $R = 1.0\,\mathrm{m}$, $t_p = 0.1\,\mathrm{m}$ (Analytical $v_T = 1007.35\,\mathrm{m\,s^{-1}}$).

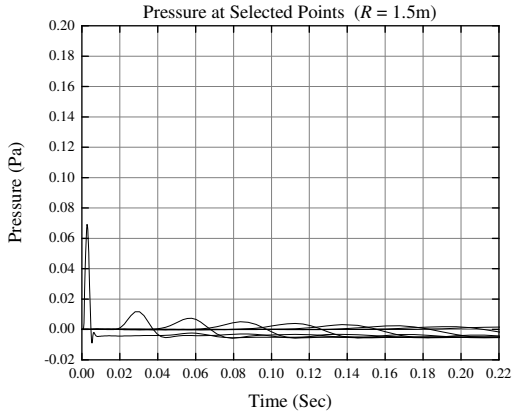

(b) $R = 1.5\,\mathrm{m}$, $t_p = 0.1\,\mathrm{m}$ (Analytical $v_T = 900.15\,\mathrm{m\,s^{-1}}$).

Figure 4.4: Tube wave response of water-filled elastic pipe at (a) $R = 1.0\,\mathrm{m}$, (b) $R = 1.5\,\mathrm{m}$.

4.6.3 Effect of Soil Medium

Next, the effect of surrounding soil formation on the water-filled elastic pipes is explored. The thickness of the cylindrical soil layer (t_s) is taken as three times the pipe radius to optimize the results. All other variables, such as, pipe dimensions (e.g. $R = 0.5\,\mathrm{m}$, $t_p = 0.1\,\mathrm{m}$), pipe properties (e.g. $E_p = 40\,\mathrm{GPa}$, $\rho_p = 2400\,\mathrm{kg\,m^{-3}}$), fluid properties (Table (4.1)) are kept as constants.

Table 4.2: Properties of the soil sample.

Soil Sample	**Soil Series (Code)**	**Density (ρ_s), $\mathbf{kg\,m^{-3}}$**	**Propagation Speed (v), $\mathbf{m\,s^{-1}}$**
Sandy Loam	Adrian (ADA)	920	373
Silt Loam	Catlin (CAB)	1270	463
Sand	Plainfield (PLA)	1510	634

Unlike the case of fluid or pipe material properties, the selection of soil properties cannot be known with same accuracy due to numerous uncertainties. The soil properties vary according to the type and the depth of the pipe. However, in this work the focus is the extent to which soil properties affect the AE signal propagation in the water-filled elastic pipes (PCCPs). Therefore, we choose three kinds of soil sample from the soil textural triangle [128], such as, Sandy Loam (Adrian soil), Silt Loam (Catlin soil) and Sand (Plainfield soil), to cover the wide range of soil elastic properties (Table (4.2) [129]).

Figures (4.5)(a), (b), and (c) show the simulation results of the AE signal propagation through the elastic pipe, which is surrounded by the Adrian, Catlin and Plainfield soil, respectively. By comparing these results with the theoretical tube wave velocities (v_T) which is given below each graph, found a good agreement. However, if we compare these results with the result of the same pipe in the air medium (Fig. (4.2)(c)), we can see that the tube wave velocities are nearly the same in all cases. This means that, the surrounding soil formation does not have any significant effect on the tube wave propagation. This is believed to arise from the fact that the stiffness of the soil medium is only one thousandth of stiffness of the PCCP. Therefore, from the graphs above, it is clear that the AE signal propagation

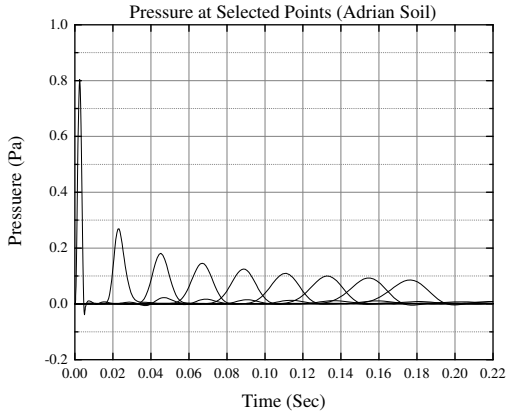

(a) Adrian soil (Analytical $v_T = 1169\,\mathrm{m\,s^{-1}}$).

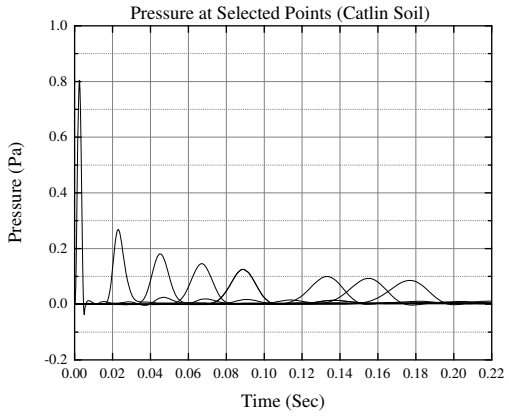

(b) Catlin soil (Analytical $v_T = 1170\,\mathrm{m\,s^{-1}}$).

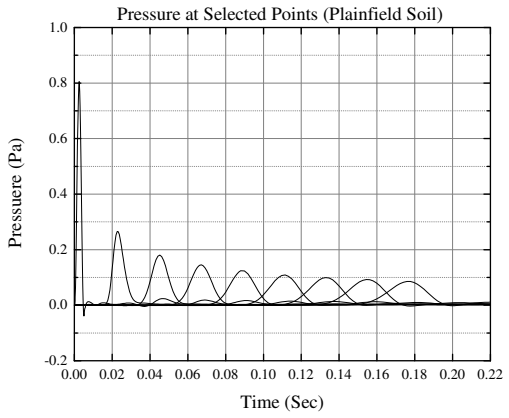

(c) Plainfield soil (Analytical $v_T = 1170\,\mathrm{m\,s^{-1}}$).

Figure 4.5: Tube wave response of water-filled elastic pipe at (a) Adrian soil, (b) Catlin soil, and (c) Plainfield soil.

in the water-filled elastic pipe (PCCP) is not affected by the surrounding soil medium.

4.6.4 Effect of Guided Path

The other effects observed in the simulation results can be explained by the effect of guided path as follows. In the model, a long circular shaped pipe is used, which acts as a cylindrical wave guide for the AE signal propagation. The excitation frequency is 200 Hz, which is below the first cut-off frequency of the pipe. Therefore, from the simulation results (Figs. (4.2), (4.3), (4.4) and (4.5)) it is observed that, there is only 'zero' order mode propagation exists in the pipe. During the propagation, the initial pulse is extended due to the dispersion of the wave's high frequency components. The signal level in the graphs decreases rapidly with the distance the wave has traveled from the source. Initially, this signal travels at a very high speed, because close to its source, it travels as a spherical wave. Later on, when the wave extends over the entire cross-sectional area of the pipe, it travels as a planar wave with the expected speed of the main signal. Therefore, the size and the shape of the path also effects the AE signal propagation.

4.7 Summary

The impact of the path on the low frequency AE signal propagation is illustrated. The tube wave effects were observed under plane-wave propagation and verified with the calculated theoretical values. The effect of surrounding formation on the acoustic signal in the fluid medium are observed for different types of soil. The simulation results are verified with the theoretical values.

The theoretical studies presented in this chapter can produce the fundamental concepts of low profile acoustic signal in the AE monitoring system.

Chapter 5

Eigenfrequency Analysis

5.1 Introduction

In industrial applications, the acoustic signals are generated through the breakage or sliding of steel wires that are prestressed to structurally enforce the pipes. These signals feature certain frequency spectral characteristics that are close to the eigenfrequency of the piping system. Through eigenfrequency analysis, many important mathematic features of such propagation can be revealed to help understand and interpret the AE testing data. The frequency domain numerical analysis of the acoustical model is carried out to determine the eigenfrequency, modes of propagation, cut-off frequency, and phase speed of acoustic wave in elastic pipes with a range of radii, stiffness and thickness of pipe and surrounding medium.

This chapter presents the numerical investigation of this problem. The significance of this analysis is described in Section 5.2. Insightful observations for eigenfrequencies and modes of propagation of the AE signal are observed using eigenfrequency and modal analysis. In Section 5.3, both the analytical and the simulation model for eigen and modal problems are presented for this purpose. The boundary conditions and the numerical study of the problem are given in Section 5.4 and 5.5, respectively. In Section 5.6, the numerical results are presented and compared with the analytical solutions. Finally, the summary of this Chapter is described in Section 5.7.

5.2 Significance of Eigenfrequency Analysis

The eigenfrequency analysis of piping system is used in thermodynamic or chemical engineering processes for many years, which are generally subjected to static or time dependent variable loads. In time dependent cases, these loads generate acoustic sources which may lead to excessive noise level in the piping system. Many researches [130]- [142] were performed on this matter for its technological importance and the performance degradation of the piping system. The eigenfrequency analysis also used in the design of Tunable Vibration Absorber (TVA) [143]- [152], which is important for noise reduction in HVAC system, aero-elastic wind tunnel investigations and turboprop noise spectra reduction in aircraft.

In the PCCP, the acoustic signals are generated through the breakage or sliding of reinforced wires. These signals feature certain frequency spectral characteristics that are close to the eigenfrequency of the piping system. This signal degrades the performance of the condition monitoring of piping system. As far as our knowledge, there is no systematic theoretical analysis on this problem in the open literature. In this chapter, the eigenfrequency analysis of these events is taken as a principal interest.

In the work, eigenfrequency analysis is used to identify the system's resonance frequencies and its effect on the acoustic signal. From the analysis, it is also possible to obtain waveguide properties for various radius, stiffness and thickness of the pipe immersed in different medium, where analytical solutions might not be known. In addition, the modal analysis is performed to identify the systems dynamic characteristics, such as, cut-off frequency, propagation constant and the number of propagating modes.

In the pipeline, the guided waves propagate with very complicated wave structures due to a mixture of multi-modes and mode conversion, which prevents guided waves from being widely used. Modal analysis and simulation of guided wave propagation are very useful for solving these problems. The use of guided waves in NDT of piping system is an attractive and widely used technique [153]- [157]. In piping system, the scope of this analysis includes the evaluation of dispersion behaviour of guided waves in hollow or liquid-filled cylinders. In long-range inspection of pipes, this guided waves largely reduces inspection time and costs

compared to the ordinary point by point testing in large pipelines [158]- [162].

5.3 Eigenfrequency and Modal Analysis

The eigenfrequencies of any mechanical system have many interesting mathematical properties and direct physical significance on the system's resonance frequencies. Each eigenfrequency represents the system's natural frequency of vibration at which the system absorbs more energy than other frequencies. At these frequencies, small or even zero driving forces can produce large amplitude vibrations, because of the stored vibrational energy. Therefore, in NDT where the measured acoustic signal is analyzed, it is important to know the eigenfrequencies of the system, since, they can change the characteristics of the propagating signal. Prior knowledge of these frequencies is therefore important to identify the actual acoustic signal.

The acoustic signals generated in the PCCP have different frequency spectra, which consist of low to high frequency signals [76,77]. These signals propagate through the fluid column inside the pipe as a guided wave. This propagation deteriorates when it passes through a number of media, such as, fluid, pipe and surrounding medium. At the beginning, this wave propagates as a spherical wave, after few moments when the wave dominates all the cross-section of the pipe it propagates with very complicated wave structures due to the mixture of multi-modes and mode conversion. At low frequencies, the wave propagates as an evanescent mode with plane wavefront. These waves can not propagate for long distances, where both pipe structure and fluid dissipates its energy due to very low viscosities and material damping [163]. At high frequencies, it has also propagating mode which exhibits oscillatory amplitude in the fluid and a decaying amplitude in the pipe structure, and propagates a far distance. The number of propagating modes grows proportional to the signal frequency. Consequently, more modes cause complicated dispersion characteristics. In elastic pipe, such waves have strong dispersive phenomena [142]; as a result, there exist several wave modes in the same propagating signal. Therefore, the modal analysis is important to determine the dynamic characteristics of the system.

5.3.1 Eigenfrequency Analysis

In the eigenfrequencies analysis, the frequency domain homogenous acoustic pressure equation is used for the numerical simulation. The homogeneous equation developed in Chapter 3 is in time domain. In frequency domain, using the time harmonic pressure Eq. (3.16) into Eq. (3.9), the homogeneous acoustic pressure equation can be obtained as

$$\nabla^2 \left(-\frac{1}{\rho_F}\right) p - \frac{\omega^2 p}{\rho_F v_F^2} = 0. \tag{5.1}$$

where p is the time harmonic pressure, ρ_F is the fluid density, v_F is the speed of signal in the fluid medium, $\omega\,(= 2\pi f)$ is the angular frequency, f is the frequency of the propagating signal.

Eq. (5.1) is used for the numerical analysis of eigenfrequencies of the AE signal propagation in the fluid inside the pipe.

For the elastic pipe this propagation is affected by the pipe and surrounding medium characteristics. Eq. (3.20) and (3.24) are used to consider the fluid to structure effect and Eq. (3.26) and (3.28) are used to consider the structure to fluid and outer medium effects in the simulation.

Eq. (5.1) shows that, the solution becomes zero except at a discrete set of eigenfrequencies with a well-defined shape of undefined magnitude.

Theoretically, the eigenfrequency of a cylindrical pipe depends on the pipe length, end condition (e.g. open or close) and speed of acoustic wave inside the pipe. The eigenfrequency equation of an open ended hollow and rigid cylindrical pipe can be expressed as [164]

$$f_e = \frac{mv}{2l}, \tag{5.2}$$

where m is the positive integer $(1, 2, 3, \cdots)$ representing the eigenmodes, v is the velocity of acoustic wave inside the pipe medium, l is the length of the pipe.

5.3.2 Modal Analysis

Let us assume that the acoustic pressure varies harmonically in longitudinal direction (say z) as shown in Fig. (5.1). Therefore, the modal description can be obtained from Eq. (3.18)

by replacing the pressure as

$$p(\mathbf{x}) = p(x, y)\, e^{-ik_z z}, \tag{5.3}$$

where k_z represents the longitudinal wave number in z direction.

Substituting Eq. (5.3) into Eq. (3.18) and eliminating all the z dependence, we have

$$\nabla^2 \left(-\frac{1}{\rho_F}\right) p - \left(\frac{\omega^2}{v_F^2} - k_z^2\right) \frac{p}{\rho_F} = g. \tag{5.4}$$

By solving Eq. (5.4) at a given frequency with a nonzero excitation, one can obtain the most axial wave numbers. These values are the propagation constants of evanescent (stoneley) or propagating (rayleigh) waveguide modes.

The frequency related to each mode is the modal or cut-off frequency of the guided path. It is the critical frequency between propagation and attenuation, which can be obtained as [165]

$$f_c = \frac{1}{2\pi} \left[\omega^2 - k_z^2 v_F^2\right]^{1/2}. \tag{5.5}$$

Theoretically, the modal frequency of fluid-filled cylindrical pipe with infinite stiffness surface can be calculated as [166]

$$f_c = \frac{v_F z_{mn}}{2\pi r} \quad \text{with} \quad J_m^{'}(z_{mn}) = 0, \tag{5.6}$$

where r is the radius of the pipe, z_{mn} is the n-th root of the first derivative of Bessel function $J_m^{'}$.

5.4 Boundary Conditions

A set of boundary conditions are used to reflect the physics properly at the interface between different layers of modeling domain and the boundaries.

5.4.1 Rigid Pipe with Infinite Stiffness

If we consider a fluid-filled rigid pipe with infinite stiffness, a Neumann (sound hard) boundary condition is required at the fluid-pipe interface. It represents a vanishing normal com-

ponent of the particle velocity at the boundary. For cylindrical pipe, this leads to [165]

$$\mathbf{n} \cdot \phi = 0 \;\; \Rightarrow \frac{\partial \phi}{\partial n} = \phi_r = 0, \tag{5.7}$$

at $r = R$ for every ϕ and z, which satisfies

$$J_m^{'}(k_{mn}R) = 0, \tag{5.8}$$

here ϕ_r is the radial component of velocity potential, R is the inner radius of the pipe, $k_{mn}R$ is the roots of the first derivative of Bessel function $J_m^{'}$, k_{mn} is the rigid pipe wave number of the m-th order wave and the n-th order Bessel function.

In the acoustic pressure model, this boundary condition can be written as [107]

$$\mathbf{n} \cdot \nabla \left(\frac{1}{\rho_F} \right) p = 0. \tag{5.9}$$

5.4.2 Elastic Pipe with Finite Stiffness

In case of elastic pipe with finite stiffness there would be an interaction between the fluid pressure and the pipe structure. As a result, the elastic wave that generated in the structure due to the acoustic signal transmits into the fluid during the wave propagation. Necessary boundary conditions are required to represent this interaction.

In the model, the continuity of pressure from the fluid to the pipe and the continuity of stresses from the pipe to the fluid are imposed. It should be noted that similar boundary conditions are also applied at the outer pipe surface when it interacts with the surrounding formation.

In the formulation, the boundary condition of continuity of pressure represented as body forces

$$\mathbf{F}^P = \mathbf{n}p. \tag{5.10}$$

This body forces causes consistent displacement and deformations inside the pipe structure. As per Newton's second law, this causes opposite, but the same amount of traction forces on the acoustic pressure. Therefore, the boundary condition of continuity of stresses represented as traction forces

$$\mathbf{F}^T = \mathbf{n}\omega^2 \nabla \mathbf{u}. \tag{5.11}$$

5.4.3 Radiation Boundary Conditions

For the outward traveling wave, the radiation boundary conditions are used on the outer perimeter of the solution domain, which provides minimal or no-reflection from the boundary.

Along the pipe axis, the plane wave radiation boundary condition is used. In time harmonic case, it can be written as [126]

$$\mathbf{n} \cdot \left(\frac{1}{\rho}\nabla p\right) + i\frac{k}{\rho}p + i\frac{\triangle_T}{2k}p = 0, \tag{5.12}$$

where $\triangle_T$ represents the Laplace operator in the tangent plane at a particular point on the boundary and $k = \frac{\omega}{v}$ is the wave number and v is the acoustic wave velocity in the medium.

At the outer cylindrical surface, the cylindrical wave radiation condition is used. In time-harmonic mode, it can be expressed as [127]

$$\mathbf{n} \cdot \left(\frac{1}{\rho}\nabla p\right) + \frac{1}{8r}\left(\frac{3 + 12ikr - 8k^2r^2}{1 + ikr}\right)\frac{p}{\rho} + \frac{r\triangle_T p}{2(1 + ikr)\rho} = 0, \tag{5.13}$$

where r is the shortest distance between source to the point of interest.

5.5 Numerical Study

Let us consider a uniform and smooth fluid-filled PCCP surrounded by a cylindrical formation and aligned along the z-direction. Typical dimensions and orientation of one pipe section (approx. 3 m long) is shown in Fig. (5.1).

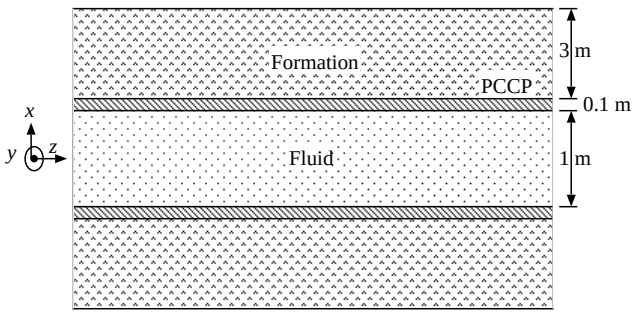

Figure 5.1: Typical model geometry with dimensions.

To optimize the computational burden with minimum boundary reflection, the dimensions and boundary conditions of solution domain are considered carefully. For simplicity, assume the pipe structure to consists of high-strength concrete only and is filled with static fluid (water). Damping is absent in all medium. In comparison with computational brevity, this simplification does not give any significant effect on the final results [9].

5.5.1 Finite Element Analysis

The commercial finite element code (COMSOL Multiphysics) is used to handle the generic 3D geometry, mathematical integrity and coupling equation between different physical layers. For the numerical computation, the model is discretized into small segment using Femlab's mesh generator. The second order polynomial basis functions are used to solve the model. The maximum element size 0.2λ (wavelength $\lambda = v/f$) is used with the second-order element to satisfy the rule-of-thumb minimum of ten degrees of freedom per wavelength for the reliable solution [107]. The longitudinal cross-sectional view of the meshed model geometry of Fig. 5.1 at 1.2 kHz frequency is shown in Fig. (5.2). The mesh consists of 826,711 tetrahedral elements and 143,709 vertices.

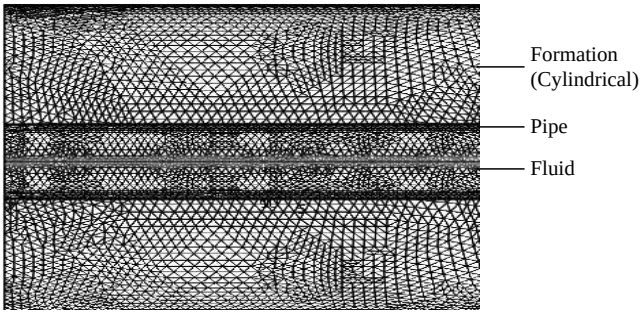

Figure 5.2: Meshed geometry for finite element analysis.

5.6 Results and Discussion

The results obtained from the rigid and elastic pipe with infinite and finite stiffness, respectively for various dimensions of the pipe and medium characteristics are presented. For the

rigid pipe the simulated results are compared with the analytical solutions using Eqs. (5.2) and (5.6). Similar analysis is also performed for elastic pipes, where analytical solutions are unknown. However, the simulated results are analyzed and validated as per theoretical and physical concept. In both cases, the phase velocity of plane wavefront inside the pipe is compared using tube wave analysis (refer Chapter 4).

The following values of the parameters have been used for the numerical study: density of fluid (water), air, concrete and soil are $997\,\mathrm{kg\,m^{-3}}$, $1.25\,\mathrm{kg\,m^{-3}}$, $2400\,\mathrm{kg\,m^{-3}}$, and $1270\,\mathrm{kg\,m^{-3}}$, respectively; acoustic wave speed in unbounded water, air and soil medium are $1500\,\mathrm{m\,s^{-1}}$, $343\,\mathrm{m\,s^{-1}}$ and $463\,\mathrm{m\,s^{-1}}$, respectively; poisson's ratio of concrete is 0.33.

Other parameters that varied during the simulation are: inner radius, $R = 0.5\,\mathrm{m}$ (default), $0.7\,\mathrm{m}$, $1.0\,\mathrm{m}$; pipe thickness, $t_c = 0.1\,\mathrm{m}$ (default), $0.15\,\mathrm{m}$, $0.2\,\mathrm{m}$; young's modulus of elasticity of concrete, $E = 20\,\mathrm{GPa}$, $30\,\mathrm{GPa}$, $40\,\mathrm{GPa}$ (default); outer formation, air, water, soil.

To avoid the computational burden, the solutions up to $6\,\mathrm{kHz}$ for cut-off frequency and up to $1.2\,\mathrm{kHz}$ for eigenfrequency were evaluated. These frequencies are sufficient to get the reasonable results for the analyses of the system presented in this study.

5.6.1 Rigid Pipe Solution

The numerical results of cut-off frequency obtained from analytical and simulated solutions are shown in Table (5.1). The modal analysis is used to obtain these simulated cut-off frequency of various radii rigid pipe. From the results it is seen that, increasing the inner radius reduces the cut-off frequency of rayleigh modes, which also satisfies the analytical solution. In this work, the analysis is computed up to 10-th mode of propagation and found only 0.2 to 0.5 % variations in the simulated results when compared to analytical solutions. And hence, the numerical solutions provide acceptable results to a reasonable level of accuracy.

The results easily identify the various propagating modes, their excitation frequency as well as the impact of the pipe radius. It is seen that, the number of propagating modes decreases with decreasing pipe radius, and vice versa. This signifies that, in the lower

Table 5.1: Analytical and simulated results of cut-off frequency of the rigid pipe.

Mode of Propaga. (m,n)	Analytical, f_c (Hz)	Simulated, f_c (Hz)	Analytical, f_c (Hz)	Simulated, f_c (Hz)	Analytical, f_c (Hz)	Simulated, f_c (Hz)
	R = 0.5 m		R = 0.7 m		R = 1.0 m	
0,0	0.00	0.00	0.00	0.00	0.00	0.00
1,1	879.01	879.10	627.87	627.92	439.51	439.55
2,1	1458.18	1458.34	1041.56	1041.64	729.09	729.14
0,1	1829.65	1820.64	1306.55	1306.81	914.58	914.75
3,1	2005.83	2006.16	1432.74	1432.84	1002.91	1002.96
4,1	2538.68	2539.71	1813.34	1813.68	1269.34	1269.49
1,2	2545.37	2546.34	1818.12	1818.41	1272.68	1272.81
5,1	3062.94	3065.03	2187.81	2188.40	1531.47	1531.68
2,2	3201.88	3204.17	2287.06	2287.56	1600.94	1601.05
0,2	3349.89	3352.79	2392.44	2393.25	1674.71	1674.94
6,1	3581.46	3585.69	2558.19	2559.10	1790.73	1790.94
3,2	3826.88	3832.40	2733.49	2734.65	1913.44	1913.69
1,3	4075.64	4083.60	2911.17	2912.83	2037.82	2038.16
7,1	4095.22	4103.42	2925.15	2927.07	2047.61	2048.09
4,2	4431.83	4442.91	3165.59	3167.96	2215.91	2216.43
8,1	4606.10	4619.99	3290.07	3293.07	2303.05	2303.66
2,3	4760.32	4775.58	3399.89	3403.11	2379.92	2380.60
0,3	4857.73	4875.47	3469.46	3473.22	2428.62	2429.38
5,2	5022.45	5042.04	3587.47	3591.78	2511.23	2512.20
9,1	5114.13	5138.25	3652.95	3658.01	2557.06	2558.03
3,3	5416.84	5446.86	3869.17	3875.39	2708.66	2709.73
6,2	5603.00	5624.15	4001.84	4000.33	2801.29	2795.82
10,1	5627.00	5627.29	4014.12	4009.20	2809.88	2802.86

diameter pipe it is difficult to detect the low frequency acoustic signal by placing the sensors at far distance. The modal analysis is also useful to determine the modes of propagation for elastic pipe with complicated structure and medium, where direct analytical solution might not be known. This information is important for the placement of sensors in AE monitoring system to locate the corroded areas.

Figure (5.3) shows the simulation result of eigenfrequency of water-filled rigid pipe at different radii. The numerical results obtained from analytical solution (using Eq. (5.2)) and simulated solution (using eigenfrequency analysis) are shown in Table (5.2).

Table 5.2: Analytical and simulated results of eigenfrequency of the rigid pipe.

n	Analytical, f_e (Hz)	Simulated, f_e (Hz) R = 0.5 m	Simulated, f_e (Hz) R = 0.7 m	Simulated, f_e (Hz) R = 1.0 m
0	0.00	0.00	0.00	0.00
1	107.143	107.142	107.142	107.142
2	214.286	214.285	214.285	214.285
3	321.429	321.429	321.429	321.429
4	428.571	428.577	428.574	428.575
5	535.714	535.730	535.724	457.378
6	642.857	642.898	632.881	469.761
7	750.000	750.084	653.402	505.090
8	857.143	857.278	662.127	535.726
-	-	914.815	687.645	559.036
-	-	921.065	728.192	626.817
-	-	939.586	750.052	642.889
-	-	-	781.437	704.464
-	-	-	844.993	750.067
-	-	-	857.211	789.091
-	-	-	916.737	837.508
-	-	-	-	844.334
-	-	-	-	857.261
-	-	-	-	864.495
-	-	-	-	878.712
-	-	-	-	897.111
-	-	-	-	940.893
9	964.286	964.585	964.454	964.519
-	-	969.667	994.923	971.906
-	-	1010.295	1010.259	972.121
-	-	-	1060.248	994.373
-	-	-	-	1056.122
-	-	-	-	1068.059
10	1071.428	1071.900	1071.721	1071.823

From the results of Fig. (5.3) and Table (5.2), it is seen that the pipe radius does not have any influence on the eigenfrequencies of the coupled system, at least, up to the first modal cut-off frequency. The analytical value of the cut-off frequency (f_c) is given below in the caption of respective graph. The eigenfrequencies, up to the first modal cut-off point, are separated at regular intervals. This satisfies the basic physical theory expressed in Eq. (5.2).

But after the first cut-off frequency (at rayleigh modes), eigenfrequencies change very rapidly. These frequencies cannot be determined analytically, as the fundamental assumption of plane wave propagation is not valid when the rayleigh modes are cut-on. The rate of information transmission grows in proportion to the frequency of the excitation. Moreover, the higher the pipe radius, the more modes propagate (as shown in Table (5.1)) and the stronger the dispersion. The presence of additional eigenfrequencies between the higher order modes is evident in the results. The analytical method, due to its simplicity, fails to identify all possible eigenferquencies when the modes start propagating within the pipe.

The result shown in Fig. (5.3) also identifies the velocity of eigen waves, where the first eigen wave represents the phase speed of acoustic wave inside the pipe in the fluid medium. In this case it is $1500\,\mathrm{m\,s^{-1}}$, which is the same as the phase speed of water in unbounded media. This velocity is comparable with the theoretical phase velocity (v_T), obtained from the tube wave analysis. The theoretical value is given below in each graph. The results show that the velocity does not change with the pipe radius and has a good agreement with the rigid pipe criteria.

The significance of this analysis is that it can be applied to determine the phase speed of acoustic signal in elastic pipes of different profile and different surrounding medium. This knowledge is important for the AE monitoring system to localize the acoustic events. Moreover, the information about the additional vibrating signal in the elastic pipe can be obtained from this analysis, which may change the characteristics of the original AE signal. In some cases, this may lead to a false or wrong signal in the sensors. Therefore, in the pipe monitoring system, eigenfrequency analysis is important for the proper information about the recorded acoustic signal.

5.6.2 Elastic Pipe with Finite Stiffness

In this case, the water-filled concrete pipe is considered as an elastic pipe with finite stiffness. The acoustic signal propagating in the water has an interaction with the pipe structure, and vice versa. As a result, eigenfrequency, cut-off frequency, modes of propagation and phase

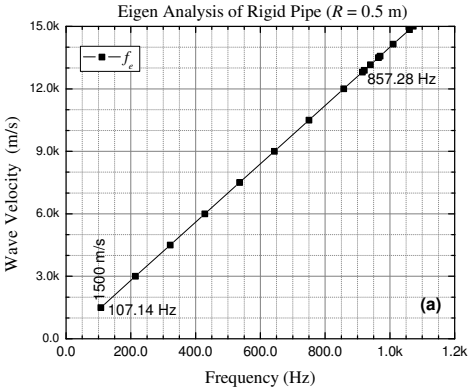

(a) Analytical f_c=879.10 Hz, v_T=1500 m s^{-1}.

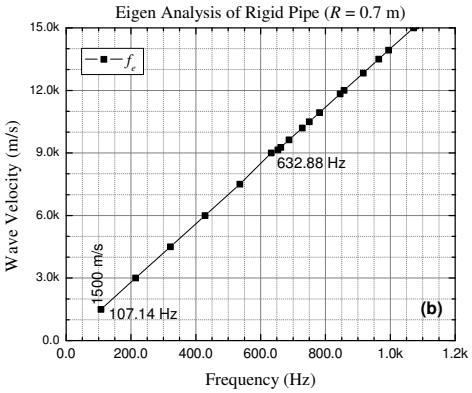

(b) Analytical f_c=627.87 Hz, v_T=1500 m s^{-1}.

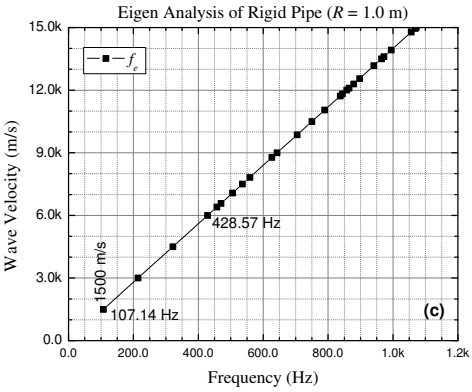

(c) Analytical f_c=439.51 Hz, v_T=1500 m s^{-1}.

Figure 5.3: Eigenfrequency of water-filled rigid pipe at (a) $R = 0.5\,\mathrm{m}$, (b) $R = 0.7\,\mathrm{m}$, and (c) $R = 1.0\,\mathrm{m}$.

speed have variable quantities based on the pipe and medium characteristics.

The eigenfrequency, cut-off frequency and phase speed of water-filled concrete pipe for different radius (R), thickness (t_c) and elastic modulus (E) of the pipe are shown in Figs. (5.4), (5.5), and (5.6), respectively. During the study, when one parameter varies, the other parameters are kept constant with their default values (as given in Section 5.6).

Figure (5.4) shows the eigenfrequency analysis of elastic pipe with finite stiffness at different radii. From the figure it is seen that, up to the first cut-off point, the eigenfrequencies are separated at regular intervals. After that, it changes very rapidly. Moreover, increasing the radius reduces the cut-off frequency of pseudo-rayleigh modes. As far as authors' knowledge, there is no analytical solution in the open literature to compare these values. However, it has a similar trend of rigid pipe as shown in Fig. (5.3) and Table (5.2). This means that, in AE monitoring system, it is possible to collect more AE events for the larger diameter pipe by placing the sensors at far distance. On the other hand, this increased radius generates additional vibrating signal which produces complicated dispersion characteristics at the receiving end (sensors). Therefore, care should be taken to indicate the active distress in the pipeline.

At low frequency stoneley mode, increasing the inner radius reduces the pipe stiffness. Consequently, both pipe structure and fluid dissipate its energy due to very low viscosities and material damping, which reduces the phase speed of the propagating acoustic signal. The phase speed of the acoustic wave inside the pipe in the fluid medium can be obtained from the velocity of the first eigen wave. The simulated result is compared with the analytical tube wave velocity (v_T), which is given below in each graph, and found a good agreement. In AE monitoring system, this phase speed is important to localize the events.

The effect of pipe thickness using eigenfrequency analysis is shown in Fig. (5.5). It is shown that if the pipe thickness increases, it increases the effective cross-sectional area of the pipe, and hence, reduces the cut-off frequency of the rayleigh modes. Consequently, it gives the same advantage of sensor placement and the disadvantage of complicated dispersion characteristics, as described earlier for Fig. (5.4).

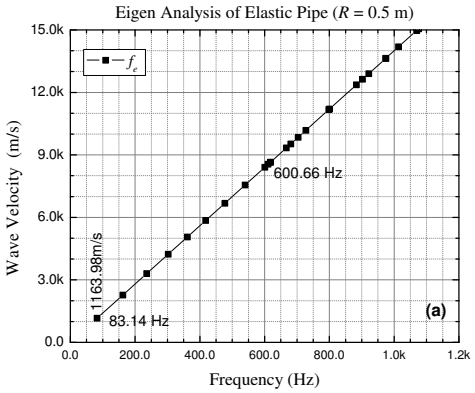

(a) Analytical v_T=1164.30 m s^{-1}.

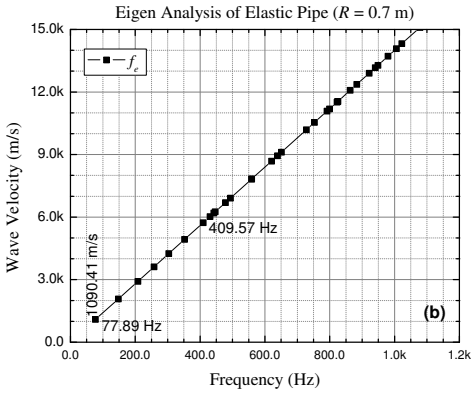

(b) Analytical v_T=1094.06 m s^{-1}.

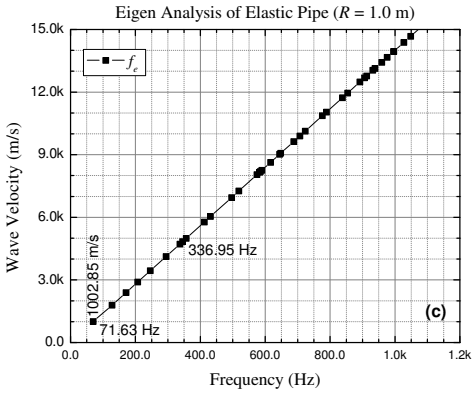

(c) Analytical v_T=1007.35 m s^{-1}.

Figure 5.4: Eigenfrequency of water-filled elastic pipe at (a) $R = 0.5\,\mathrm{m}$, (b) $R = 0.7\,\mathrm{m}$, and (c) $R = 1.0\,\mathrm{m}$.

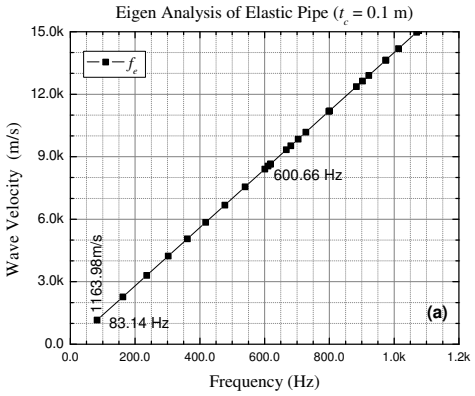

(a) Analytical v_T=1164.30 m s^{-1}.

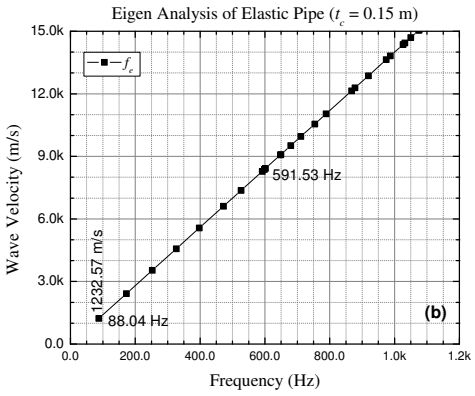

(b) Analytical v_T=1235.39 m s^{-1}.

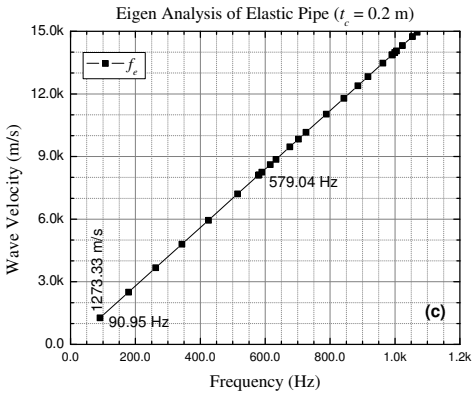

(c) Analytical v_T=1275.58 m s^{-1}.

Figure 5.5: Eigenfrequency of water-filled elastic pipe at (a) $t_c = 0.1\,\mathrm{m}$, (b) $t_c = 0.15\,\mathrm{m}$, and (c) $t_c = 0.2\,\mathrm{m}$.

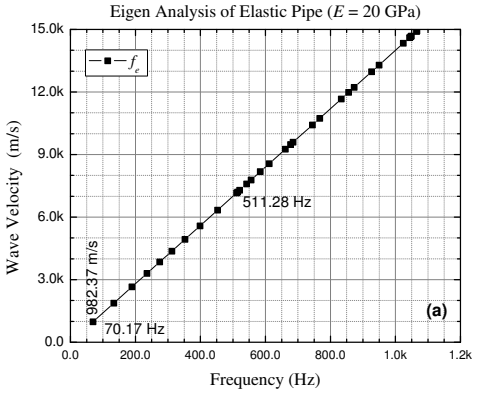

(a) Analytical v_T=985.12 m s^{-1}.

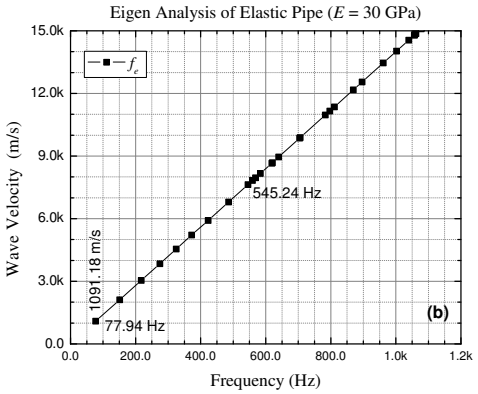

(b) Analytical v_T=1094.72 m s^{-1}.

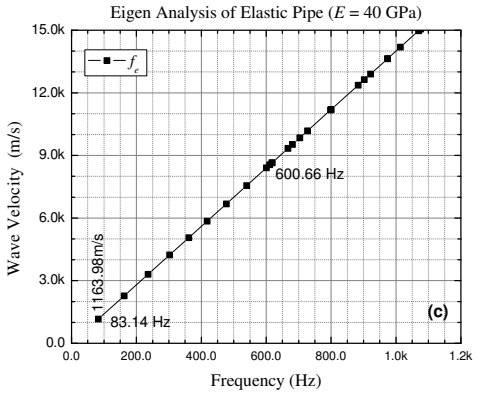

(c) Analytical v_T=1164.30 m s^{-1}.

Figure 5.6: Eigenfrequency of water-filled elastic pipe at (a) $E = 20\,\mathrm{GPa}$, (b) $E = 30\,\mathrm{GPa}$, and (c) $E = 40\,\mathrm{GPa}$.

On the other hand in stoneley mode, when the thickness increases, the stiffness of the pipe reduces and hence, lowers the material damping, which causes more energy radiation from the inside to the outside. As a result, the phase speed decreases. The phase speed obtained from the simulated result is also comparable with the theoretical tube wave velocity (v_T), which is given below in the caption of respective graph.

Figure (5.6) shows the effect of pipe elasticity on system rigidity using eigenfrequency analysis. It shows that with the increasing of the elasticity, the material damping increases. Consequently, the pipe rigidity increases, which reduces the effective cross-section of the pipe area. As a result, the cut-off frequency of the pseudo-rayleigh modes is increased. Therefore, less number of propagating mode exists in the pipe. This means that, as the strength of the pipe material increases it increases the pipe elasticity, and hence, reduces the number of propagating acoustic signal. Consequently, it reduces the effect of complicated dispersion characteristics at the receiving end.

In stoneley mode, increasing the rigidity causes increased stiffness, and hence, increases the material damping of the pipe. Therefore, less energy propagates from the acoustic signal. As a result, the phase speed is increased, which is an important parameter for event localization in AE monitoring system. This phase speed is obtained from the velocity of the first eigen wave, which matches well with the theoretical value (v_T), given below in each graph.

From the above parametric studies it is clear that, the pipe dimensions and stiffness have an effect on the acoustic signal propagation through the fluid medium. From the eigenfrequency analysis it is possible to determine the stoneley and rayleigh modes of the propagation, cut-off frequency, phase speed and dispersion behavior of different elastic pipe. This knowledge is important for AE signal detection when the pipes are buried in different medium.

5.6.3 Elastic Pipe with Outer Formation

The effect of surrounding formation on the acoustic signal propagation of the buried water-filled elastic pipe is observed in this section. These pipes are generally located below the surface ground for large-scale distribution and transmission of water and waste-water. This long pipeline may be surrounded by different kinds of soil formation when it is below the ground, or by the water or air when it is above the surface ground. In the analysis, only Catlin soil is considered as a soil formation from the soil textural triangle [128]; while fresh water and air are considered for other types of formation. The selection of these formations only focuses on the extent to which type of formation affects the acoustic signal propagation in buried water-filled PCCP.

From Fig. (5.7), it is very difficult to identify the cut-off frequency. However, it is seen that eigenfrequency and phase velocity of the acoustic signal inside the pipe changes according to the stiffness of the outer formation (medium). Higher acoustic speed of the outer formation causes a lower number of propagating modes. This fact is due to the high stiffness effect. Therefore, complicated dispersion curve is produced in the fluid when the pipe is surrounded by the soil or air compared to the water. This information has a significant importance for the AE monitoring system when the testing is under different surrounding formation.

In this case, higher phase speed of the outer formation also causes less effect on phase speed of acoustic signal inside the pipe. The effect on phase speed of the acoustic wave is shown in the simulated result, which is the velocity of the first eigen wave. This simulated phase speed is comparable with the theoretical results (v_T), which is given below in each graph, and shows a reasonable agreement. This knowledge can be implemented in the AE monitoring system.

5.7 Summary

The impacts of the rigid pipe radius on the stoneley and the rayleigh modes, and the phase speeds of the system are described. The eigenfrequency, modes of propagation, cut-off fre-

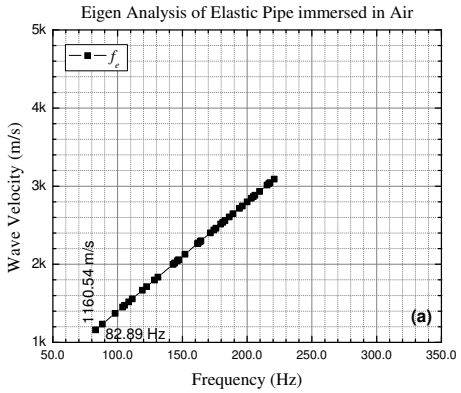

(a) Analytical v_T=1164.30 m s^{-1}.

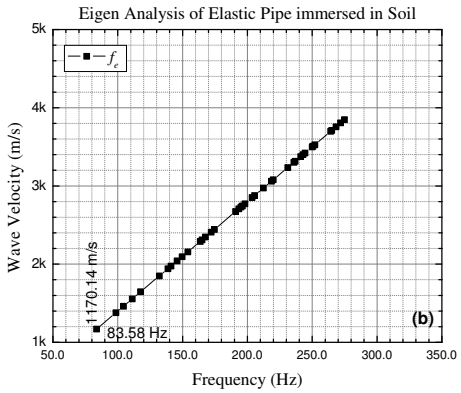

(b) Analytical v_T=1172.82 m s^{-1}.

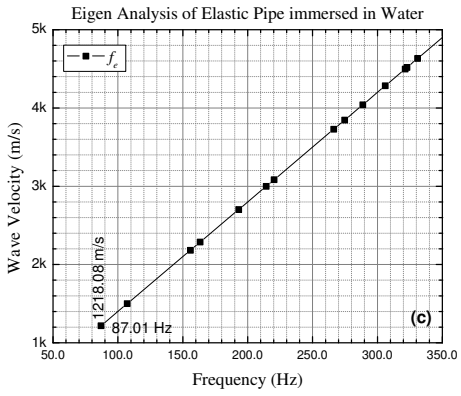

(c) Analytical v_T=1222.33 m s^{-1}.

Figure 5.7: Eigenfrequency of water-filled elastic pipe surrounded by (a) Air, (b) Soil , and (c) Water.

quency, and phase speed of acoustic wave in elastic pipes with a range of radii, stiffness and thickness of pipe and surrounding medium are observed.

It is found that, the speed of the acoustic signals propagating through pipes is not constant and is affected by the pipe profiles and the surrounding formations. The acoustic signals recorded by the sensors may have been noised by the system resonance.

These eigen wave solutions are the fundamentals for a number of more complex wave propagation studies, such as system vibration, pulse propagation and perturbation analysis. Therefore, the study produces the fundamentals on which better non-destructive pipe performance testing technologies can be designed.

Chapter 6

High Frequency Analysis

6.1 Introduction

In this study, the primary objective is to investigate the acoustical wave propagation of high frequency AE signal in the fluid-filled pipe. During the numerical simulation, sonic/ultrasonic frequencies are used as an excitation signal frequency. The time domain acoustical model is used to explore the impact of the impulse response of the pipe and the surrounding medium on the spectral profile of the high frequency excitation signal. As an excitation signal, we use a single sine pulse with different amplitude to observe the effect of AE signal's flow strength on the acoustical wave propagation.

The basic purpose of the high frequency analysis is described in Section 6.2. The time domain acoustical model which is used for numerical analysis is presented in Section 6.3. Section 6.4 described the sine wave shape of AE source model. The procedure of numerical implementation is described in Section 6.5. In Section 6.6, the numerical results are presented and discussed. Finally, the summary of this Chapter is described in Section 6.7.

6.2 Significance of High Frequency Analysis

An AE monitoring technique is a powerful method to detect dynamic deformation and fracture of materials with a high sensitivity. In recent years, the high frequency AE signal analysis has become a viable technique in the condition monitoring of many applications [167]-

[172]. This type of analysis has superior sensitivity over low frequency vibration analysis, which can provide an earlier indication of incipient faults such as frictional rubbing [173]. In the pipeline inspection, this can provide an earlier indication of wire break or slip related developing faults of the PCCP.

In convention, it is considered that the AE in the pipeline creates high-frequency mechanical wave which propagate along the pipe at high frequencies (above 100 kHz), and in the pressurizing medium inside the pipe at lower frequencies (about 30 kHz) [72]. Therefore, in current AE technology the usable frequency range of the sensor, that is used for the AE signals detection of PCCP, can go up to 40 kHz [4]. And hence, theoretical analysis and knowledge of the AE signal propagation at these excitation frequencies is important for the evaluation of wire break or slip related event.

As far as our knowledge, there is no systematic theoretical analysis of high frequency AE signal propagation through water-filled PCCP. In this work, we investigate the AE signal propagation through the fluid column inside the pipe within the range of sonic/ultrasonic frequency of 20 to 40 kHz. The time domain acoustical model with high frequency sine wave excitation signal is carried out for the numerical analysis of the rigid and the elastic pipe (PCCP) with a range of radii, thickness, and stiffness of the pipe and the surrounding soil medium.

6.3 Acoustical Model

In this study, the time domain acoustical model is used for the high frequency analysis. The inhomogeneous acoustical pressure model can be written from Eq. (3.15) as

$$\nabla^2 \left(-\frac{1}{\rho_F} \right) P + \frac{1}{\rho_F v_F^2} \frac{\partial^2 P}{\partial t^2} = G, \tag{6.1}$$

where P is the transient pressure, ρ_F is the fluid density, v_F is the speed of signal in the fluid medium, and G is the source of AE signal in time domain.

The model given in Eq. (6.1) is used for the transient analysis of high frequency AE signal propagation in the fluid inside the pipe.

As long as it is assumed that the pipe is rigid with infinite stiffness, the pressure distribution of acoustic signal in the fluid inside the pipe can be obtained by using Eq. (6.1). Instead in case of elastic pipe with finite stiffness, it is important to consider the interaction between the fluid pressure, the pipe and the surrounding medium, which results path impact on the spectral profiles of the original acoustical signal.

In this study, Eqs. (3.19) and (3.23) are used to calculate the displacement effect in the pipe structure due to the acoustic pressure and Eqs. (3.25) and (3.27) are used to calculate the acoustic pressure variation in the fluid column due to the traction forces on the pipe wall.

6.4 AE Source Model

As an excitation signal, in this work we use a single sine pulse with variable amplitude to observe the impact of AE signal's flow strength on the wave propagation. For this purpose, consider a single pulse sinusoidal wave as shown in Fig.(6.1).

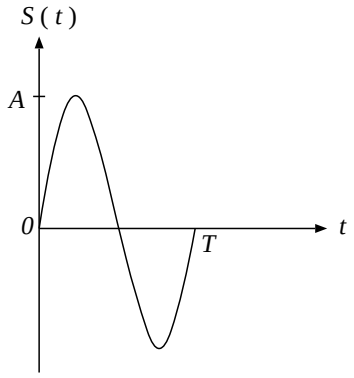

Figure 6.1: Characteristics of source signal.

Mathematically, the source flow strength S(t) of transient source model given in Eq. (3.14) can be represented as

$$S(t) = \begin{cases} A\sin(\omega t), & 0 < t < T \\ 0, & \text{otherwise} \end{cases} \tag{6.2}$$

where A is the amplitude, t is the time, T is the time period and $\omega\,(=2\pi f)$ is the angular frequency, f is the frequency of the excitation signal.

Equation (3.14) with the source pulse of Eq. (6.2) is used as a AE signal source.

6.5 Numerical Implementation

Let us consider a uniform fluid column surrounded by the smooth cylindrical layered medium. The typical dimensions and orientation of the model is shown in Fig.6.2.

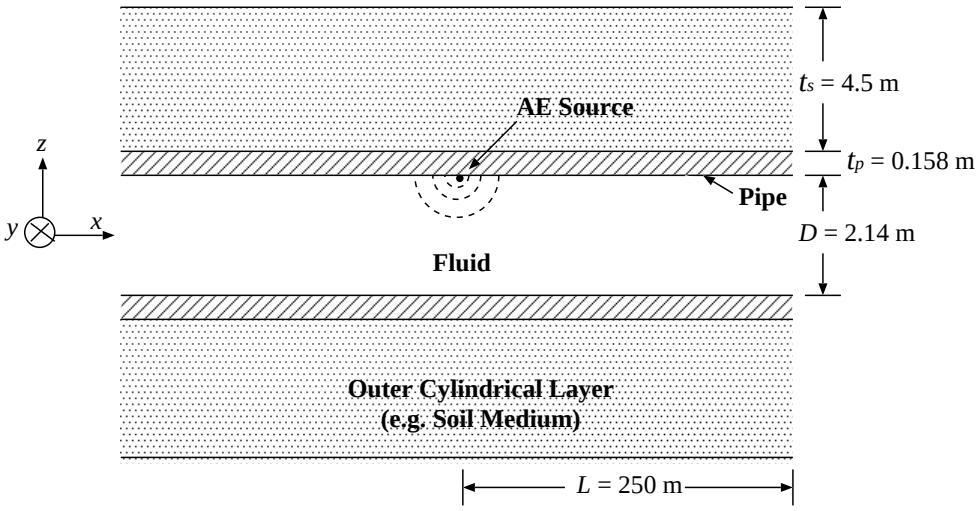

Figure 6.2: Schematic of typical model geometry and dimensions.

For simplicity, assume the pipe structure consists of high-strength concrete only, and filled with motionless fluid. This assumption does not give any significant effect on the final result [9]. For the shake of computational brevity, it is assumed that the damping is absent in all medium.

The model shown in Fig.(6.2) is solved numerically by using Eq. (6.1) for the acoustic pressure (P) distribution of AE signal through fluid-column only. The impact of the path on this propagating signal, due to the fluid-structure and the structure-fluid and -surrounding medium interaction, are considered by using coupling Equations (3.19), (3.23), (3.25) and (3.27).

6.5.1 Boundary Conditions

The boundary conditions that are applied to the model boundary are same as it is described in Chapter-4. The Eqs. (4.4) and (4.5) are used for the continuity of pressure and acceleration from the fluid to the pipe structure and from the structure to the fluid and the outer medium, respectively. The Eqs. (4.6) and (4.7) are used for the radiation boundary condition along the pipe axis and the outer cylindrical boundary, respectively.

The boundary conditions outlined above are used for elastic pipe with finite stiffness. In case of rigid pipe with infinite stiffness, the sound-hard boundary condition that is described in Eq. (5.9) is used on the fluid-pipe interface. This represents the vanishing normal component of the fluid particle velocity at this boundary. In addition, Eq. (4.6) is used along the pipe axis for the radiation boundary condition.

6.5.2 Discretization

The model is discretized into small segment using Femlab's mesh generator for the numerical simulation. The maximum element size 0.2λ (wavelength $\lambda = v/f$) is used with the second-order element to satisfy the rule-of-thumb minimum of ten degrees of freedom per wavelength for the reliable solution [107].

6.6 Results and Discussion

The numerical results of the impact of the path on the spectral profiles of the high frequency AE signal in different locations throughout the pipe have been obtained by the time domain acoustical model outlined above. The commercial finite element code COMSOL Multiphysics is used for this purpose. The model is applied in four scenarios: (i) fluid-filled rigid pipe, (ii) fluid-filled elastic pipe, (iii) fluid-filled elastic pipe surrounded by soil, and (iv) fluid-filled elastic pipe surrounded by different types of soil. In each case, different dimensions and stiffness of the layered medium are considered. This illustrates the effect of different path profile on the acoustic signal propagation.

The following values of the parameters have been used for the numerical study: density of fluid (water) (ρ_F), air (ρ_a), and pipe (concrete) structure (ρ_P) are 997 kg m^{-3}, 1.25 kg m^{-3} and 2,400 kg m^{-3}, respectively; acoustic wave speed in unbounded water (v_F), and air (v_a) medium are 1,500 m s^{-1} and 343 m s^{-1}, respectively; poisson's ratio of concrete (ν_P) is 0.33.

As an outer formation, we choose three kinds of soil sample, such as, Adrian, Catlin and Plainfield, from the soil textural triangle [128], to cover the wide range of soil elastic properties. This selection only focuses on the extent of soil properties affect the acoustic wave propagation in buried fluid-filled pipe. The density (ρ_s) and the compressional wave velocity (v_L) of these soils are: 920 kg m^{-3} and 373 m s^{-1} for Adrian soil, 1,270 kg m^{-3} and 463 m s^{-1} for Catlin soil (default), and 1,510 kg m^{-3} and 634 m s^{-1} for Plainfield soil, respectively. The poisson's ratio of the soil (ν_s) is assumed 0.4, which is used to calculate the shear wave velocity (v_S) of the soil.

To observe the pipe profile effect, we choose three different dimensioned pipe from the manufacturer's data sheet [81]. These pipes are generally used for different purposes. As for example, pipe with inner radius, $R = 1.07$ m (default), and thickness $t_p = 0.158$ m (default) is used in California, USA as a drainage culvert under a major highway. The pipe with $R = 1.22$ m, and $t_p = 0.184$ m is used in San Diego Aqueduct, USA for transporting potable water to a large metropolitan area. The pipe with $R = 1.37$ m, and $t_p = 0.209$ m is used as the tunnel liner in a water transmission pressure-system tunnel.

As an excitation signal frequency, we choose sonic/ultasonic frequency of $f = 20$ kHz, 30 kHz (default), 40 kHz. This selection only focuses on the extent of high frequency AE signal effect in the acoustic wave propagation of buried fluid-filled pipe. In convention, the frequency of AE signal that propagates in the pressurized fluid inside the pipe is about 30 kHz [72]. Therefore, this selection is sufficient enough to observe the spectral profile of the propagating signal with in the range of measurement.

Other parameters that are varied during the simulation are: pipe thickness, $t_p = 0.139$ m, 0.158 m, 0.182 m; young's modulus of elasticity of concrete, $E = 30$ GPa, 40 GPa, 50 GPa (default); amplitude of sine pulse, $A = 1$ m^3 s^{-1}, 3 m^3 s^{-1} (default), 5 m^3 s^{-1}.

In order to observe the impact of the path and signal characteristics on the spectral profile of the vibrating acoustic signals, the time response of the system is taken at selected points (such as, 50 m, 100 m, 150 m and 200 m) in the pipe.

6.6.1 Fluid-filled Rigid Pipe

In this case, we considered the fluid (water) filled pipe with infinite stiffness (i.e., rigid pipe). The numerical results of this model are obtained by using Eq. (6.1) with appropriate source and boundary conditions (as described in Section 6.4 and 6.5.1). During the simulation, the amplitude and the frequency of the source, radius of the pipe varies as, $A = 1\,\mathrm{m^3\,s^{-1}}$, $3\,\mathrm{m^3\,s^{-1}}$, $5\,\mathrm{m^3\,s^{-1}}$; $f = 20\,\mathrm{kHz}$, $30\,\mathrm{kHz}$, $40\,\mathrm{kHz}$; $R = 1.07\,\mathrm{m}$, $1.22\,\mathrm{m}$, $1.37\,\mathrm{m}$, respectively. In the study, when one parameter varies, the other parameters are kept constant with their default values (as given in Section 6.6). The results obtained from these simulation are shown in Fig. (6.3), (6.4) and (6.5).

Figures (6.3), (6.4) and (6.5) show that, the fluid-filled rigid pipe has an axially propagating wave with velocity equal to the intrinsic velocity of the acoustic wave in unbounded media. This velocity remain same at all sources (as seen in Fig. (6.3)), frequencies (as seen in Fig. (6.4)) and pipe dimensions (as seen in Fig. (6.5)). The simulated result of wave velocity is comparable with the tube wave velocity ($v_T = 1500\,\mathrm{m\,s^{-1}}$, calculated using Eq. (4.1)), which is used for the low frequency (below the system cut-off frequency) propagation. From the results, it is also seen that when the velocity of an axially propagating wave in a fluid cylinder equals the intrinsic sound velocity, the wavefront is planner and purely longitudinal.

From Fig. (6.3) it is seen that, if the signal strength increases, it increases the system noise due to the reverberations from the pipe boundary, consequently, the signal can propagate for long distance. Figure (6.4) shows that, increasing frequency decreases the signal strength, since the significant part of the energy of the signal is carried by the higher modes. Similarly, in Fig. (6.5), increasing cross-sectional dimension decreases the signal strength, due to the increased spatial energy dissipation.

Other information that can be observed from these figures are as follows. The initial

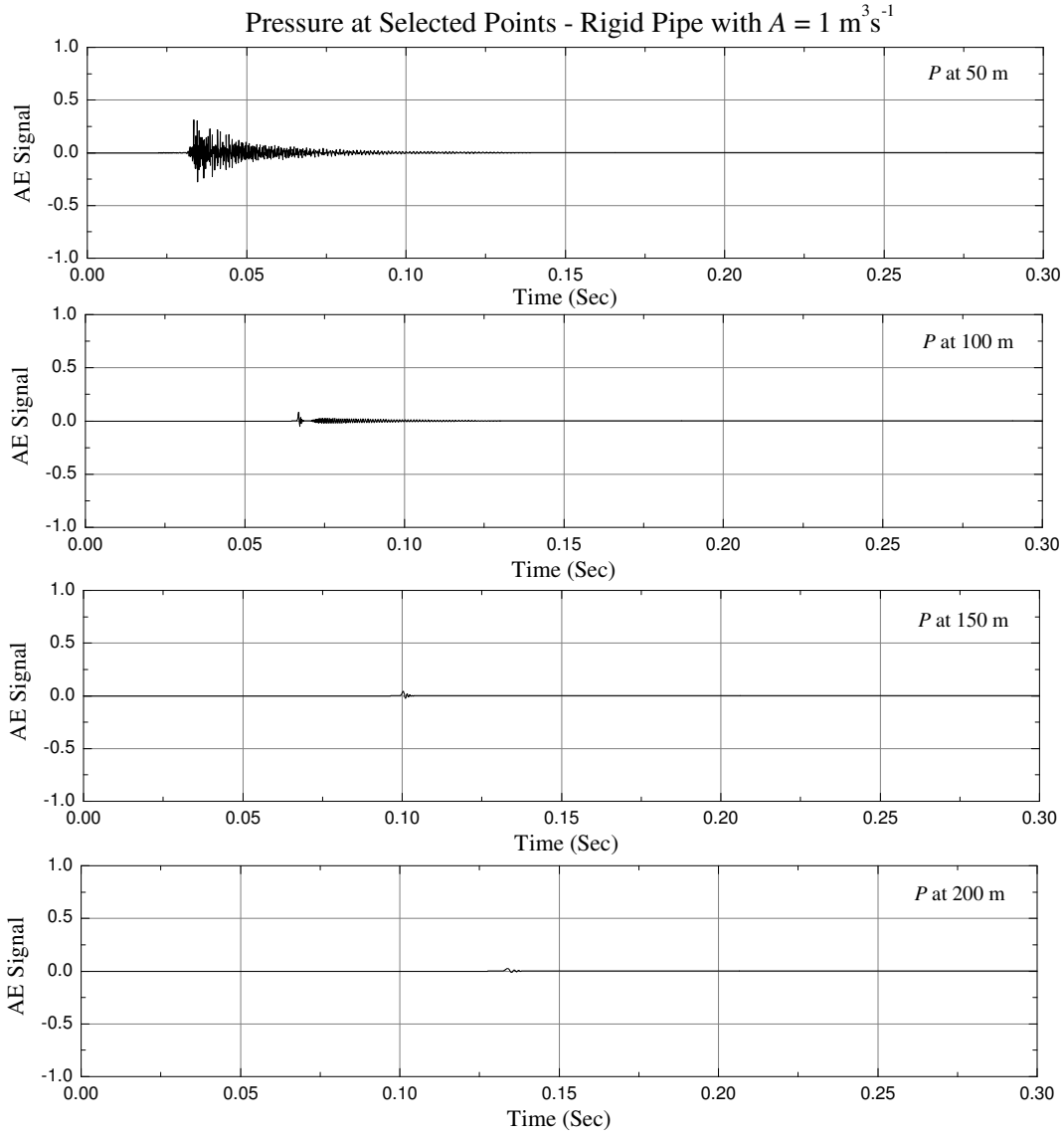

(a) Analytical $v_T = 1{,}500\,\mathrm{m\,s^{-1}}$.

Figure 6.3: Spectral response of water-filled rigid pipe at (a) $A = 1\,\mathrm{m^3\,s^{-1}}$.

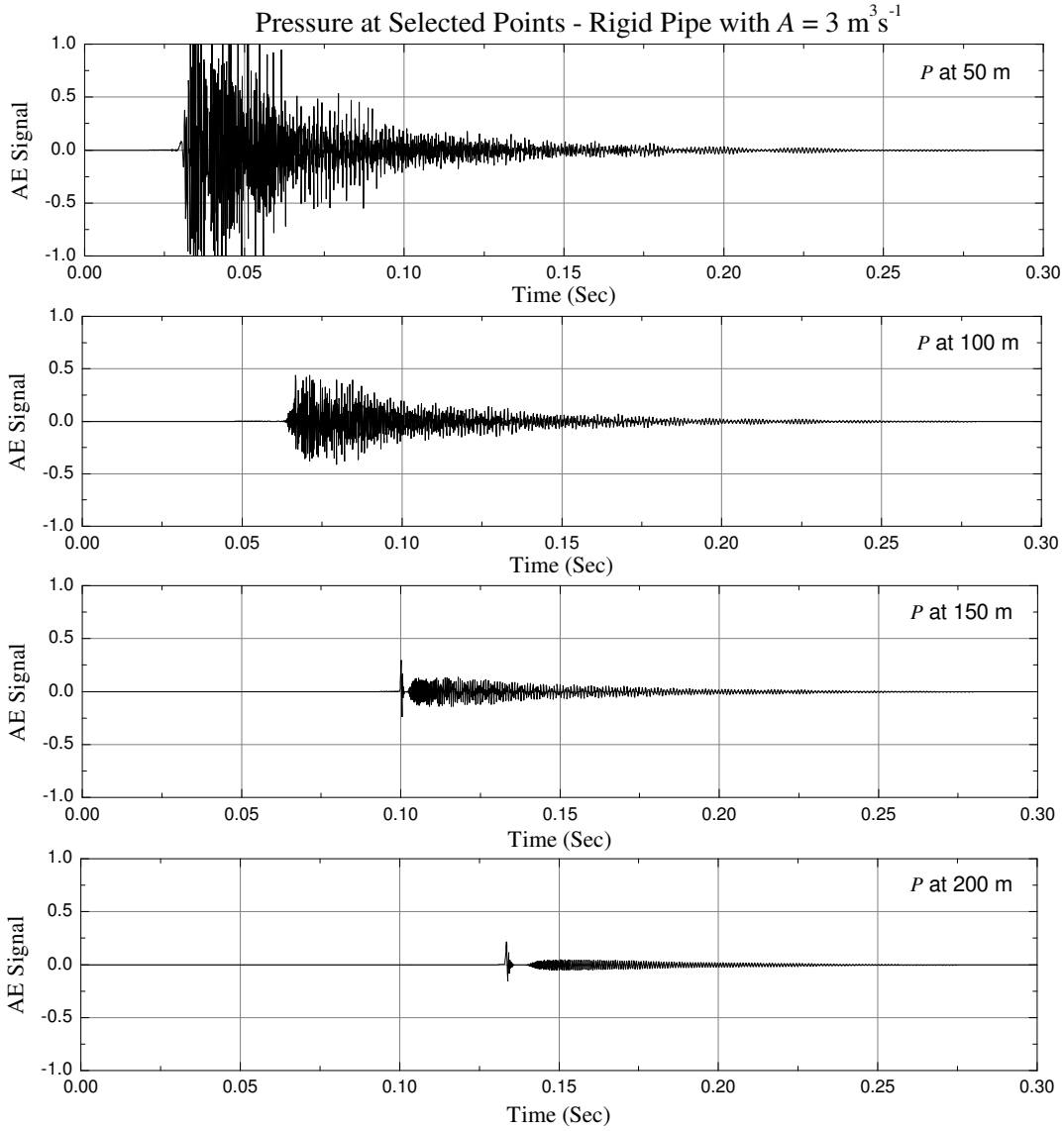

(b) Analytical $v_T = 1{,}500\,\mathrm{m\,s^{-1}}$.

Figure 6.3: Spectral response of water-filled rigid pipe at (b) $A = 3\,\mathrm{m^3\,s^{-1}}$.

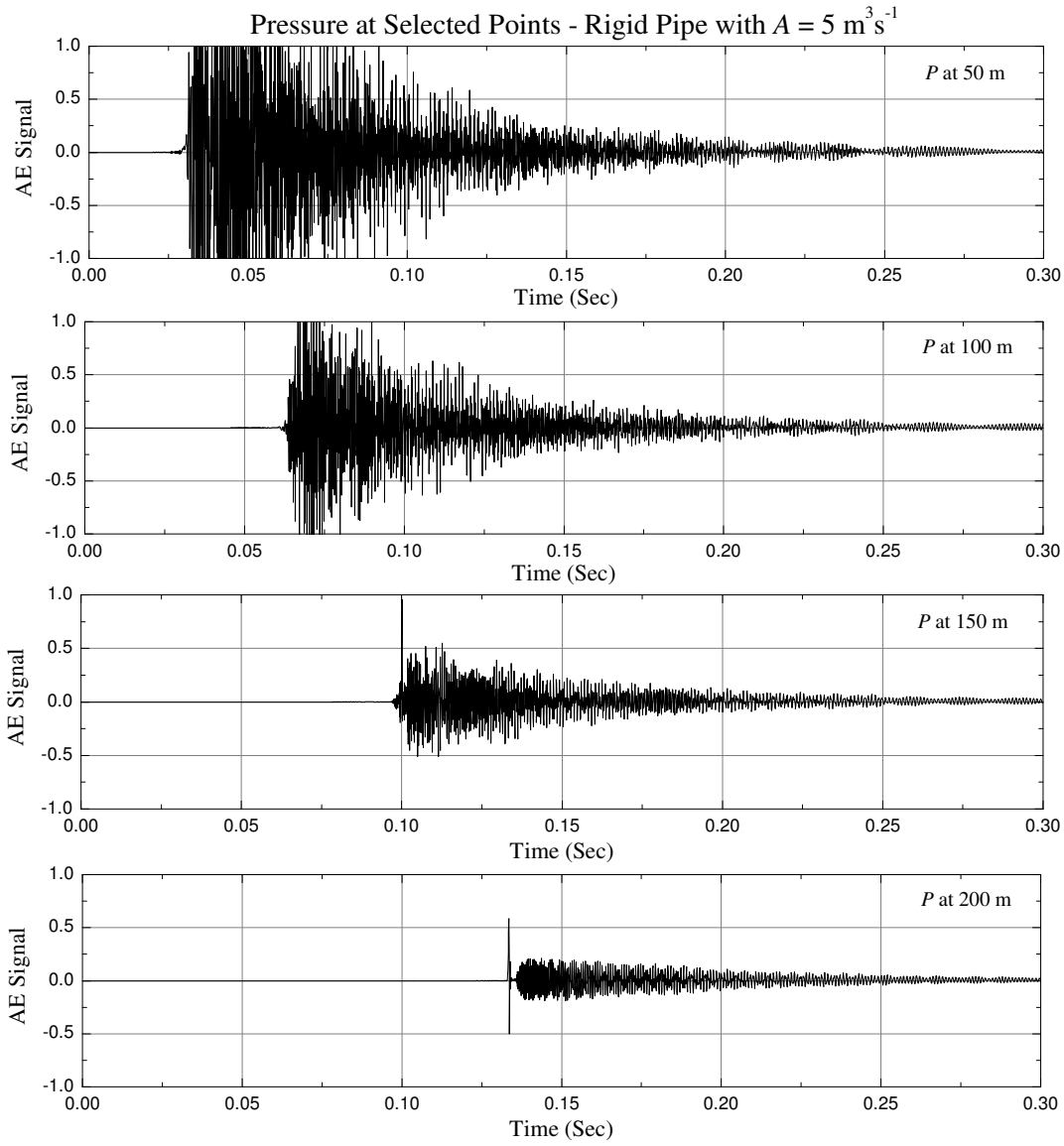

(c) Analytical $v_T = 1{,}500\,\mathrm{m\,s^{-1}}$.

Figure 6.3: Spectral response of water-filled rigid pipe at (c) $A = 5\,\mathrm{m^3\,s^{-1}}$.

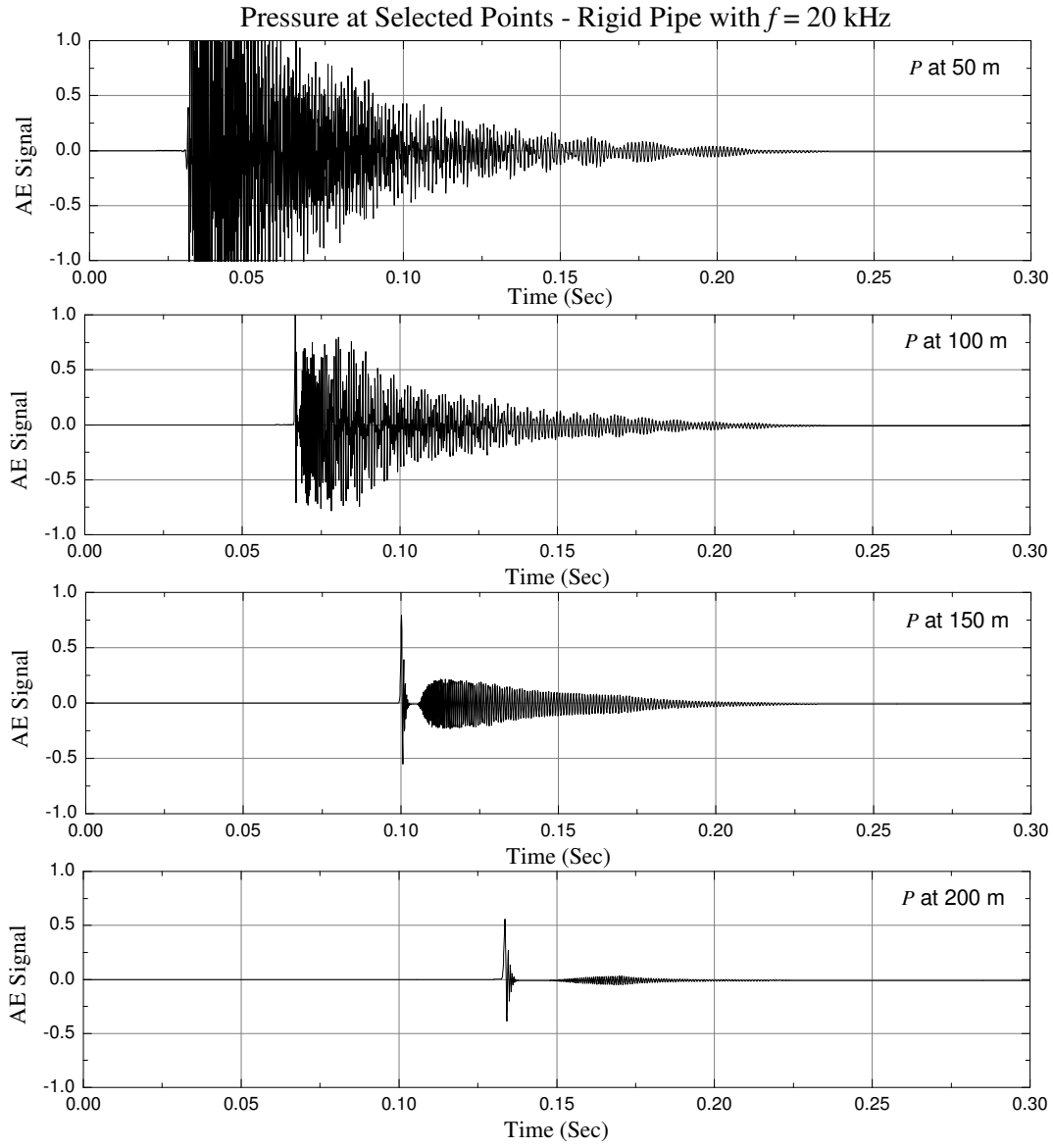

(a) Analytical $v_T = 1{,}500\,\mathrm{m\,s^{-1}}$.

Figure 6.4: Spectral response of water-filled rigid pipe at (a) $f = 20\,\mathrm{kHz}$.

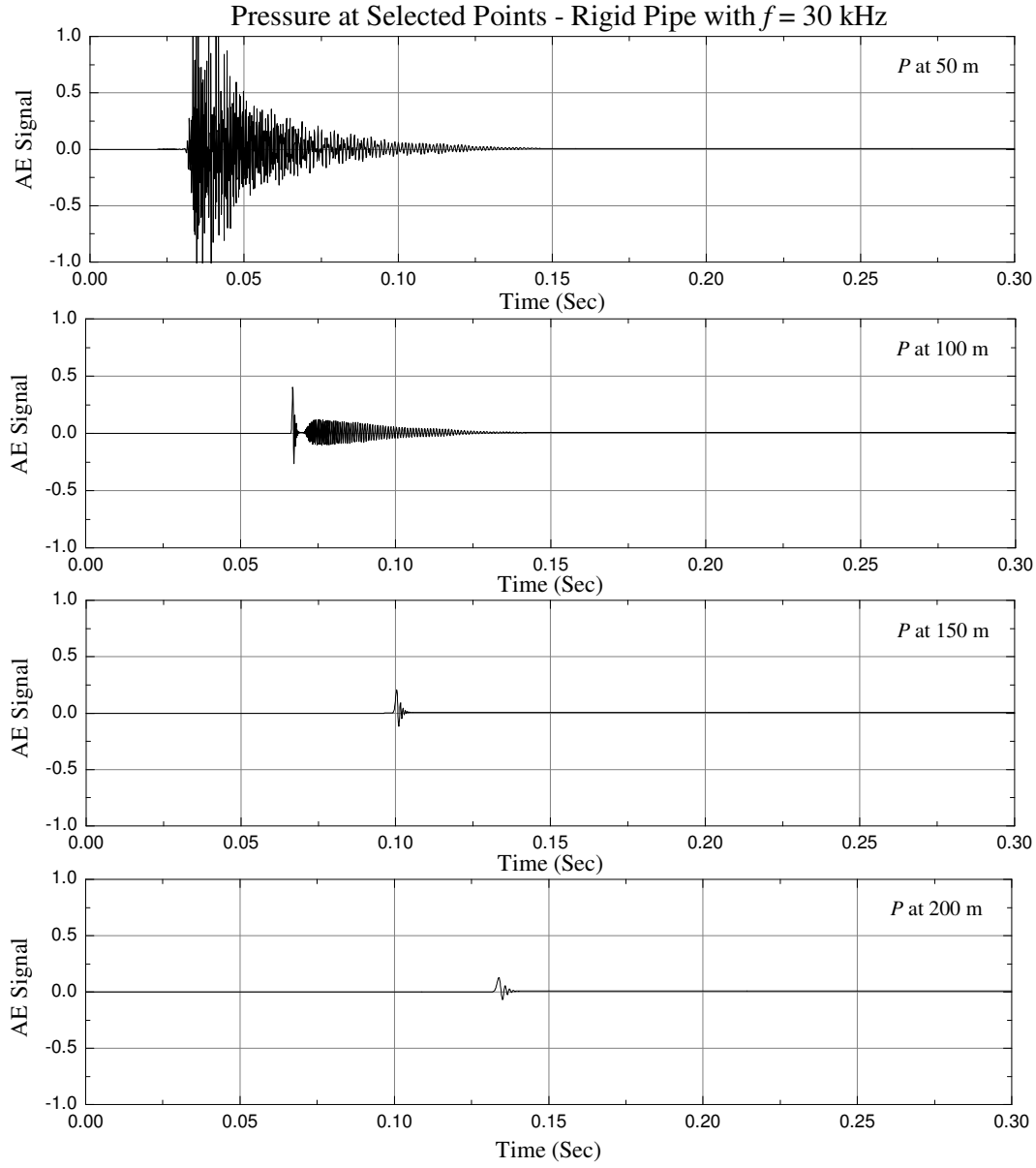

(b) Analytical $v_T = 1{,}500\,\mathrm{m\,s^{-1}}$.

Figure 6.4: Spectral response of water-filled rigid pipe at (b) $f = 30\,\mathrm{kHz}$.

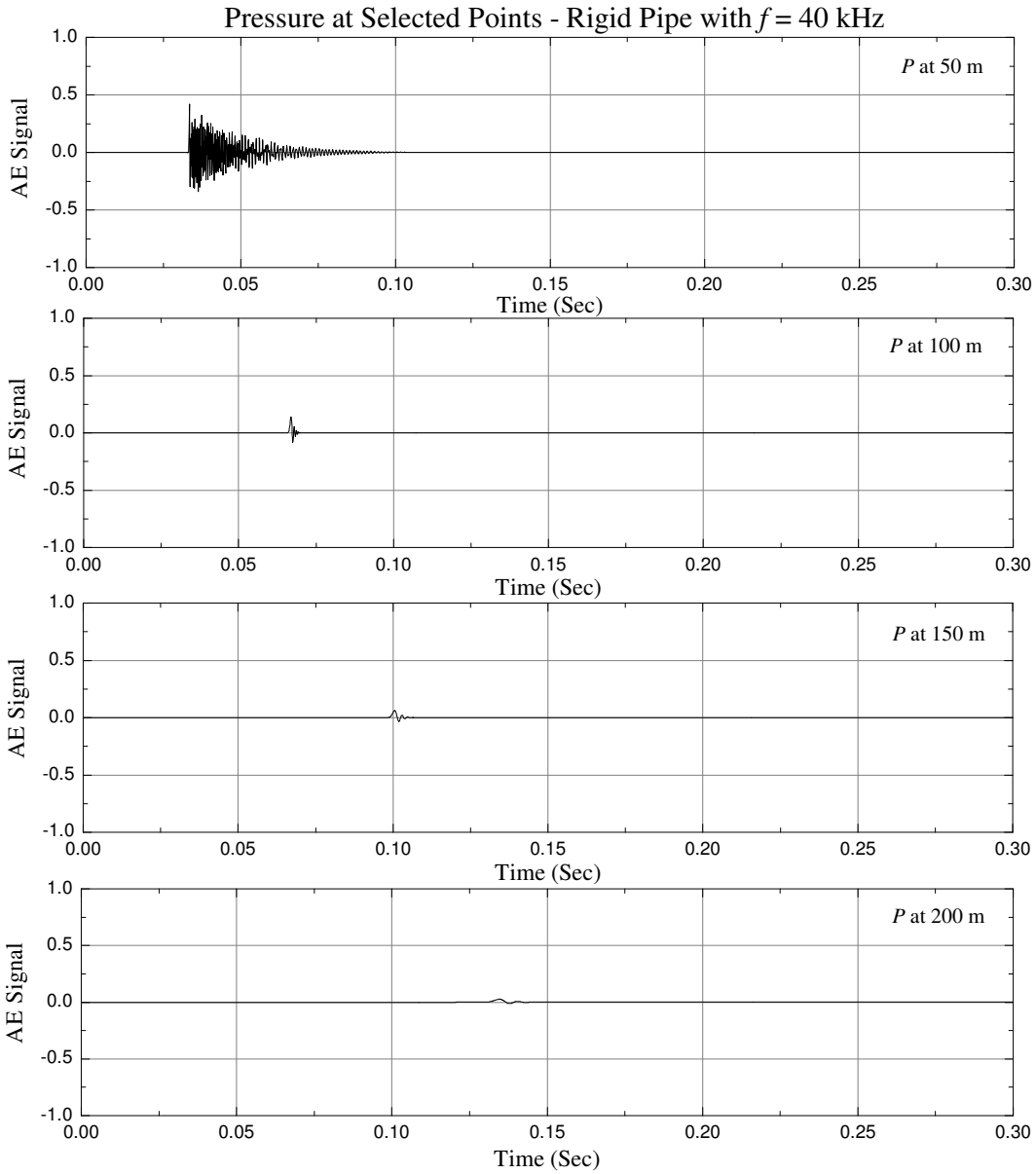

(c) Analytical $v_T = 1{,}500\,\mathrm{m\,s^{-1}}$.

Figure 6.4: Spectral response of water-filled rigid pipe at (c) $f = 40\,\mathrm{kHz}$.

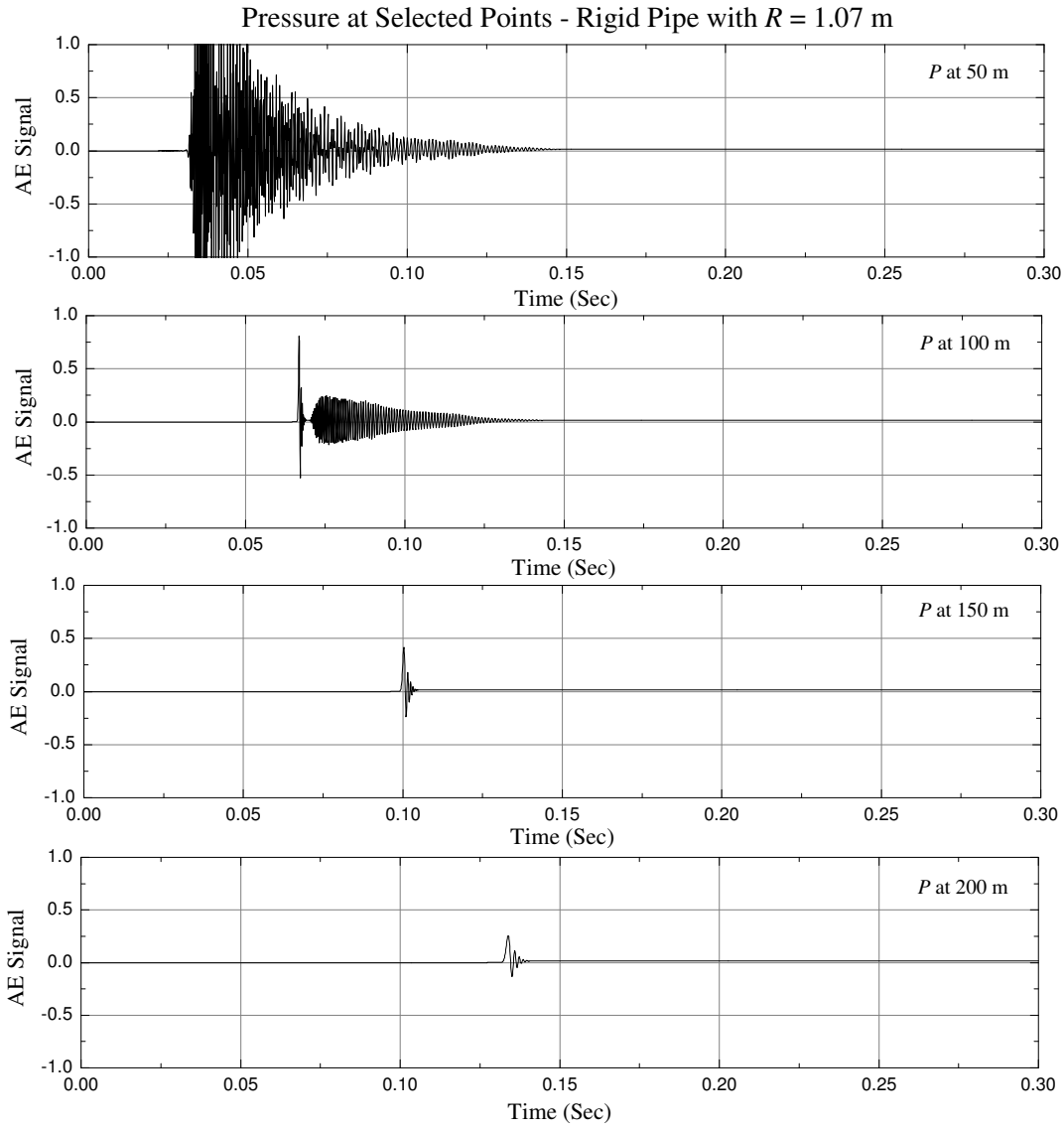

(a) Analytical $v_T = 1{,}500\,\mathrm{m\,s^{-1}}$.

Figure 6.5: Spectral response of water-filled rigid pipe at (a) $R = 1.07\,\mathrm{m}$.

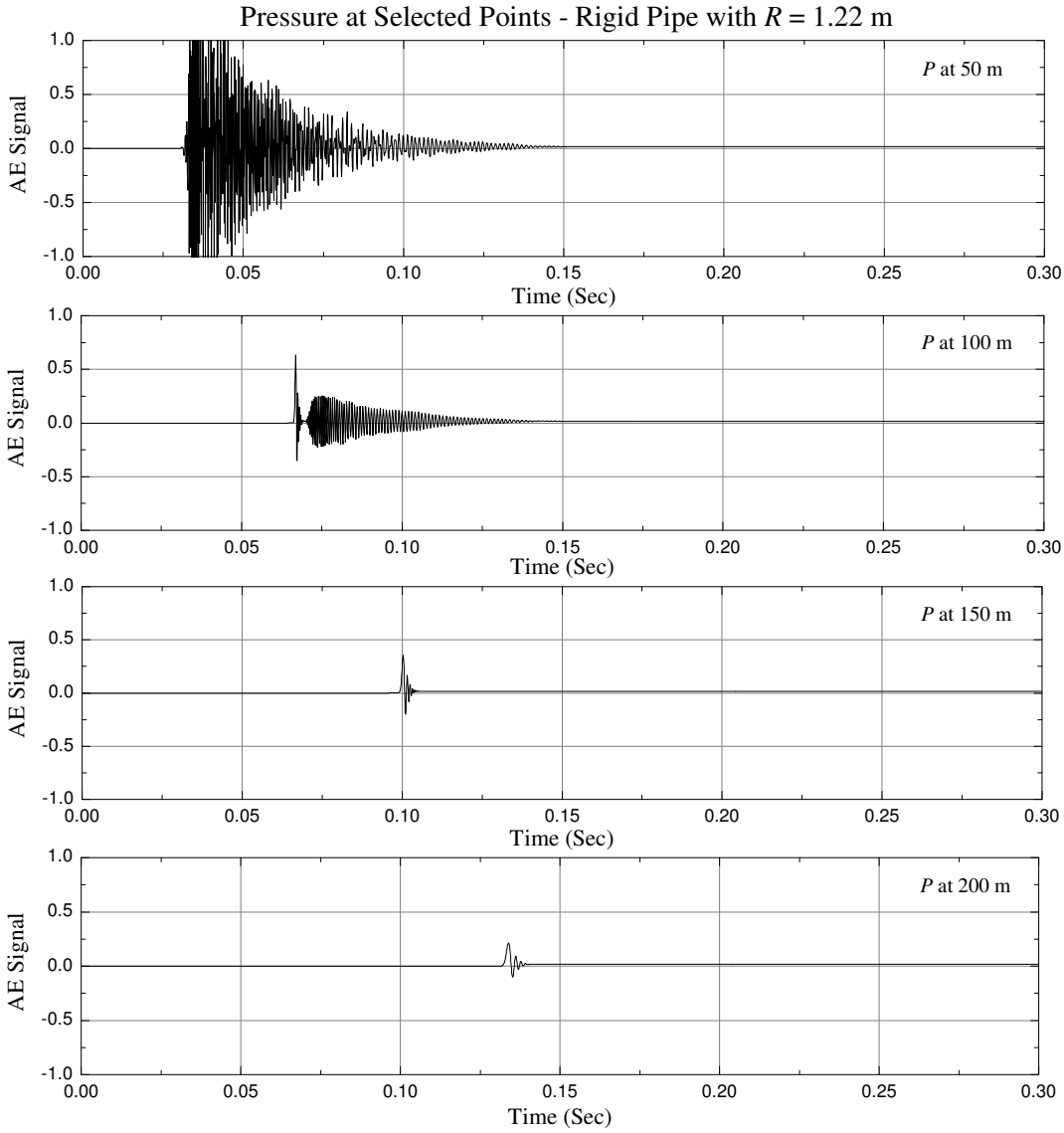

(b) Analytical $v_T = 1{,}500\,\mathrm{m\,s^{-1}}$.

Figure 6.5: Spectral response of water-filled rigid pipe at (b) $R = 1.22\,\mathrm{m}$.

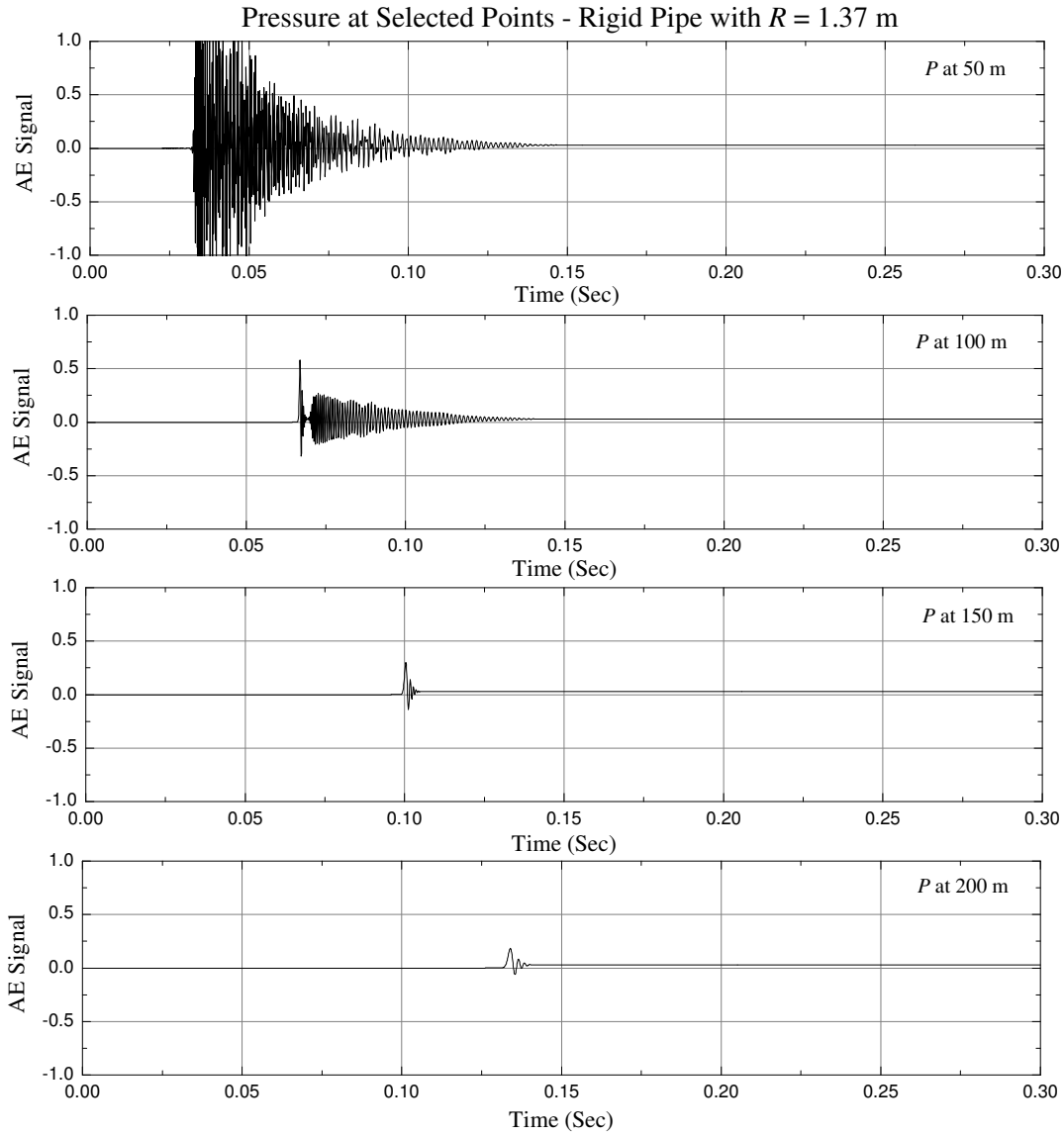

(c) Analytical $v_T = 1{,}500\,\mathrm{m\,s^{-1}}$.

Figure 6.5: Spectral response of water-filled rigid pipe at (c) $R = 1.37\,\mathrm{m}$.

signal pulse is extended and the smoothing out of the pulse's starting and ending regions due to the slight dispersion of the wave's higher frequencies (attenuation of the higher modes). Therefore, after certain propagation distance, we can get a signal of less strength with an extended duration which resembles the original one. The noise dies out after propagating a relatively small distance compared to the main signal. This fact is due to the noise that resembles with higher modes, which are attenuated faster than the fundamental mode. Consequently, at large distance, the main signal can sustain its strength much more than the noise following it.

In the pipeline condition monitoring system, the importance of this analysis is to obtain fundamental concept of acoustic wave propagation through fluid-column under different situation. This type of analysis is also important for the solid pipe filled with gas type medium, where it can be assumed that the pipe boundary motion is negligible.

6.6.2 Fluid-filled Elastic Pipe

In this study, consider a water-filled concrete pipe as a fluid-filled elastic pipe (PCCP) with finite stiffness. The parameters that changes during the simulation are: $A = 1\,\mathrm{m^3\,s^{-1}}$, $3\,\mathrm{m^3\,s^{-1}}$, $5\,\mathrm{m^3\,s^{-1}}$; $f = 20\,\mathrm{kHz}$, $30\,\mathrm{kHz}$, $40\,\mathrm{kHz}$; $E = 30\,\mathrm{GPa}$, $40\,\mathrm{GPa}$, $50\,\mathrm{GPa}$; $t_p = 0.139\,\mathrm{m}$, $0.158\,\mathrm{m}$, $0.182\,\mathrm{m}$. When one parameter varies, the other parameters are kept constant with their default values (as given in Section 6.6). The impact of pipe profile and the signal characteristics on the spectral profiles of the propagating signal are observed from these analyses. The results obtained from these simulation are shown in Fig. (6.6), (6.7), (6.8) and (6.9).

Figure (6.6) shows the spectral profile of the AE signal propagation throughout the pipe at different signal strength. As same as rigid pipe, increasing signal strength increases the system noise due to the reverberations from the pipe boundary. Higher signal strength also increases the traveling distance.

From Fig. (6.7) it is seen that, increasing the frequency increases the attenuation, which decreases the signal strength, because the significant part of energy of the signal is carried

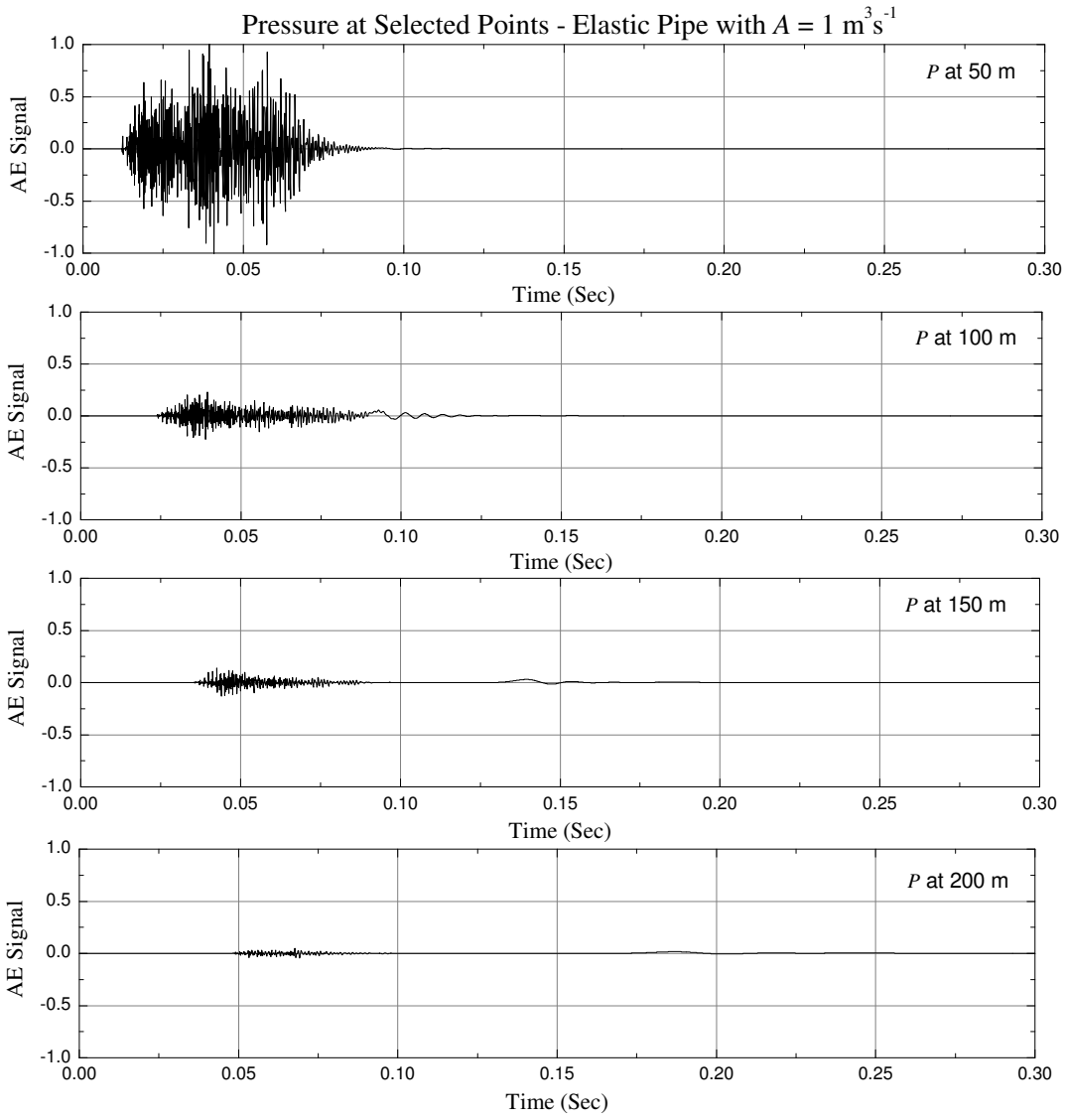

(a) Analytical $v_T = 1{,}100\,\mathrm{m\,s^{-1}}$.

Figure 6.6: Spectral response of water-filled elastic pipe at (a) $A = 1\,\mathrm{m^3\,s^{-1}}$.

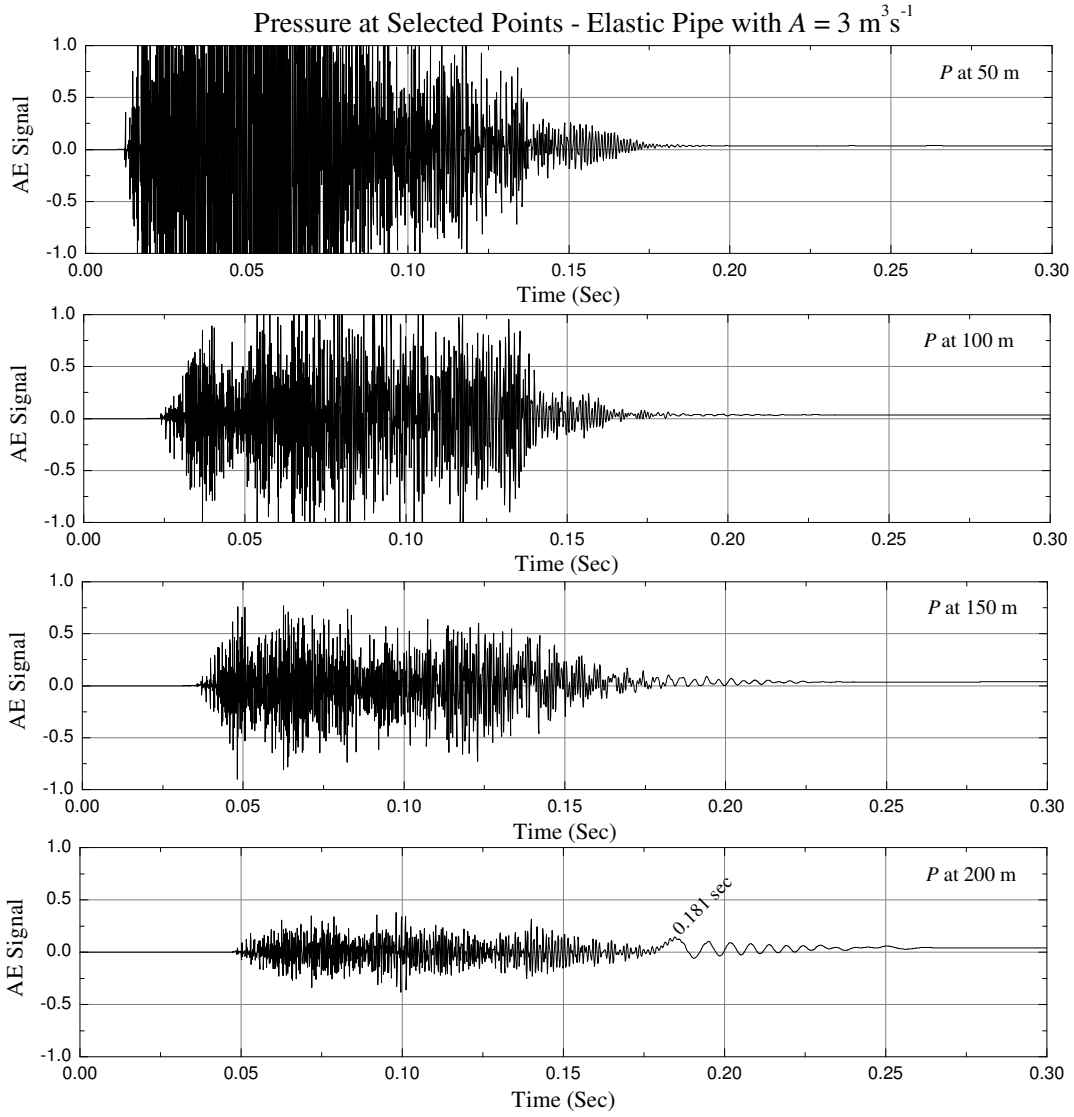

(b) Analytical $v_T = 1{,}100\,\mathrm{m\,s^{-1}}$.

Figure 6.6: Spectral response of water-filled elastic pipe at (b) $A = 3\,\mathrm{m^3\,s^{-1}}$.

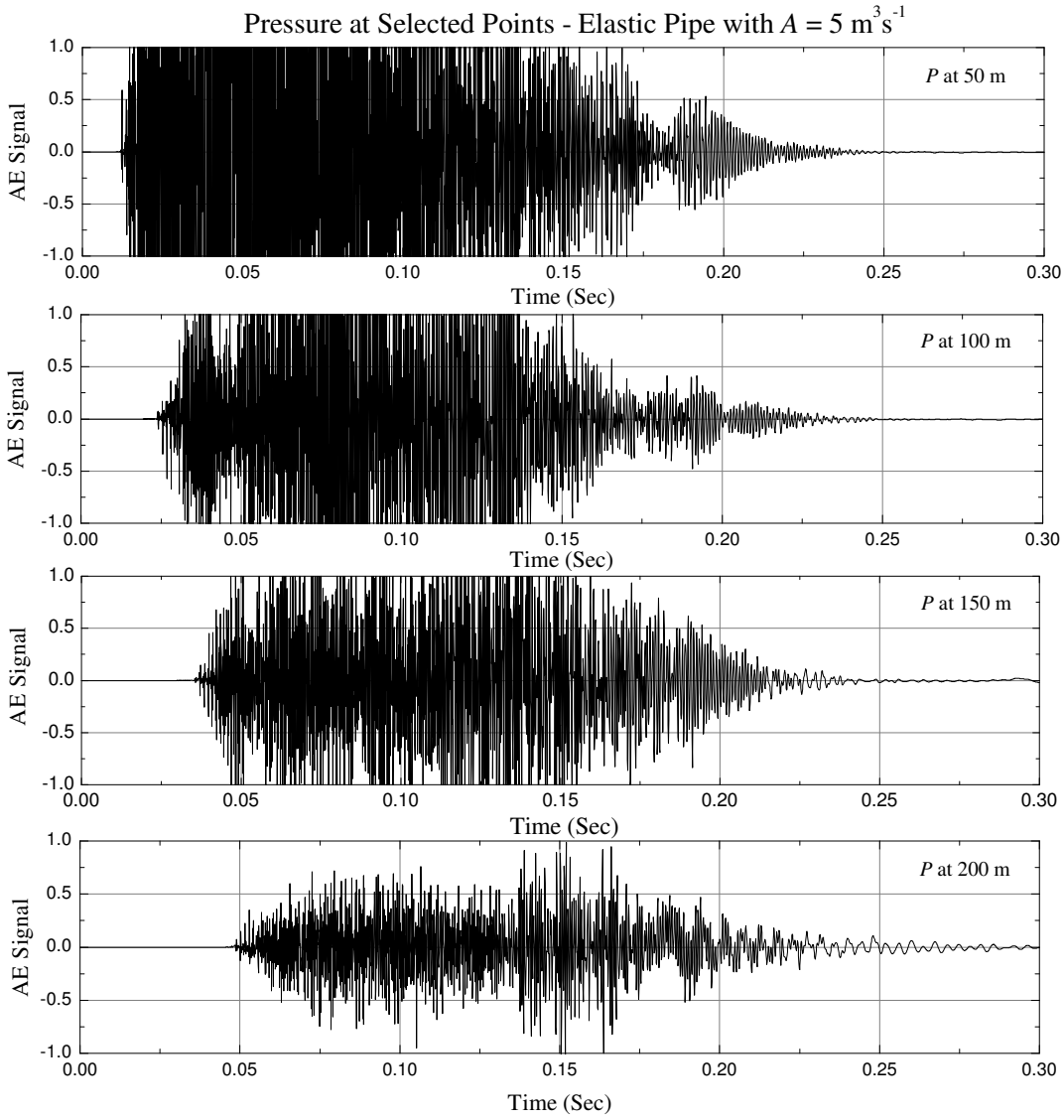

(c) Analytical $v_T = 1{,}100\,\mathrm{m\,s^{-1}}$.

Figure 6.6: Spectral response of water-filled elastic pipe at (c) $A = 5\,\mathrm{m^3\,s^{-1}}$.

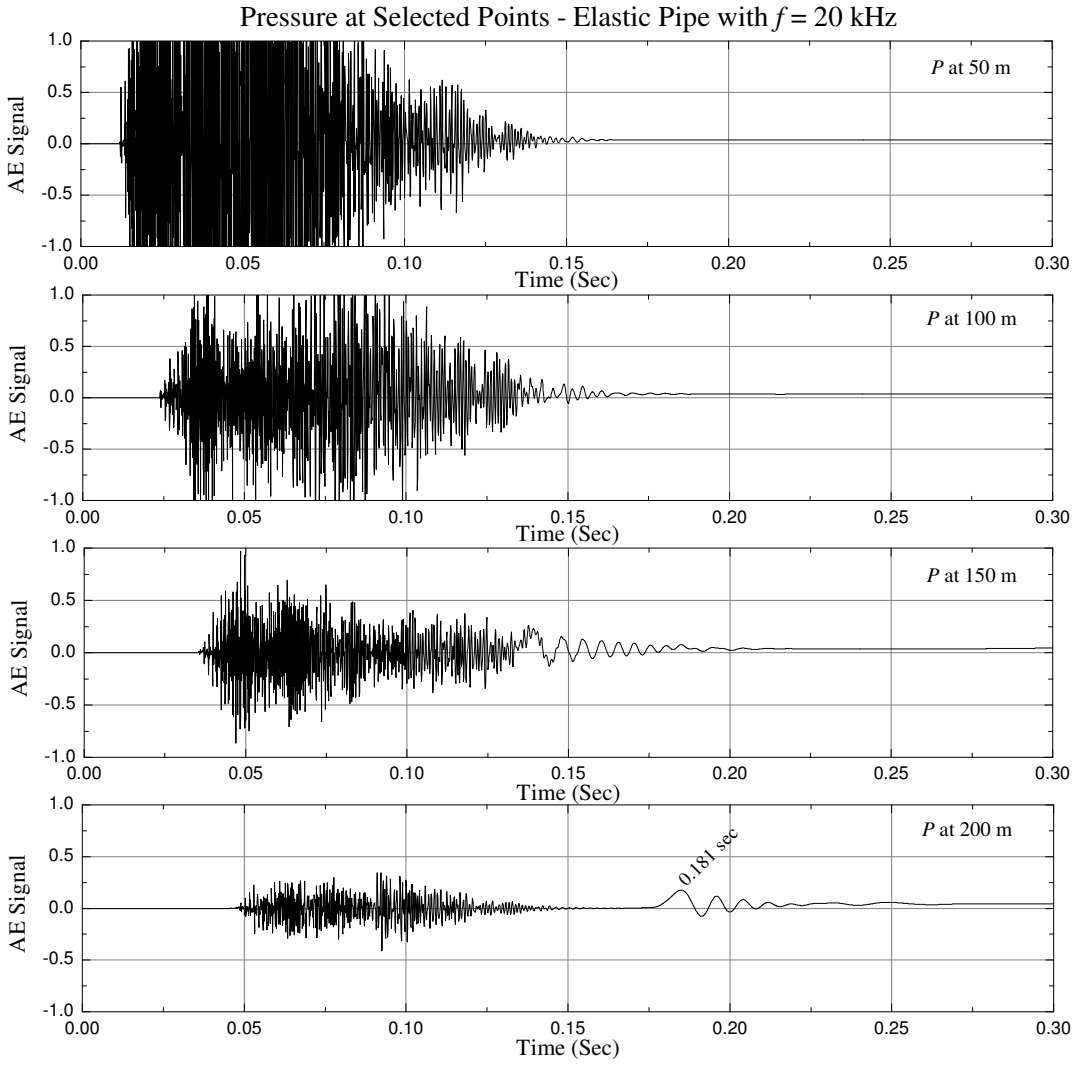

(a) Analytical $v_T = 1{,}100\,\mathrm{m\,s^{-1}}$.

Figure 6.7: Spectral response of water-filled elastic pipe at (a) $f = 20\,\mathrm{kHz}$.

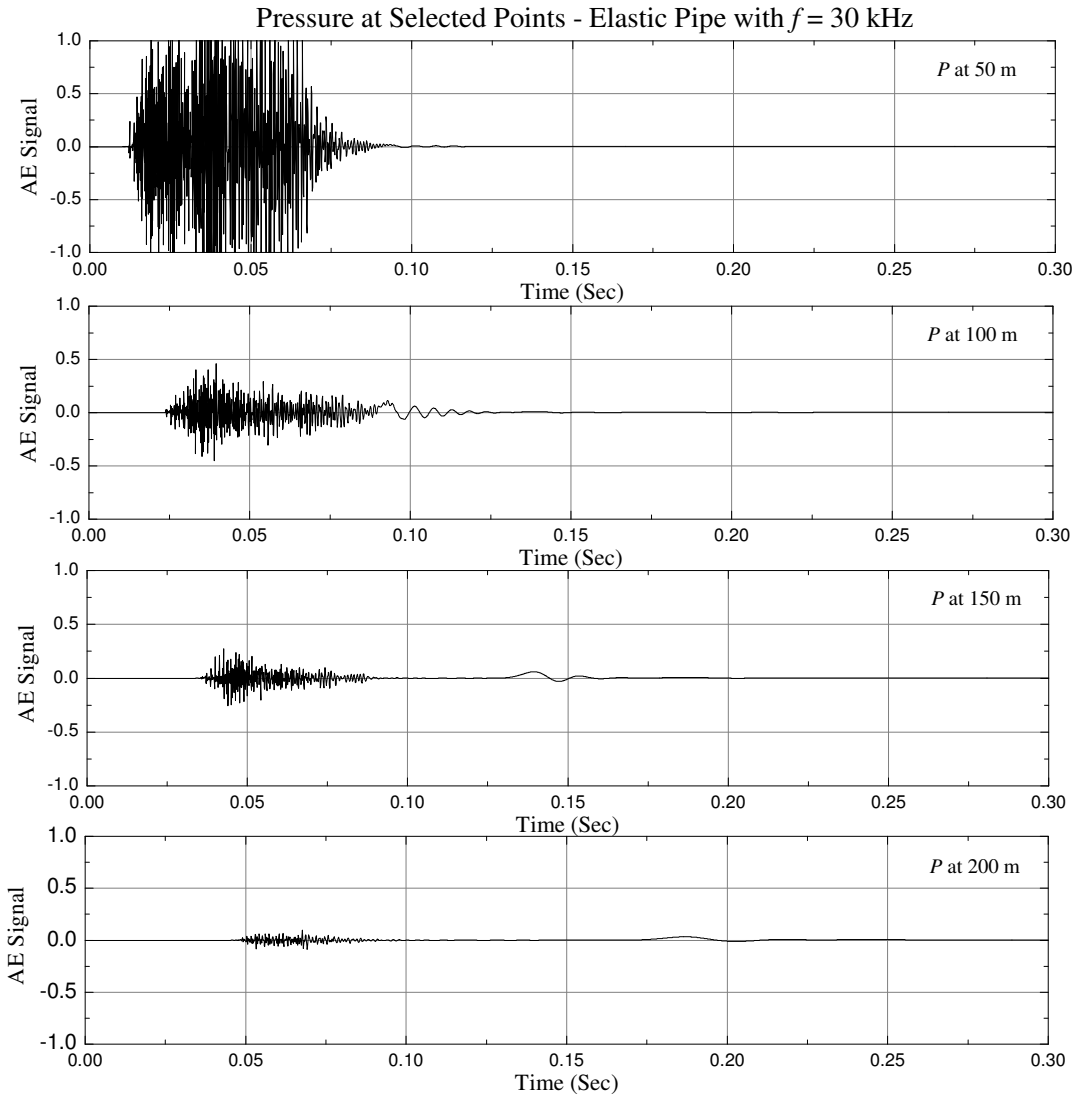

(b) Analytical $v_T = 1{,}100\,\mathrm{m\,s^{-1}}$.

Figure 6.7: Spectral response of water-filled elastic pipe at (b) $f = 30\,\mathrm{kHz}$.

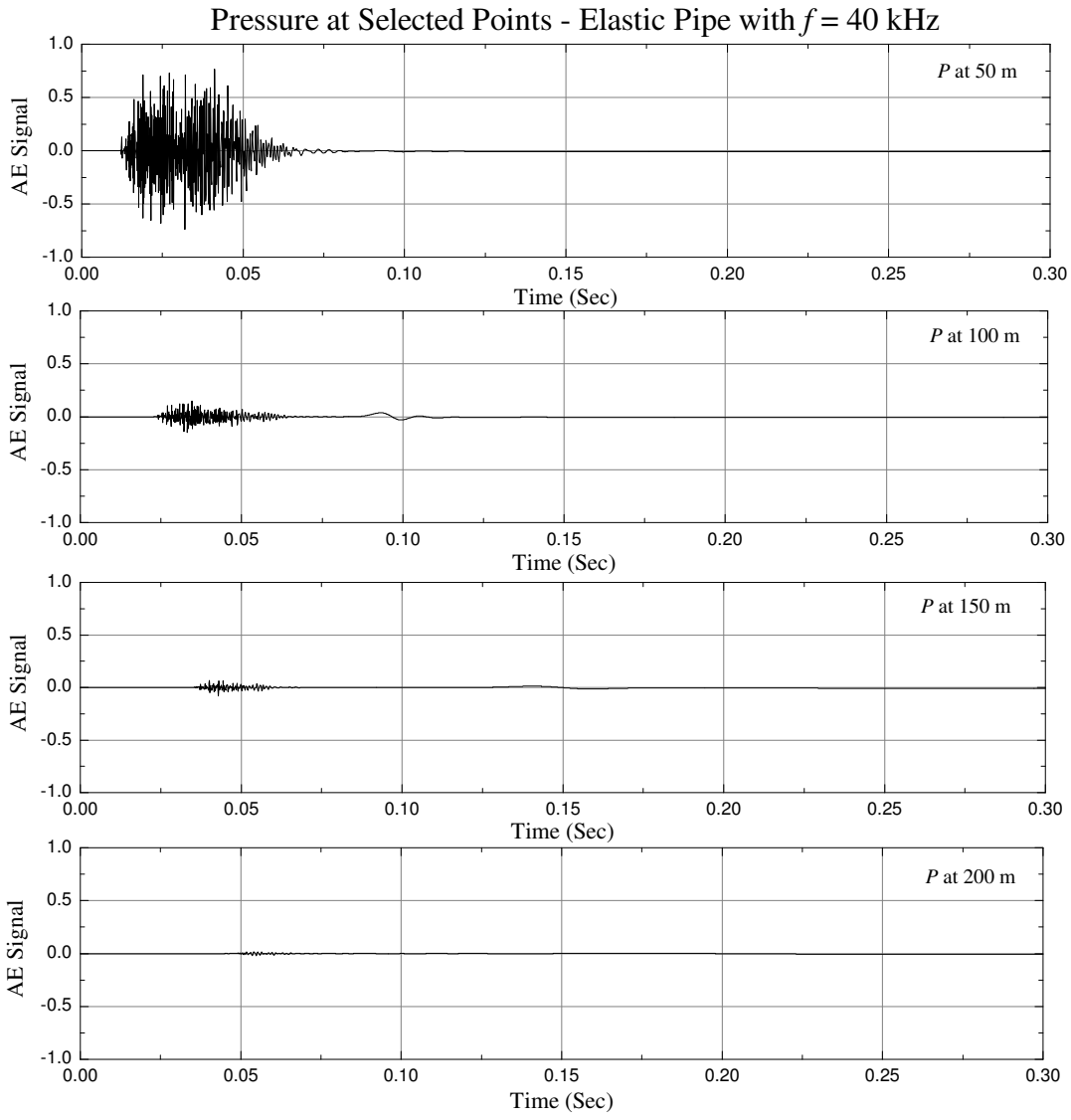

(c) Analytical $v_T = 1{,}100\,\mathrm{m\,s^{-1}}$.

Figure 6.7: Spectral response of water-filled elastic pipe at (c) $f = 40\,\mathrm{kHz}$.

by the higher modes. This information signifies that, in the far-field measurement of long-range pipe inspection, the high frequency AE signal can not be detected, due to its high attenuation.

The effect of pipe elasticity on system rigidity is shown in Fig. (6.8). From figure it is seen that, increasing elasticity increases the pipe stiffness, which reduces the effective cross-sectional area of the pipe. As a result, less energy radiated from the inside to the outside. Consequently, the signal strength is stronger in the high stiffness pipe.

Figure (6.9) shows the effect of pipe thickness on the AE signal propagation. It is seen that if the pipe thickness increases, it increases the effective cross-section of the pipe, which decreases the pipe stiffness. And hence, more energy is radiated from the inside to the outside, as a result, wave speed is decreases.

The figures also show that, a distinct signal is propagating throughout the pipe, which is faster than the system noise signal. Initially, this signal has small amplitude compared to the reverberations caused by the high frequency pulses and traveled at the same speed. Therefore, it can not be detected at this stage. After some distance, the noise level reduces well below this signal, because the higher modes are attenuated much faster than the fundamental mode. Moreover, at the beginning the noise signal travels at a very high speed, because at start it travels as a spherical wave with in the pipe. Later on, when the wave dominates all the cross-sectional area of the pipe, it also travels throughout the surrounding elastic layers (e.g. pipe, outer soil medium) and reflect back into the fluid inside the pipe. As a result, due to the pipe wall and elastic effect of the surrounding layers, it travels as a wave front with the slower speed of the main signal. Thus, the main signal can be distinguish clearly after short distance with less noise background. The magnitude and velocity of this signal is affected by the pipe and signal characteristics, which can be explained by the tube wave analysis. As for example in Fig. (6.8)(c), the calculated v_T is 1,155 $\mathrm{m\,s^{-1}}$, therefore, the time required to travel the AE signal from the source to 150 m distance is 0.129 sec, which is same as it is seen in the graph. Similarly, we can verify the simulation results for other distances. The characteristics of this distinct signal signifies that, it is the original AE

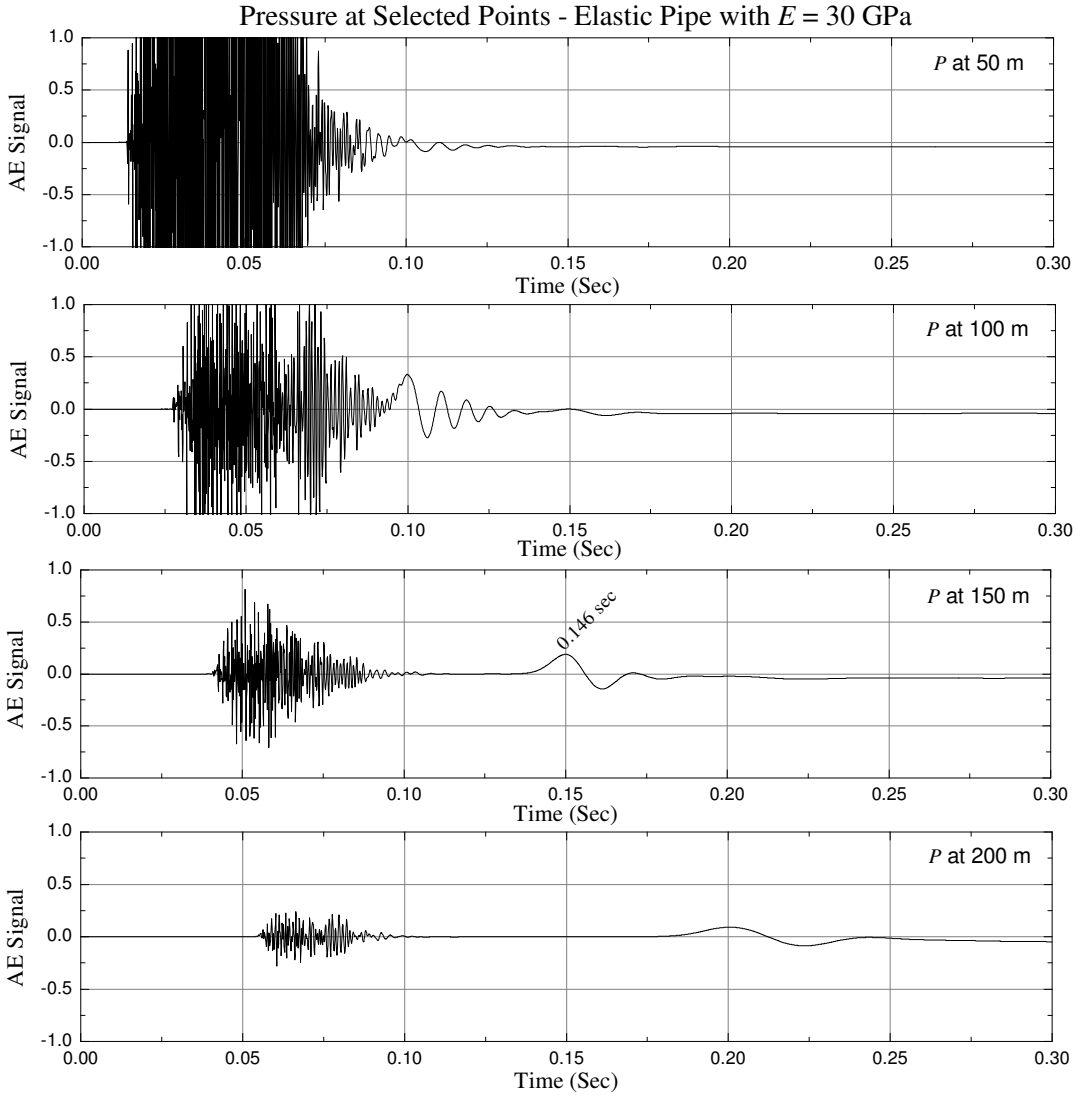

(a) Analytical $v_T = 1{,}024\,\mathrm{m\,s^{-1}}$.

Figure 6.8: Spectral response of water-filled elastic pipe at (a) $E = 30\,\mathrm{GPa}$.

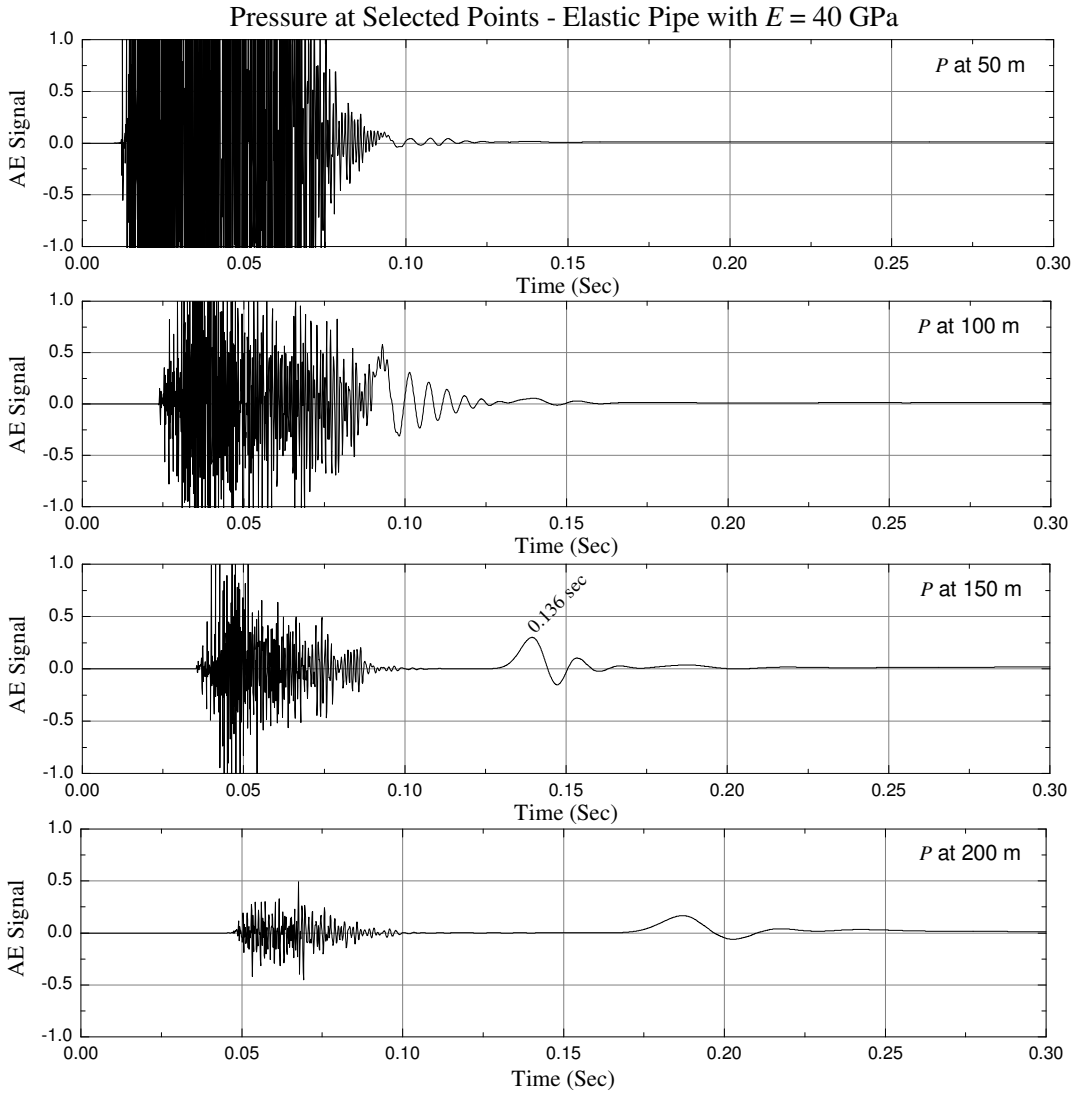

(b) Analytical $v_T = 1{,}100\,\mathrm{m\,s^{-1}}$.

Figure 6.8: Spectral response of water-filled elastic pipe at (b) $E = 40\,\mathrm{GPa}$.

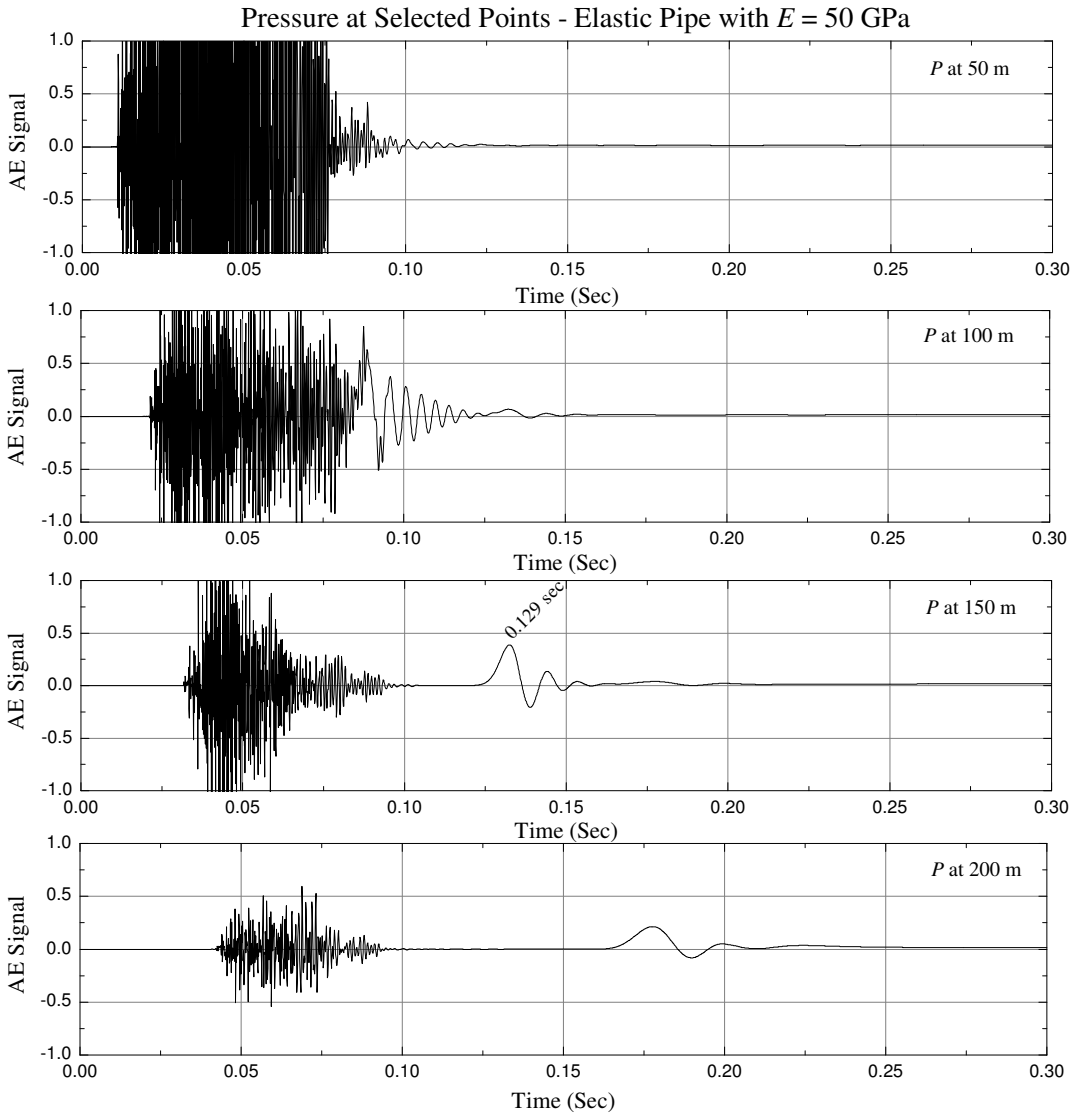

(c) Analytical $v_T = 1{,}155\,\mathrm{m\,s^{-1}}$.

Figure 6.8: Spectral response of water-filled elastic pipe at (c) $E = 50\,\mathrm{GPa}$.

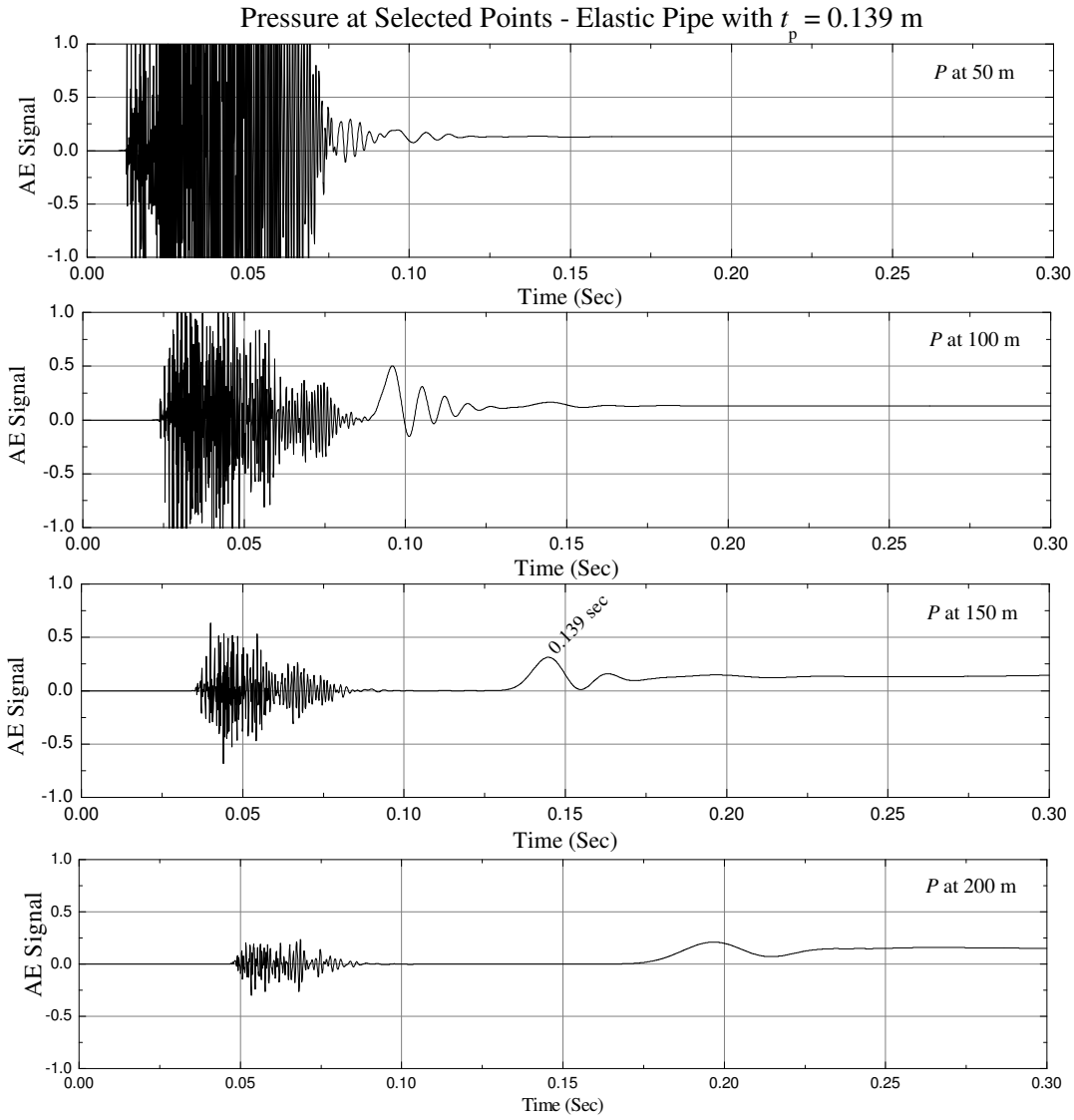

(a) Analytical $v_T = 1{,}071\,\mathrm{m\,s^{-1}}$.

Figure 6.9: Spectral response of water-filled elastic pipe at (a) $t_p = 0.139\,\mathrm{m}$.

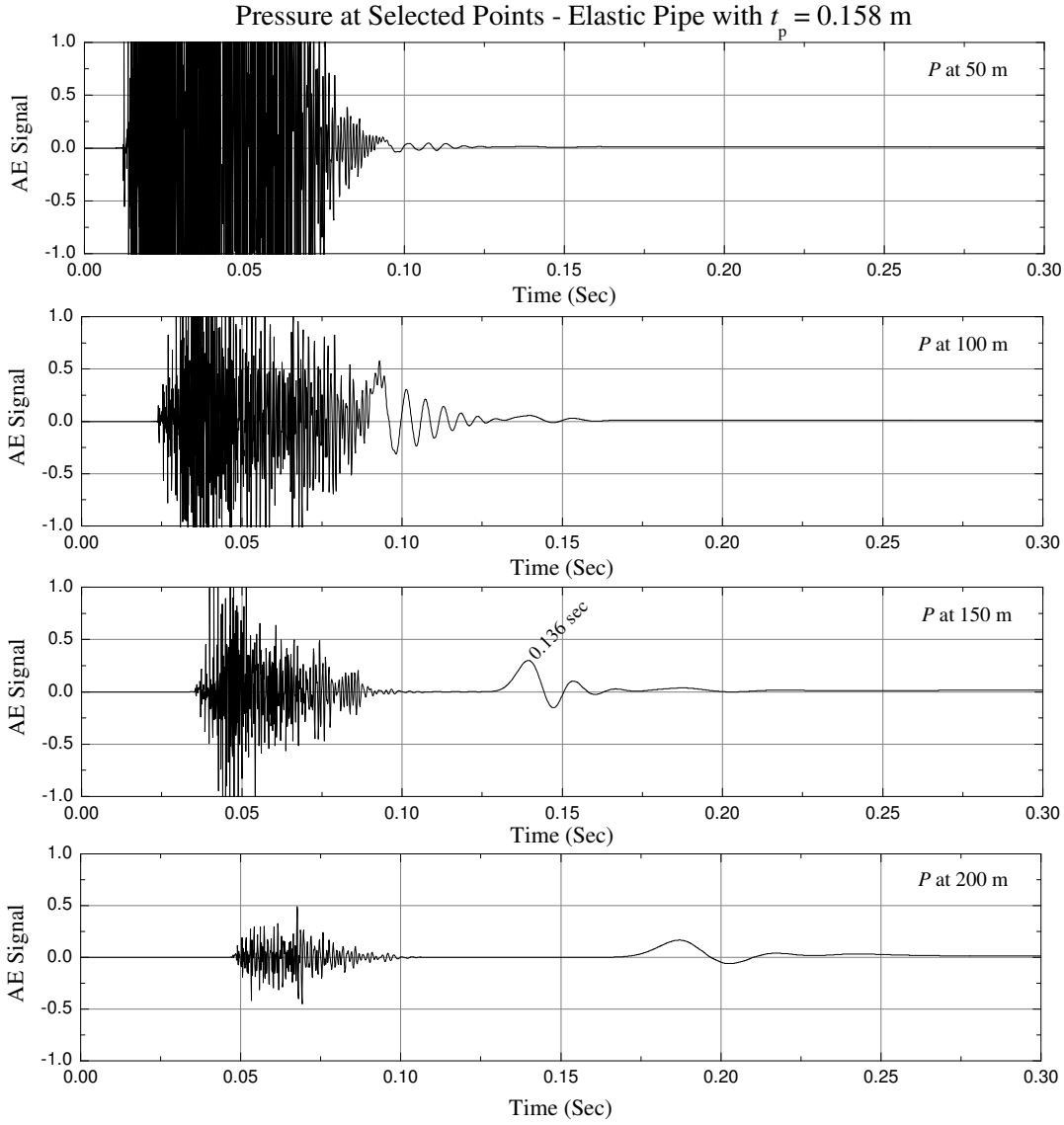

(b) Analytical $v_T = 1{,}100\,\mathrm{m\,s^{-1}}$.

Figure 6.9: Spectral response of water-filled elastic pipe at (b) $t_p = 0.158\,\mathrm{m}$.

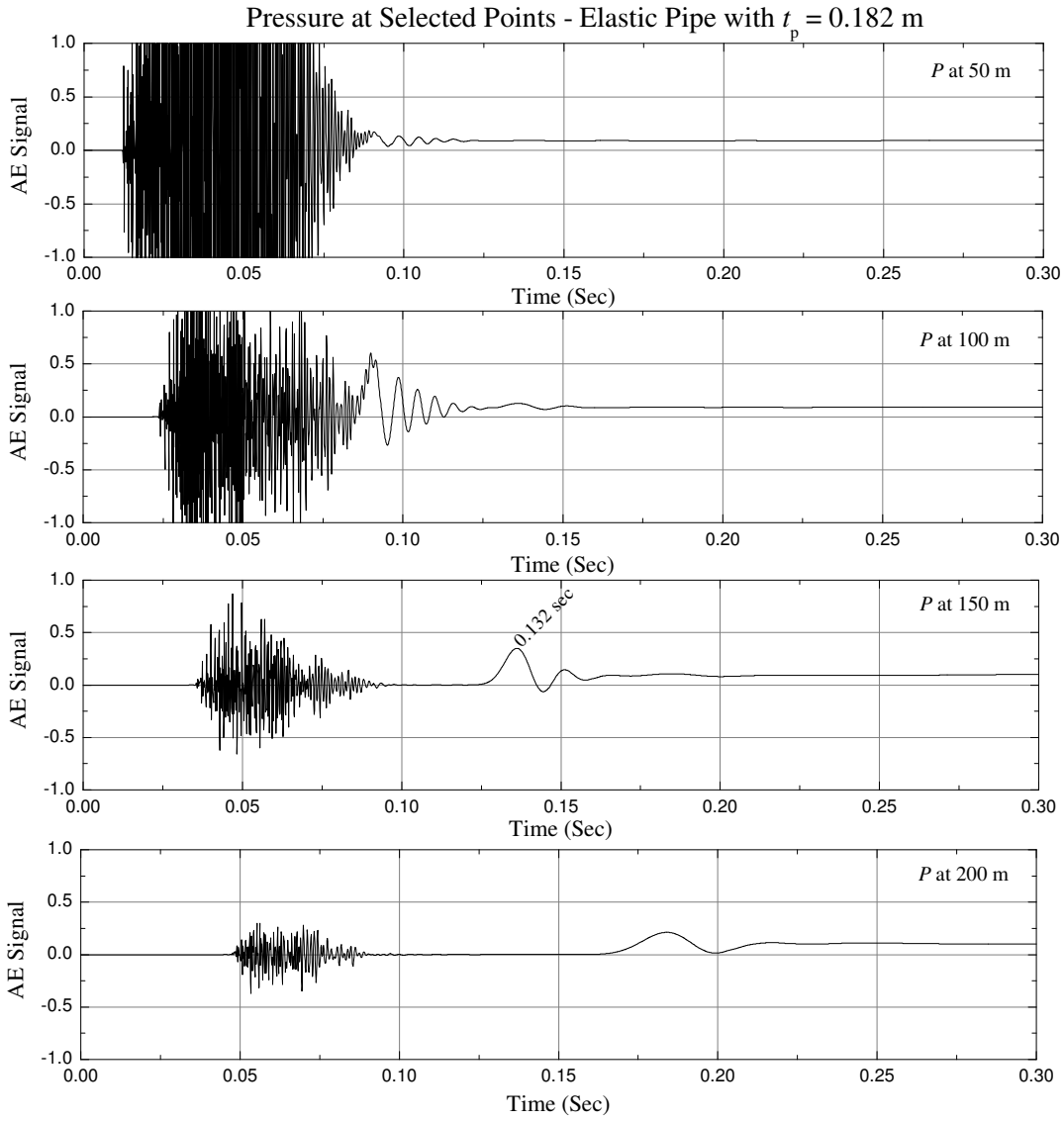

(c) Analytical $v_T = 1{,}131\,\mathrm{m\,s^{-1}}$.

Figure 6.9: Spectral response of water-filled elastic pipe at (c) $t_p = 0.182\,\mathrm{m}$.

signal generated from high frequency AE event. If we compare the signal and the noise with the rigid pipe solution, it is seen that the speed of the system noise of elastic pipe is slower than the original AE signal. This is due to the elastic effect of the pipe structure. Other characteristics of the original AE signal are same as it is described in Subsection 6.6.1.

From the analyses it is seen that, the excitation signal and the pipe characteristics has an effect on the acoustic signal propagation through the fluid medium. Moreover, at high frequency the original AE signal is separated from the system noise after some distance. Therefore, it can be easily detected in the condition monitoring system. This knowledge is important to determine the phase speed of AE signal in the elastic pipe with different profile surrounded by different outer medium.

6.6.3 Fluid-filled Elastic Pipe Surrounded by Soil

The effect of outer soil formation on the AE signal propagation of water-filled elastic pipe at different signal and pipe profile is discussed in this section. The pipes are generally placed below the earth in the soil formation. In this study, we choose three different types of pipe, such as, pipe with radius $R = 1.07\,\mathrm{m}$, $1.22\,\mathrm{m}$, $1.37\,\mathrm{m}$ and thickness $t_p = 0.158\,\mathrm{m}$, $0.184\,\mathrm{m}$, $0.209\,\mathrm{m}$, respectively (as given in Section 6.6). These pipes (PCCP) can carry a wide range of load conditions. As for example, $1.37\,\mathrm{m}$ radius pipe is used as waterline with $290\,\mathrm{m}$ pressure head and $4.5\,\mathrm{m}$ of earth cover [81]. During the simulation, we use this earth cover as a thickness of the outer cylindrical soil layer (t_s). Other parameters that changes during the simulation are: $A = 1\,\mathrm{m^3\,s^{-1}}$, $3\,\mathrm{m^3\,s^{-1}}$, $5\,\mathrm{m^3\,s^{-1}}$; $f = 20\,\mathrm{kHz}$, $30\,\mathrm{kHz}$, $40\,\mathrm{kHz}$; $E = 30\,\mathrm{GPa}$, $40\,\mathrm{GPa}$, $50\,\mathrm{GPa}$; $t_p = 0.139\,\mathrm{m}$, $0.158\,\mathrm{m}$, $0.182\,\mathrm{m}$. When one parameter varies, the other parameters are kept constant with their default values (as given in Section 6.6). The results obtained from these simulation are shown in Fig. (6.10), (6.11), (6.12), (6.13) and (6.14).

From Fig. (6.10) it is seen that, if the signal strength increases, it increases the system noise, as well as increases the propagating signal amplitude, which can propagate for long distance. As same as elastic pipe (as seen in Section 6.6.2), the original AE signal is separated

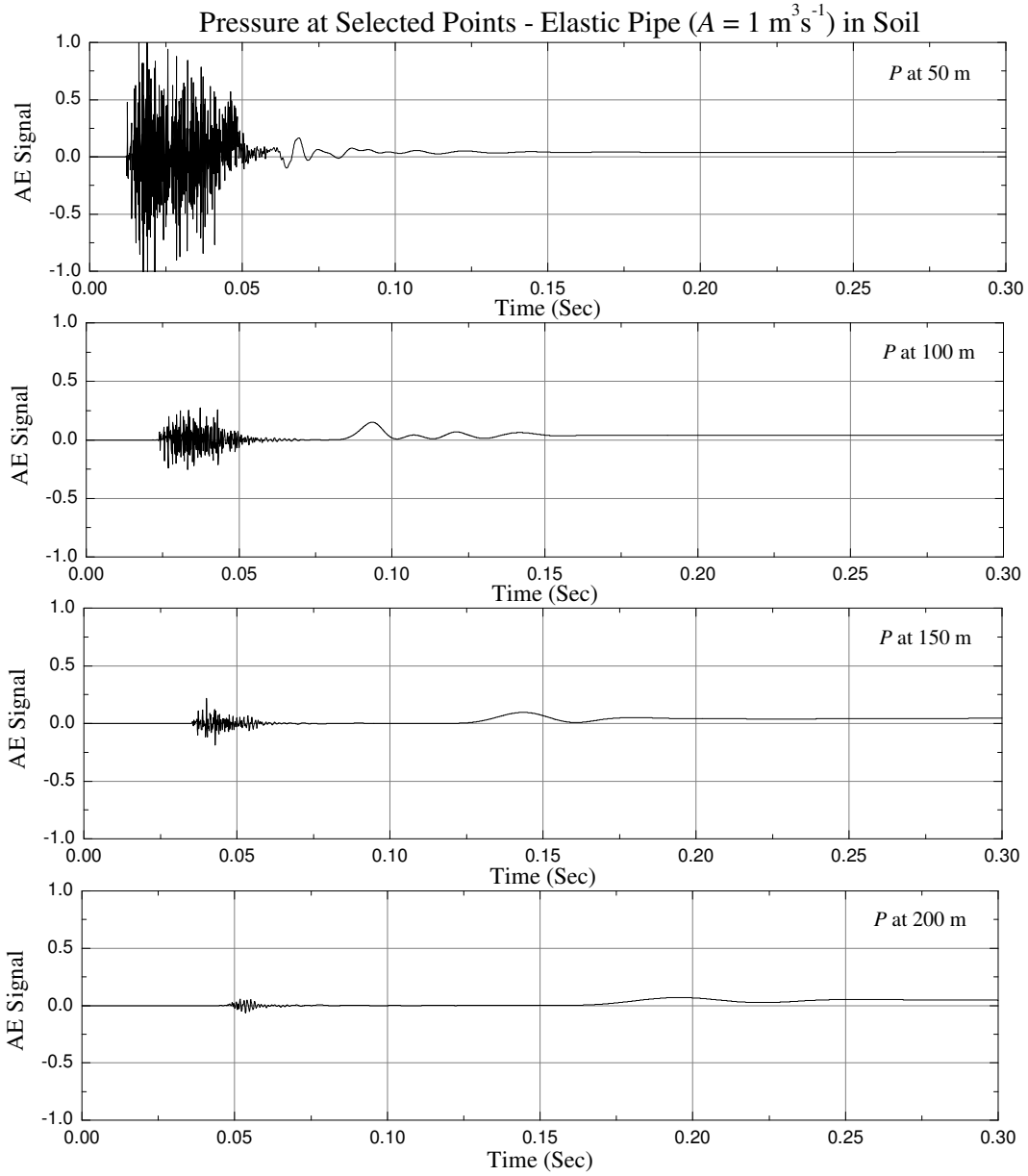

(a) Analytical $v_T = 1{,}103\,\mathrm{m\,s^{-1}}$.

Figure 6.10: Spectral response of water-filled elastic pipe surrounded by soil at (a) $A = 1\,\mathrm{m^3\,s^{-1}}$.

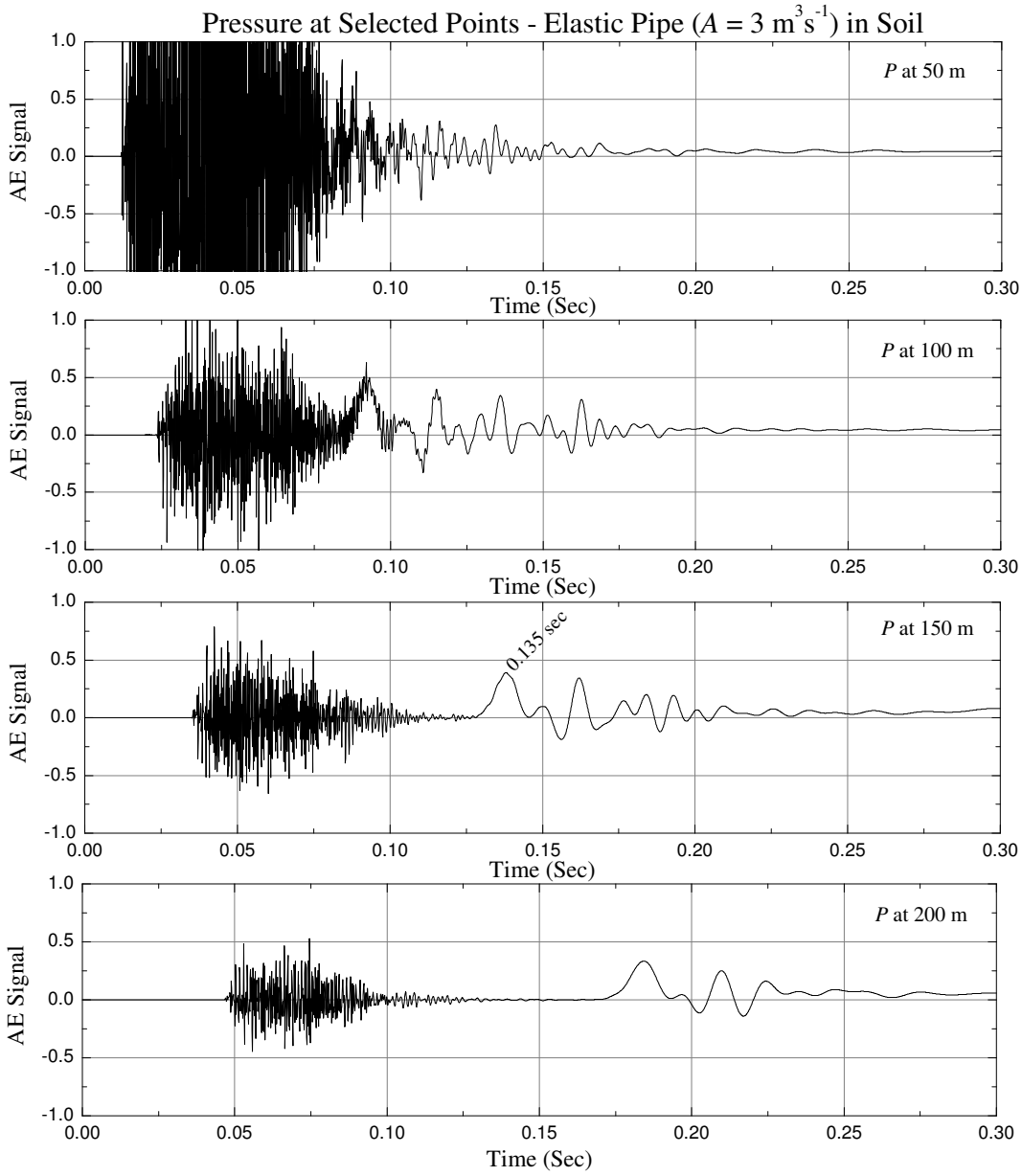

(b) Analytical $v_T = 1{,}103\,\mathrm{m\,s^{-1}}$.

Figure 6.10: Spectral response of water-filled elastic pipe surrounded by soil at (b) $A = 3\,\mathrm{m^3\,s^{-1}}$.

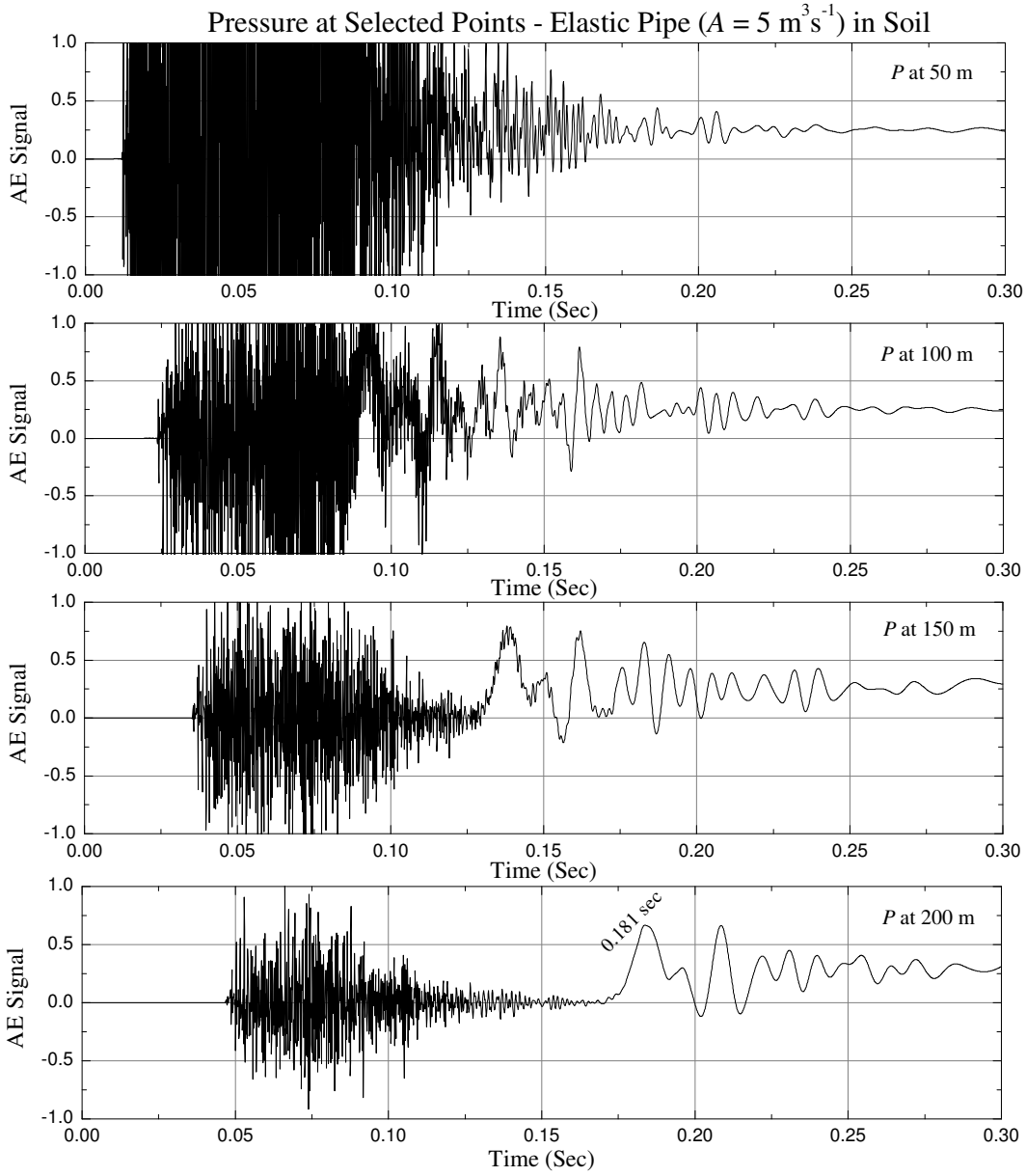

(c) Analytical $v_T = 1{,}103\,\mathrm{m\,s^{-1}}$.

Figure 6.10: Spectral response of water-filled elastic pipe surrounded by soil at (c) $A = 5\,\mathrm{m^3\,s^{-1}}$.

from the system noise during its propagation. It is possible, because the noise signals are generated from the reflection, diffraction and refraction of the original signal during its propagation. Therefore, the noise signal is suffered by the elastic effect of the pipe and outer soil medium. Consequently, the original signal is traveling faster than the background noise. From the investigation it is seen that, the velocity of this wave is same as the tube wave velocity ($v_T = 1{,}103\,\mathrm{m\,s^{-1}}$), which can be calculated using Eq. (4.1). The simulation result (as shown in Fig. (6.10)(b)) has a good agreement with the analytical result, which is given below in each graph. Since, the tube wave velocity does not depend on the source strength, therefore, in all cases the velocity remain same.

Figure (6.11) shows that, increasing the excitation frequency, increases the signal attenuation which decreases the signal strength, because the significant part of the energy of the signal is carried by the higher modes. The results has the same relationship with the elastic pipe case (as seen in Fig. (6.7)), except the signal is distorted due to the elastic effect of outer soil medium. Therefore, form the analysis we can conclude that, in the far-field measurement of long-range pipe inspection, the high frequency AE signal measurement is not important for the AE event localization. Although, it has superior sensitivity to detect the incipient faults of wire break or slip at the earlier stage, in that case, the near-field measurement with the high resolution (e.g. frequency, sensitivity) measuring instruments are required to detect this signal.

As same as previous case, the velocity of the original signal can be computed from the tube wave velocity ($v_T = 1{,}103\,\mathrm{m\,s^{-1}}$). The simulation result (shown in Fig. (6.11)) has a good agreement with analytical result, which is given below in each graph. This velocity is independent from the frequency.

Figure (6.12) shows the pipe elasticity effect on the system rigidity. If the elasticity increases, it increases the pipe stiffness, which reduces the effective cross-sectional area of the pipe. As a result, less energy is radiated from the inside to the outside. Consequently, the signal strength in the high stiffness pipe is more stronger than the lower stiffness pipe. Moreover, in high stiffness pipe the signal can propagate with higher speed. This wave

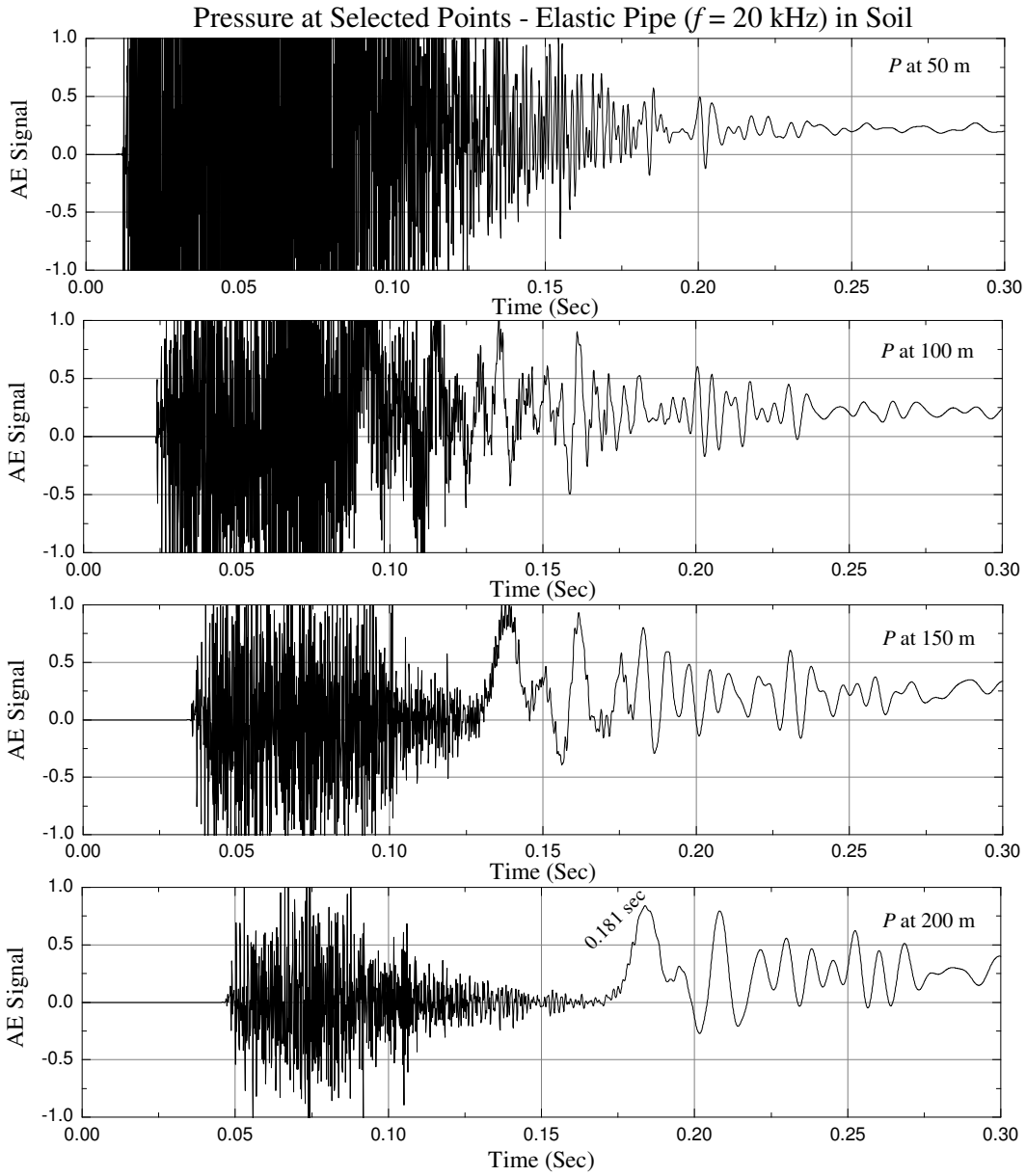

(a) Analytical $v_T = 1{,}103\,\mathrm{m\,s^{-1}}$.

Figure 6.11: Spectral response of water-filled elastic pipe surrounded by soil at (a) $f = 20\,\mathrm{kHz}$.

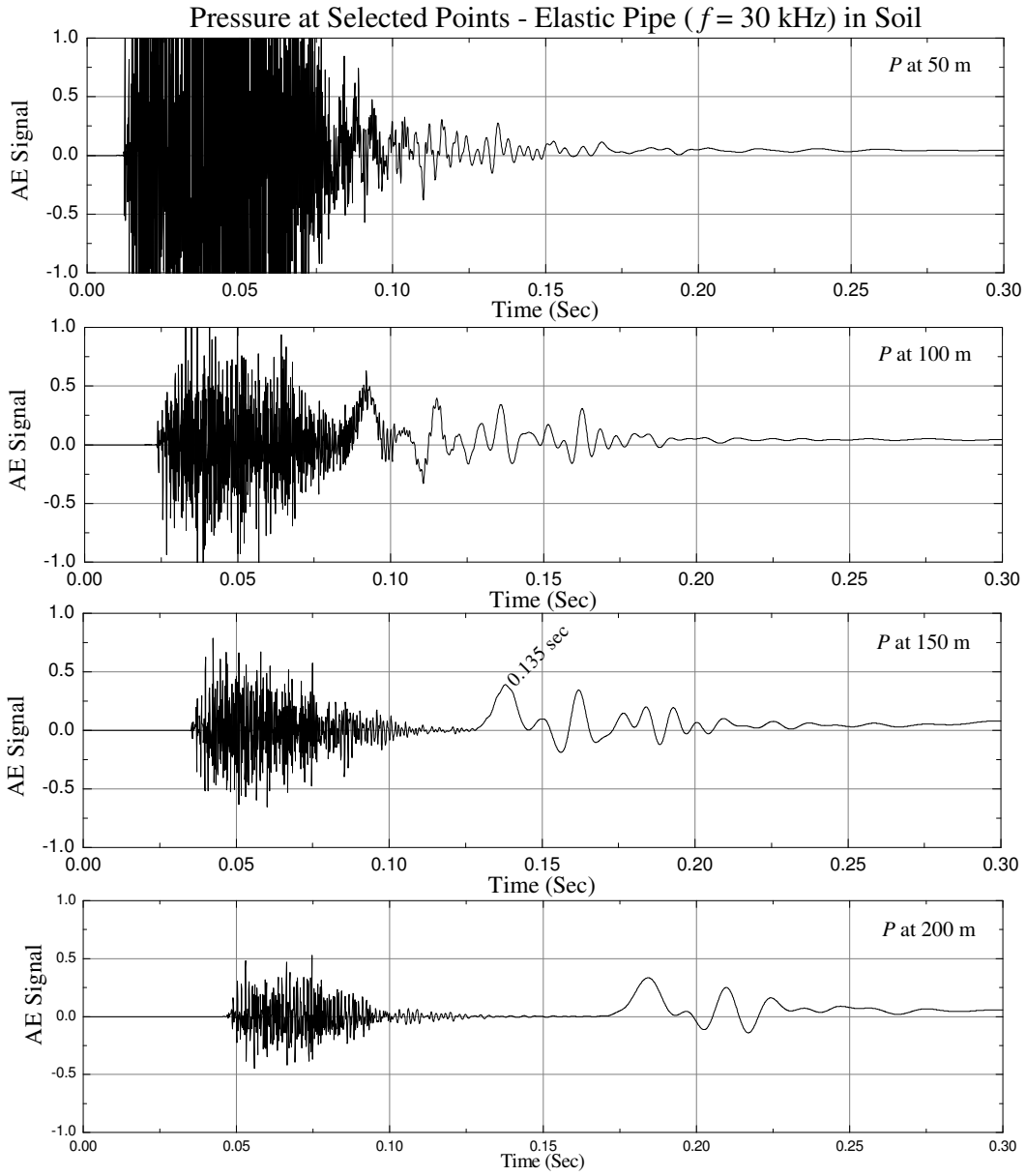

(b) Analytical $v_T = 1{,}103\,\mathrm{m\,s^{-1}}$.

Figure 6.11: Spectral response of water-filled elastic pipe surrounded by soil at (b) $f = 30\,\mathrm{kHz}$.

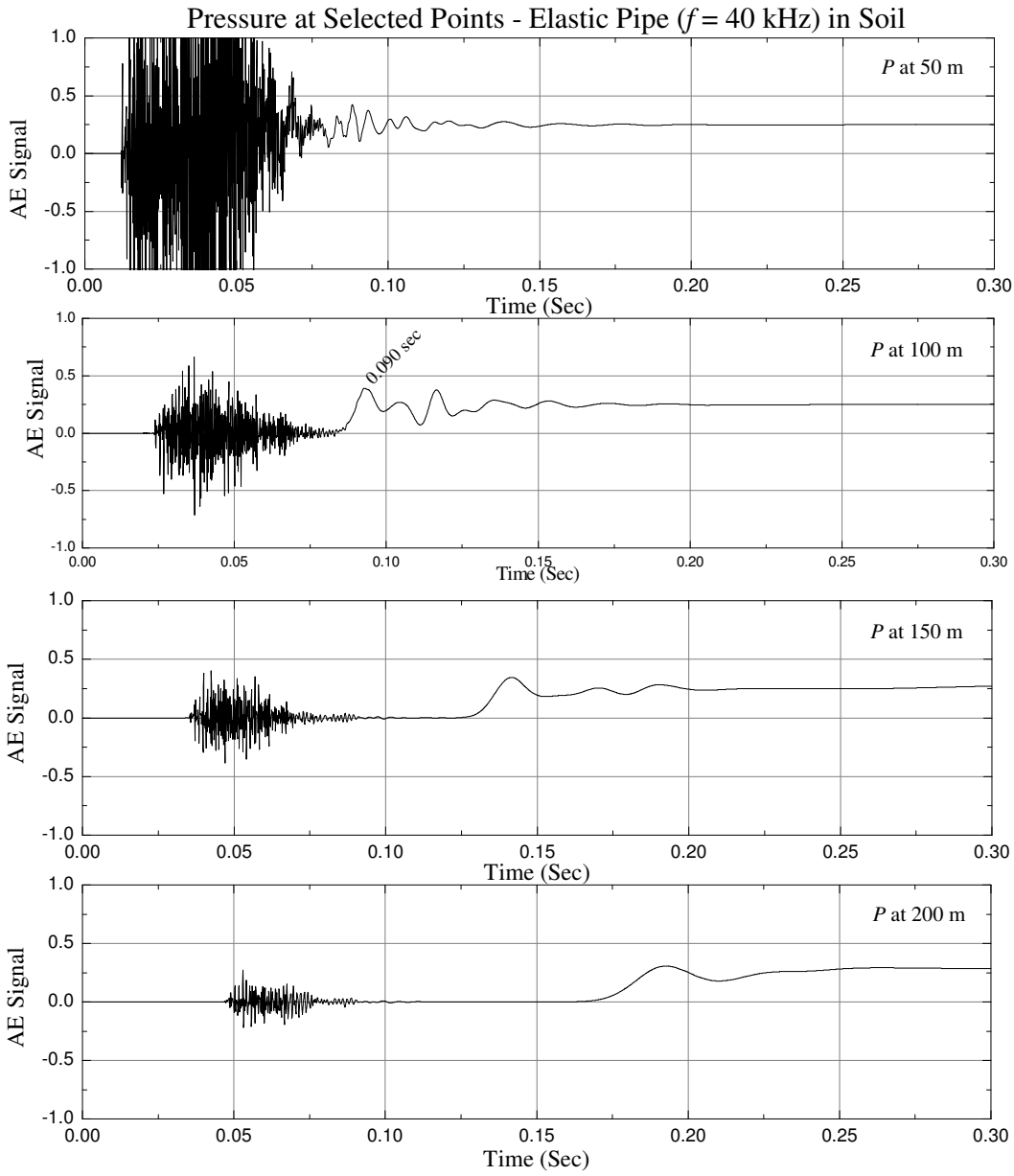

(c) Analytical $v_T = 1{,}103\,\mathrm{m\,s^{-1}}$.

Figure 6.11: Spectral response of water-filled elastic pipe surrounded by soil at (c) $f = 40\,\mathrm{kHz}$.

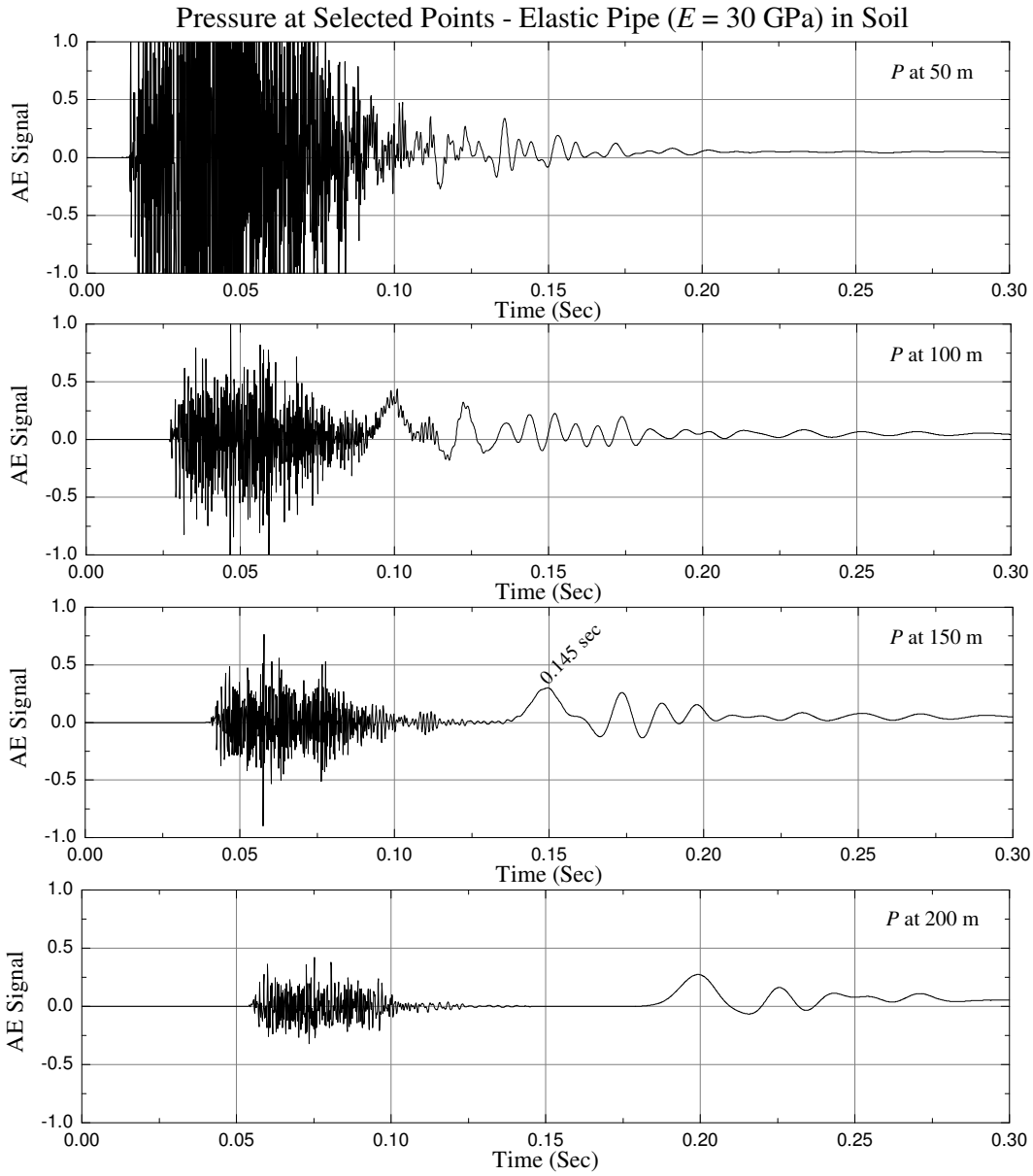

(a) Analytical $v_T = 1{,}028\,\mathrm{m\,s^{-1}}$.

Figure 6.12: Spectral response of water-filled elastic pipe surrounded by soil at (a) $E = 30\,\mathrm{GPa}$.

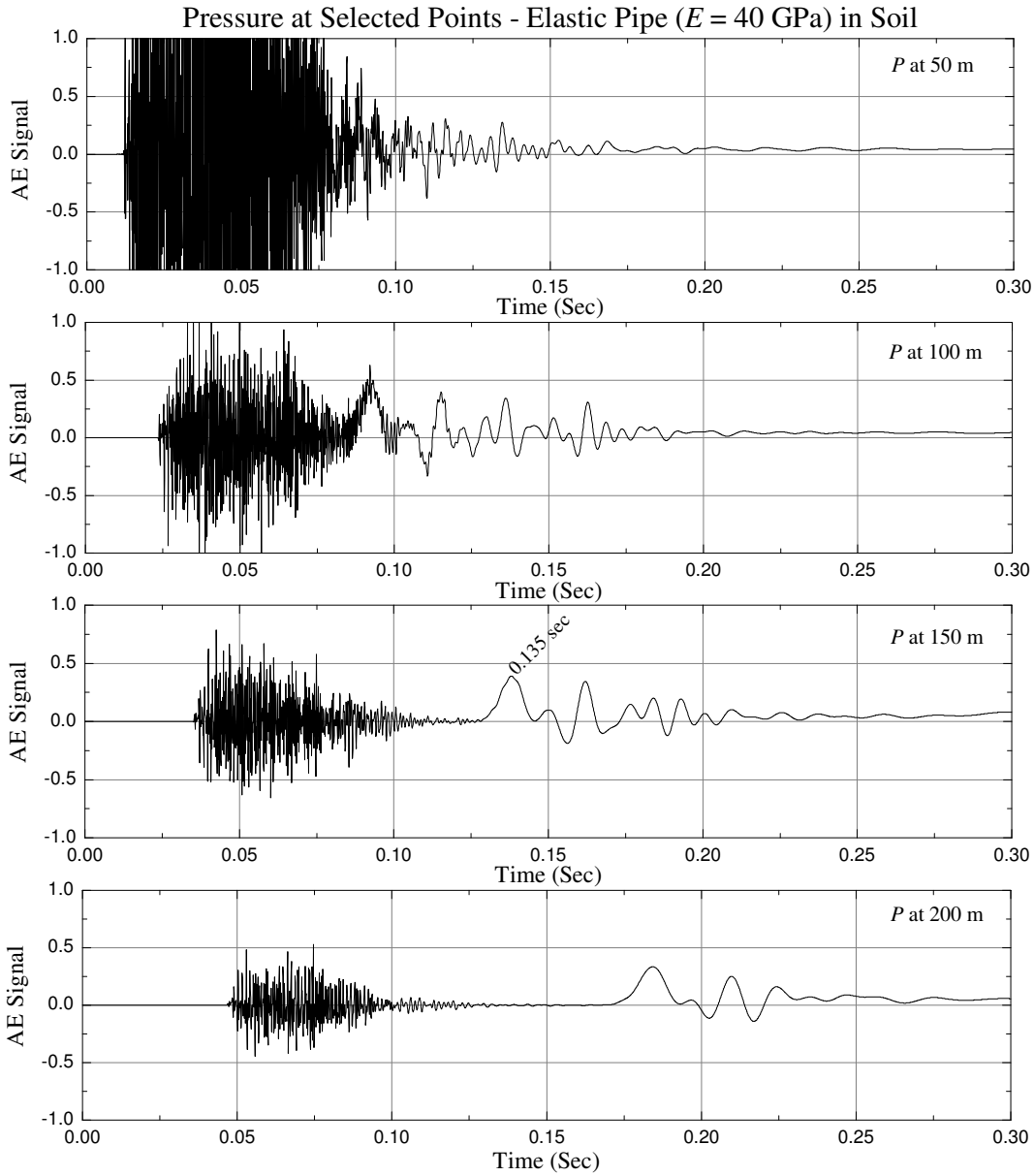

(b) Analytical $v_T = 1{,}103\,\mathrm{m\,s^{-1}}$.

Figure 6.12: Spectral response of water-filled elastic pipe surrounded by soil at (b) $E = 40\,\mathrm{GPa}$.

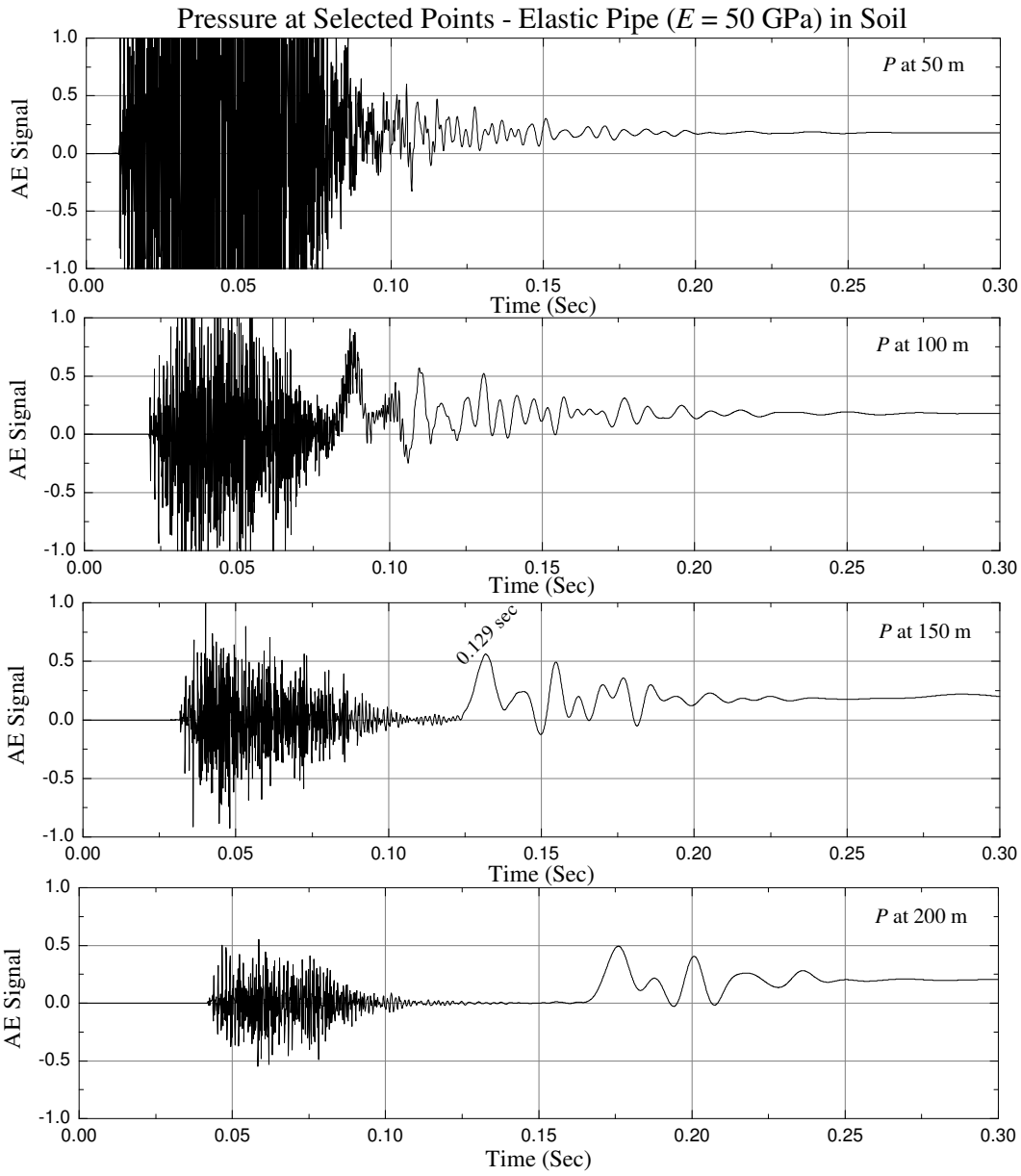

(c) Analytical $v_T = 1{,}157\,\mathrm{m\,s^{-1}}$.

Figure 6.12: Spectral response of water-filled elastic pipe surrounded by soil at (c) $E = 50\,\mathrm{GPa}$.

speed can be calculated by the tube wave equation, which is given below in each graph. The simulated results have a good agreement with these analytical result, which is shown on each graph at arbitrary position. Other effects are same as discussed earlier for elastic pipe.

The effect of pipe thickness is shown in Fig. (6.13). The figure shows that, if the pipe thickness increases, it increases the effective cross-section of the pipe, which decreases the pipe stiffness. Consequently, more energy is penetrated from the inside to the outside. Due to this energy penetration, the original signal becomes weaker and slower. The analytical and simulated velocity of this wave is shown below in each graph and at the arbitrary position on the graph, respectively.

The Fig. (6.14) shows the effect of pipe radius on the AE signal propagation. If the pipe cross-sectional dimension increases, it increases the spatial energy dissipation, which reduces the propagating signal strength. In this case, we use three different types of pipe with different radius and thickness, where thickness also increases with the increasing of radius. As a result, the wave speed increases. The analytical results of these waves can compare with the simulated results, which are given below and on the graph, respectively.

If we compare the results of this section with the results of Section 6.6.2 it is seen that, there is no significant changes on the wave speed due to the outer soil formation. Because, the wave speed mainly depends on the elastic properties of the medium, where elasticity of the PCCP is more dominant among the others. Therefore, the analyses of this section has (nearly) the same tube wave effect as describe in Section 6.6.2. But if we compare the wave shape and strength, some significant changes can be observed, due to the energy dissipation in the soil medium. Other characteristics of the propagating AE signal are same as it is described in Subsection 6.6.1 and 6.6.2. This knowledge is important for the AE monitoring system to determine the phase speed of AE signal in water-filled elastic pipe (PCCP) with different profile surrounded by different outer medium.

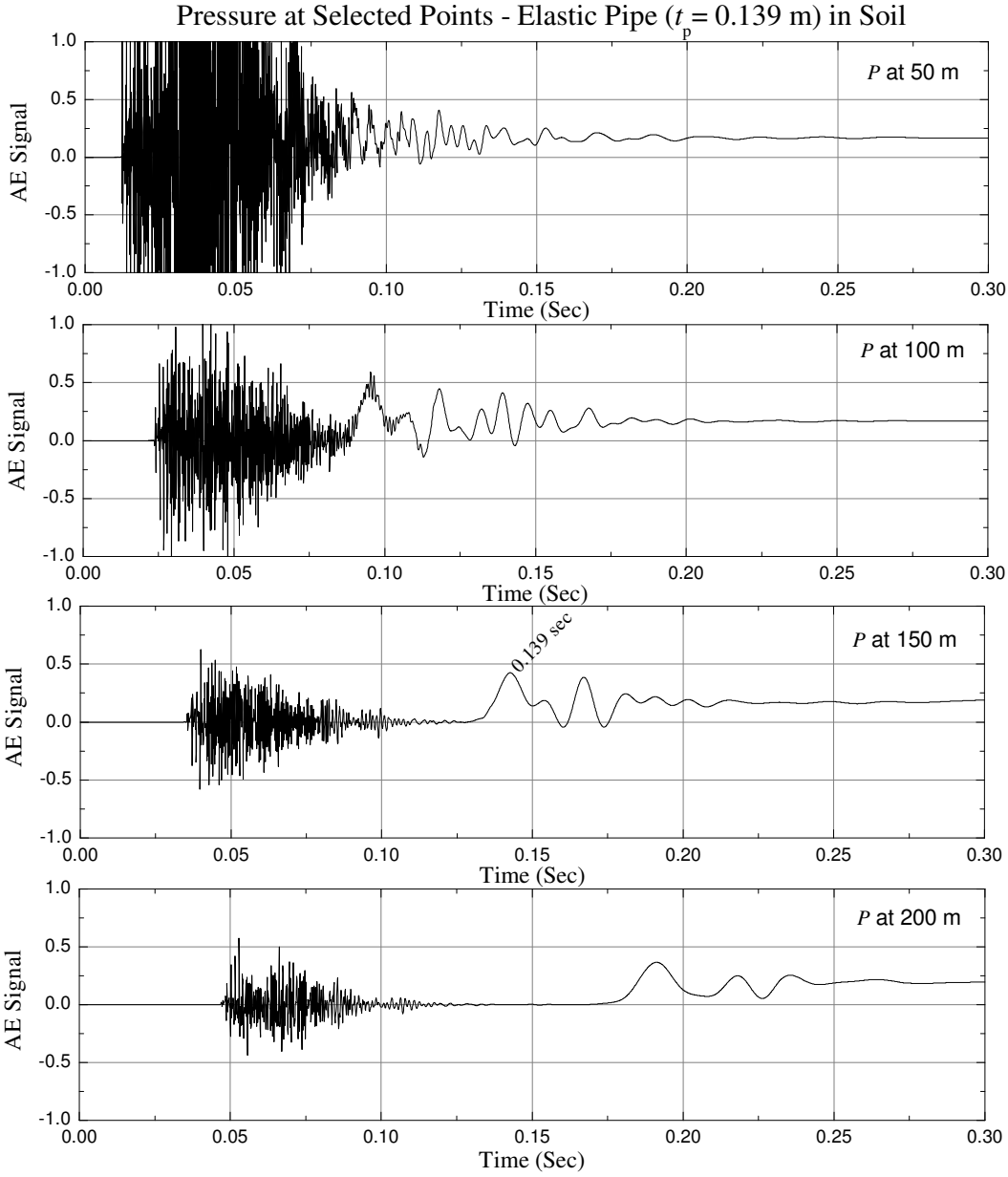

(a) Analytical $v_T = 1{,}074\,\mathrm{m\,s^{-1}}$.

Figure 6.13: Spectral response of water-filled elastic pipe surrounded by soil at (a) $t_p = 0.139\,\mathrm{m}$.

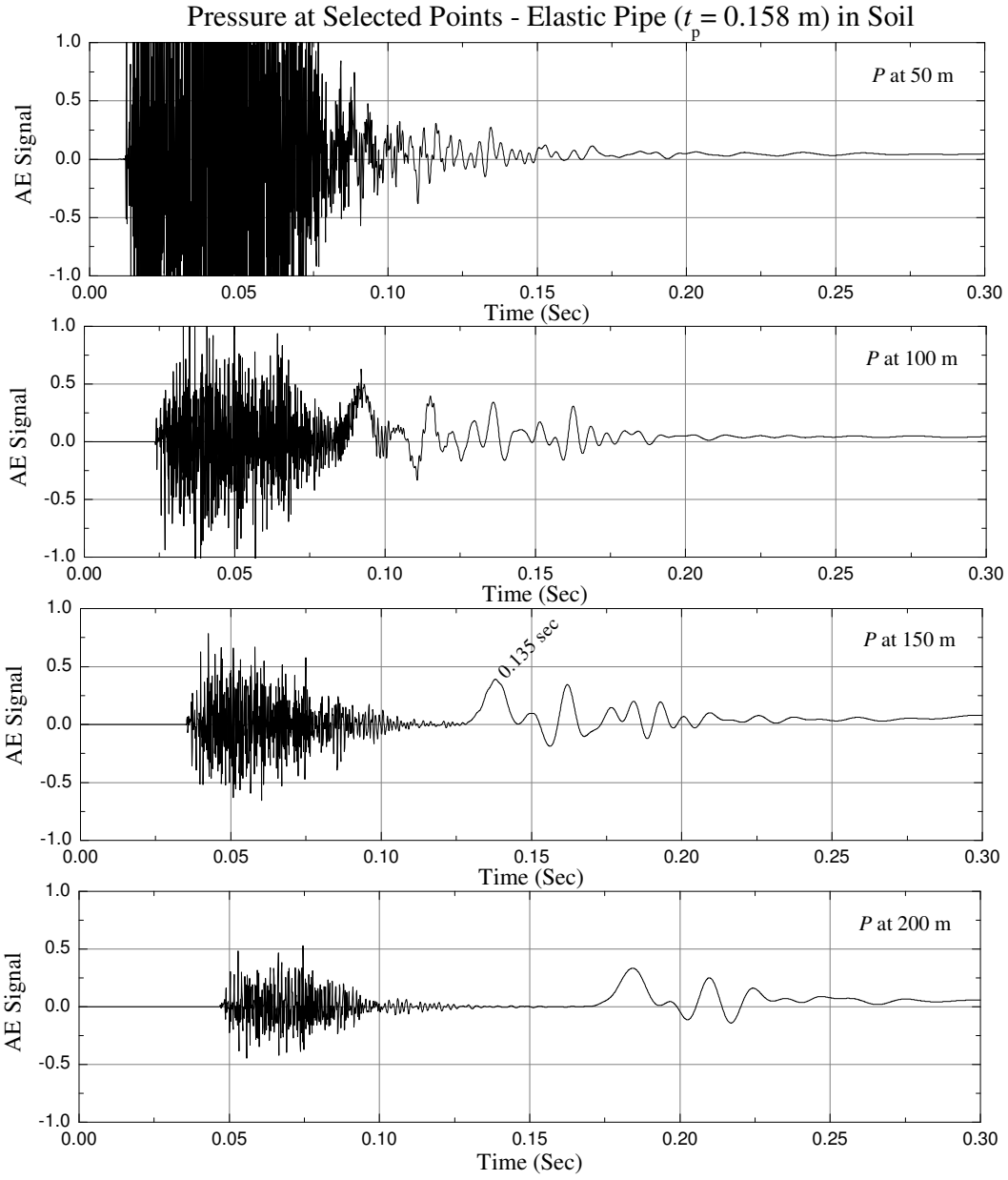

(b) Analytical $v_T = 1{,}103\,\mathrm{m\,s^{-1}}$.

Figure 6.13: Spectral response of water-filled elastic pipe surrounded by soil at (b) $t_p = 0.158\,\mathrm{m}$.

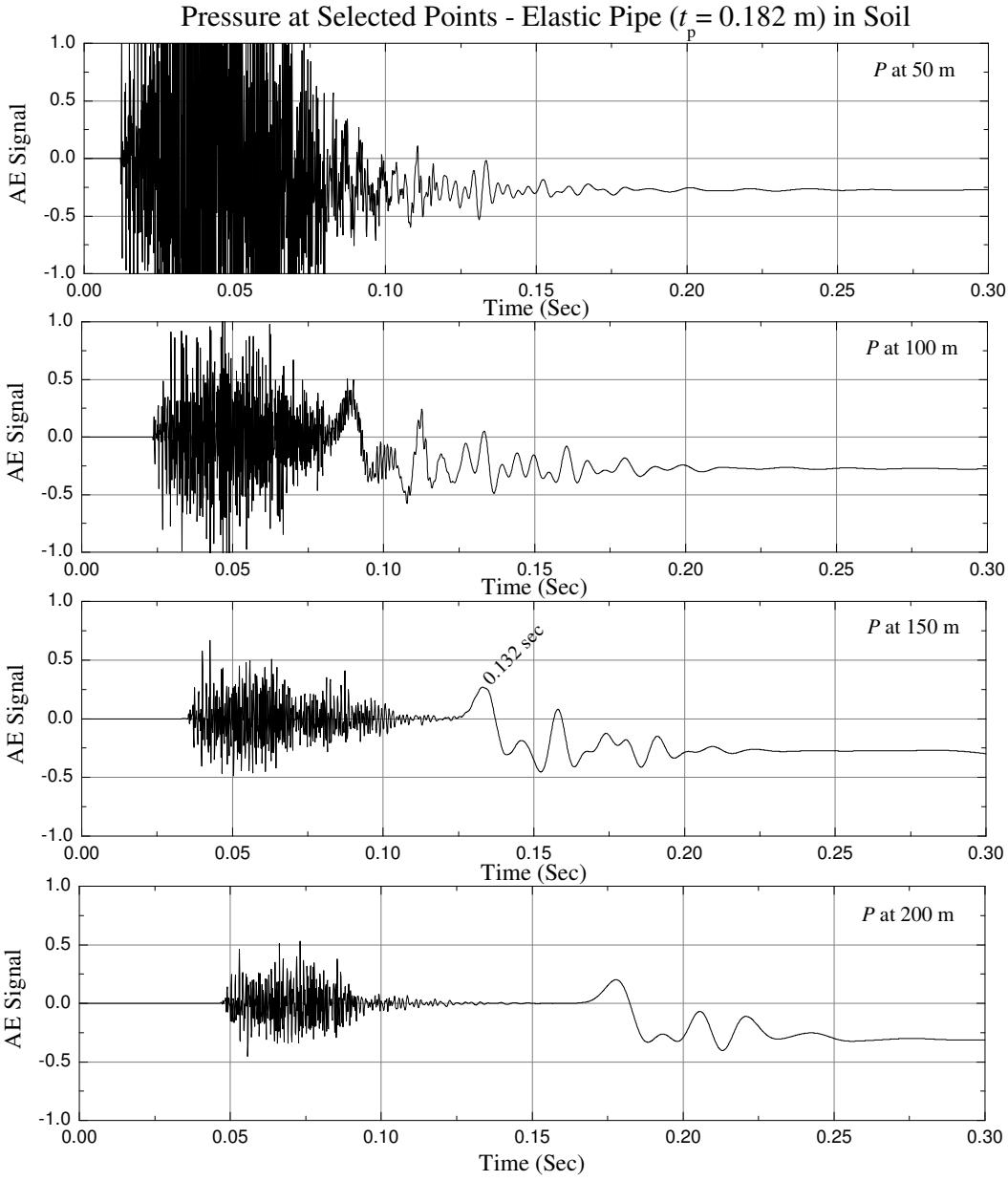

(c) Analytical $v_T = 1{,}133\,\mathrm{m\,s^{-1}}$.

Figure 6.13: Spectral response of water-filled elastic pipe surrounded by soil at (c) $t_p = 0.182\,\mathrm{m}$.

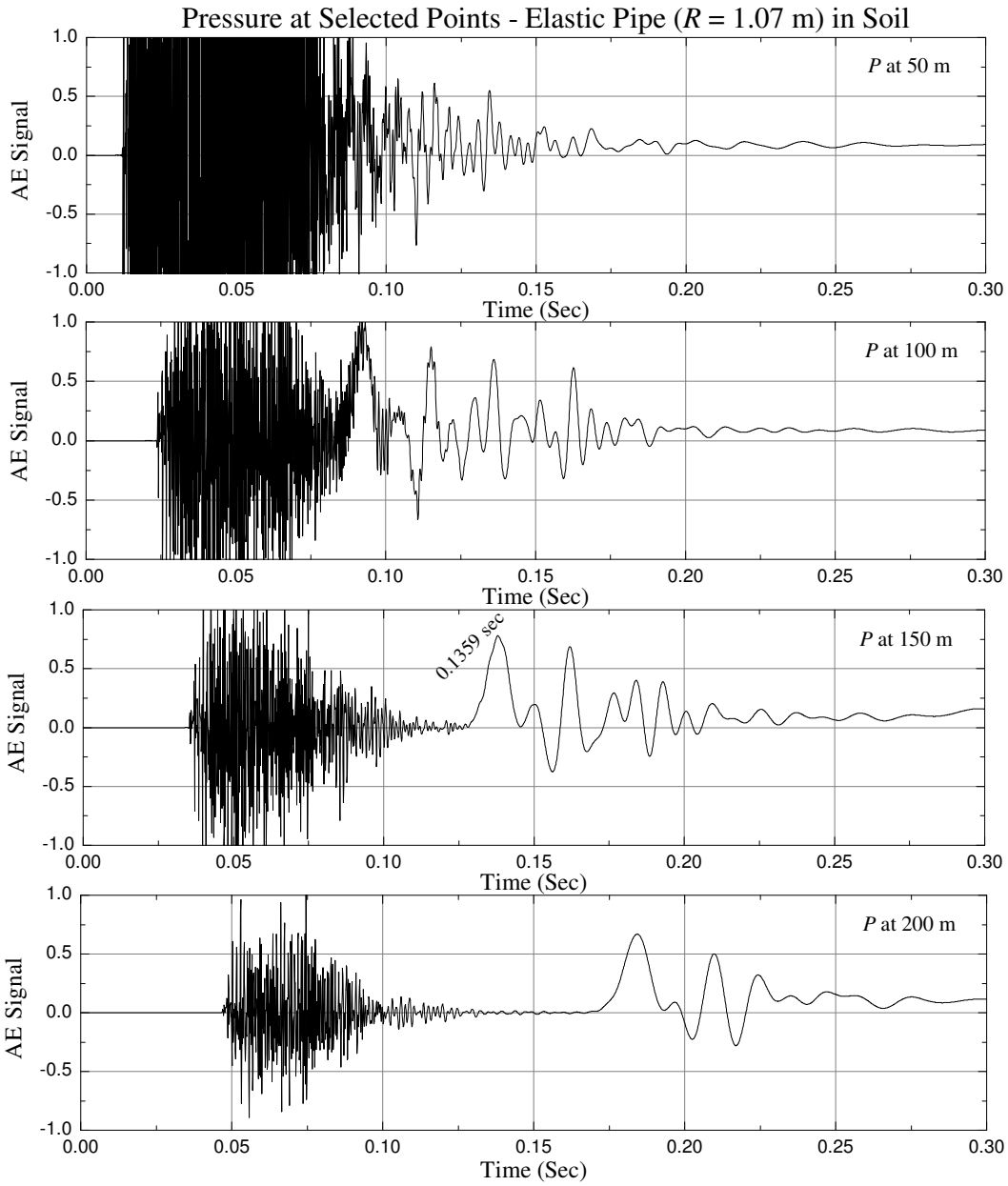

(a) Analytical $v_T = 1{,}103\,\mathrm{m\,s^{-1}}$.

Figure 6.14: Spectral response of water-filled elastic pipe surrounded by soil at (a) $R = 1.07\,\mathrm{m}$, $t_p = 0.158\,\mathrm{m}$.

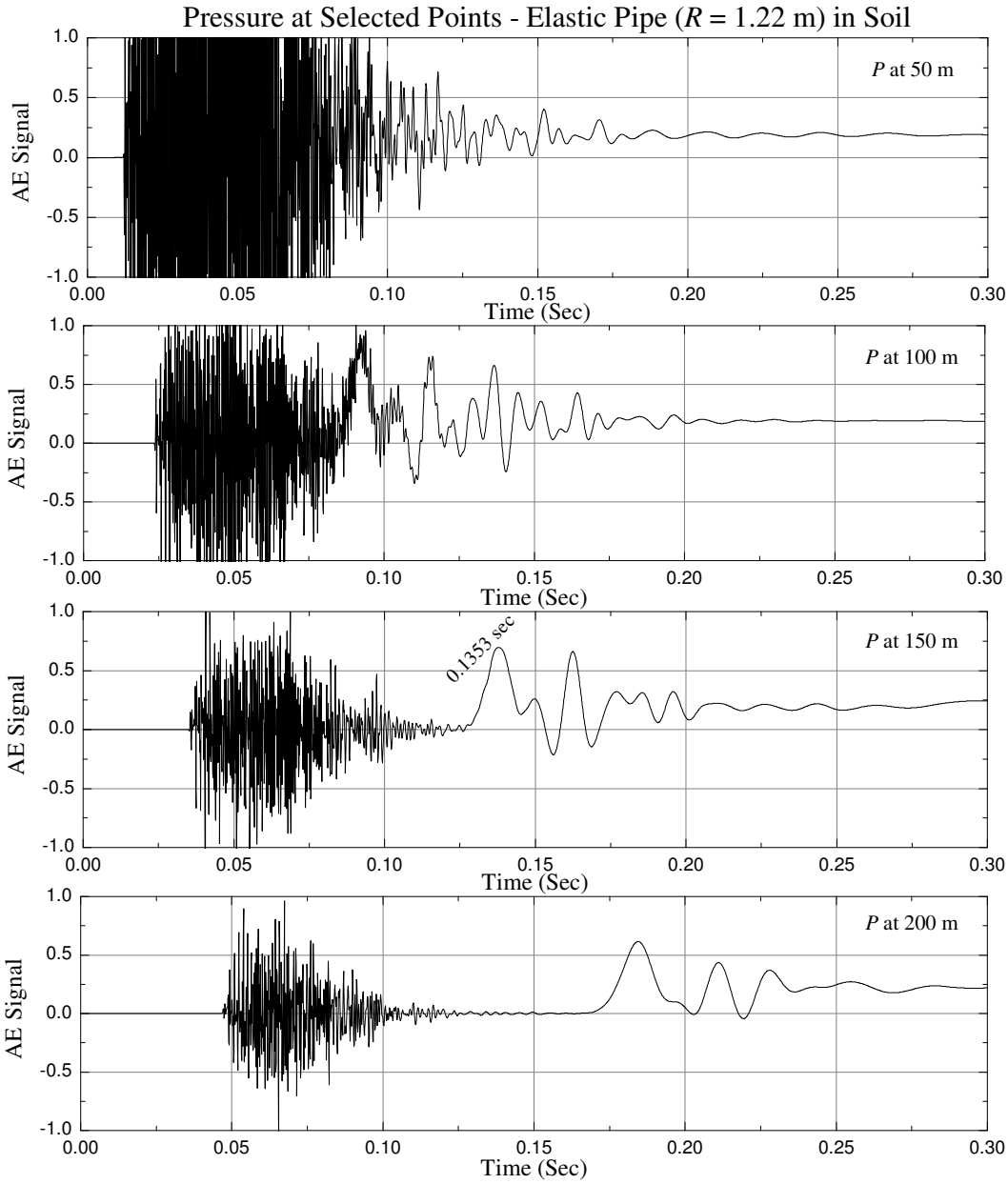

(b) Analytical $v_T = 1{,}108\,\mathrm{m\,s^{-1}}$.

Figure 6.14: Spectral response of water-filled elastic pipe surrounded by soil at (b) $R = 1.22\,\mathrm{m}$, $t_p = 0.184\,\mathrm{m}$.

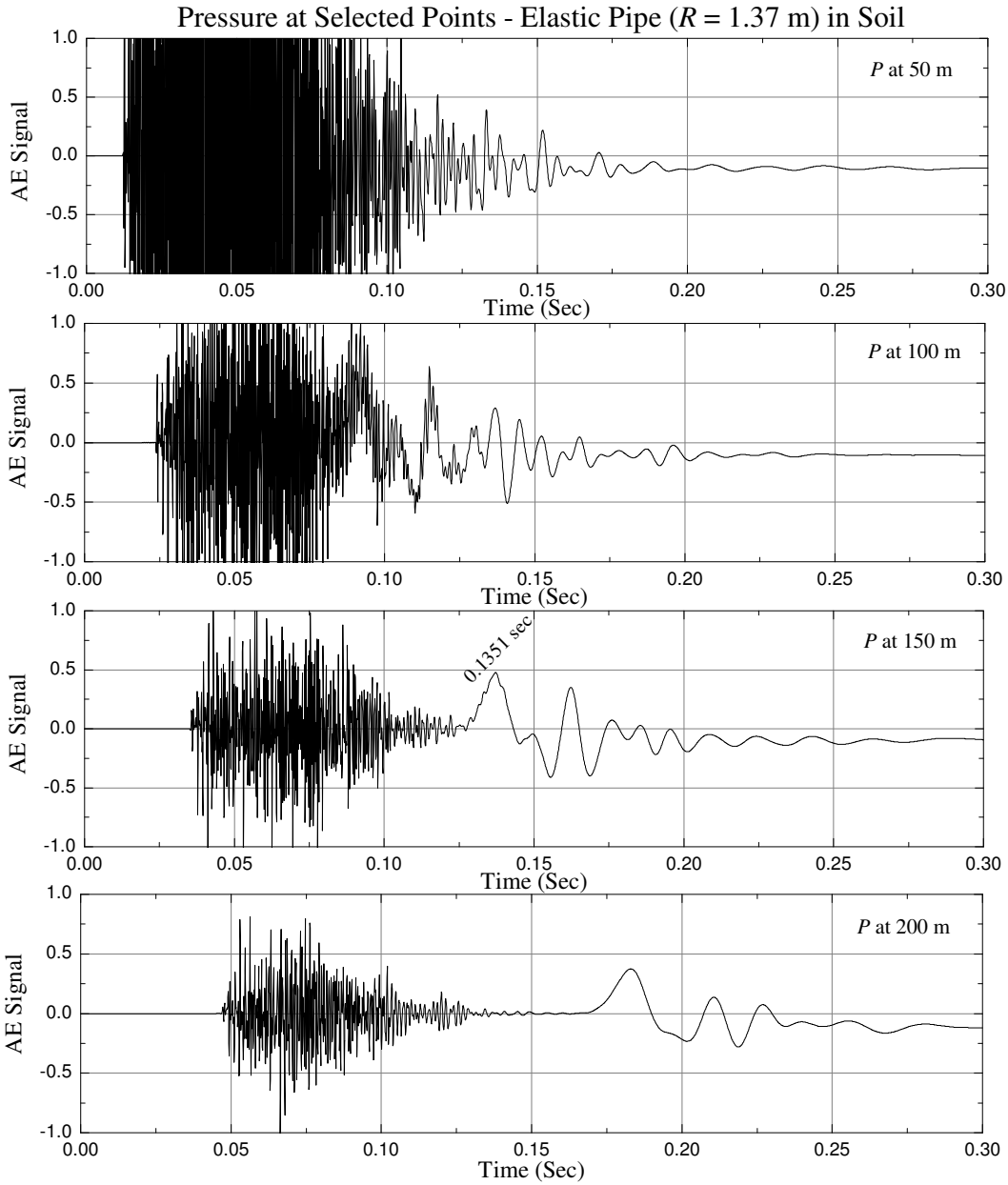

(c) Analytical $v_T = 1{,}110\,\mathrm{m\,s^{-1}}$.

Figure 6.14: Spectral response of water-filled elastic pipe surrounded by soil at (c) $R = 1.37\,\mathrm{m}$, $t_p = 0.209\,\mathrm{m}$.

6.6.4 Fluid-filled Elastic Pipe Surrounded by Different Soil

The PCCP are generally placed below the surface ground in the soil for the large-scale transmission and distribution of potable- and waste-water. The properties of the surrounded soil depends on the depth and geographical location of the pipe. However, in this study we choose three different types of soil: Sandy Loam (Adrian soil), Silt Loam (Catlin soil) and Sand (Plainfield soil), from the Canadian soil texture triangle [128], to observe the different types of soil effect on the AE signal propagation. The properties of these soils are given in Section 6.6. The thickness of the soil (t_s) is same as Subsection 6.6.3. Other parameters, such as, pipe dimensions (e.g. $R = 1.07\,\mathrm{m}$, $t_p = 0.158\,\mathrm{m}$), elastic properties (e.g. $E = 40\,\mathrm{GPa}$, $\rho_P = 2{,}400\,\mathrm{kg\,m^{-3}}$), fluid properties (e.g. $v_F = 1{,}500\,\mathrm{m\,}s^{-1}$, $\rho_P = 2{,}400\,\mathrm{kg\,m^{-3}}$), and excitation signal properties (e.g. $A = 3\,\mathrm{m^3\,s^{-1}}$, $f = 30\,\mathrm{kHz}$) are kept as constants.

Figures (6.15)(a), (b) and (c) show the time response of AE signal propagation through water-filled elastic pipe at selected points, which is surrounded by Adrian, Catlin and Plainfield soil, respectively. From the figures it is seen that, the velocity of the acoustical wave has a good agreement with the analytical result, which is given below in each graph.

If we compare the results of Fig. (6.15) with the same pipe in vacuum or air medium as discussed in Subsection 6.6.2 (e.g. Fig (6.6)(b)), it is noticed that the characteristics of propagating acoustical wave (e.g. velocity) are nearly same in all cases, except the wave shape and the amplitude. This means that, the outer soil formation has less impact on the propagating wave velocity inside the pipe in the fluid medium. This fact is due to the velocity of acoustical wave inside the pipe, which is greatly affected by the high stiffness of pipe characteristics. Usually, the pipe stiffness is thousand times greater than the soil stiffness.

On the other hand, the signal shape and the strength mainly depends on the surrounding medium characteristics. Different medium has different reflection, diffraction and refraction characteristics. Each of this has different delayed version of AE signal due to multipath propagation. The acoustical wave in the fluid inside the pipe is the superposition of these delayed signal. Therefore, wave shape and strength are affected by the characteristics of

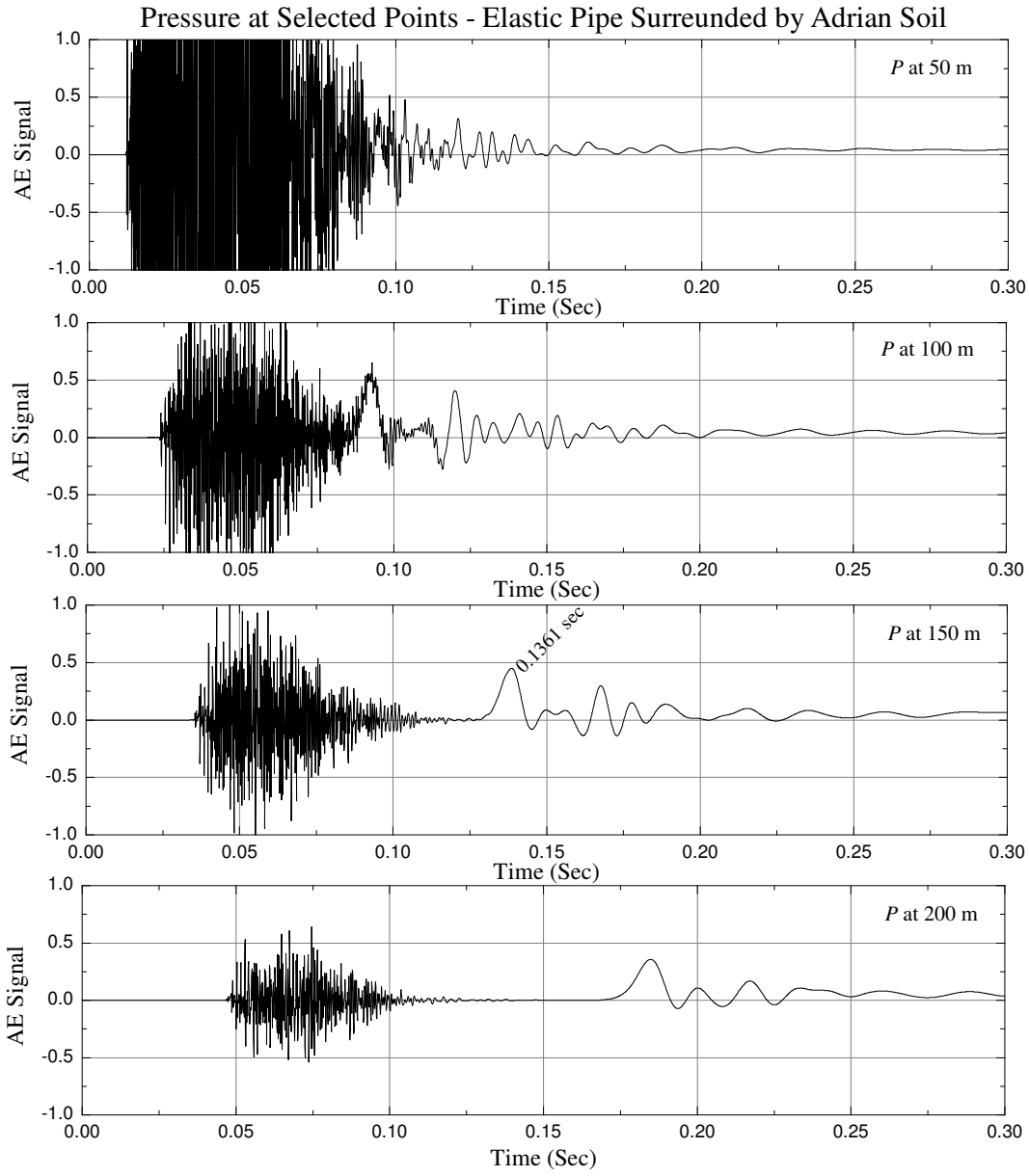

(a) Analytical $v_T = 1{,}102\,\mathrm{m\,s^{-1}}$.

Figure 6.15: Spectral response of water-filled elastic pipe surrounded by (a) Adrian soil.

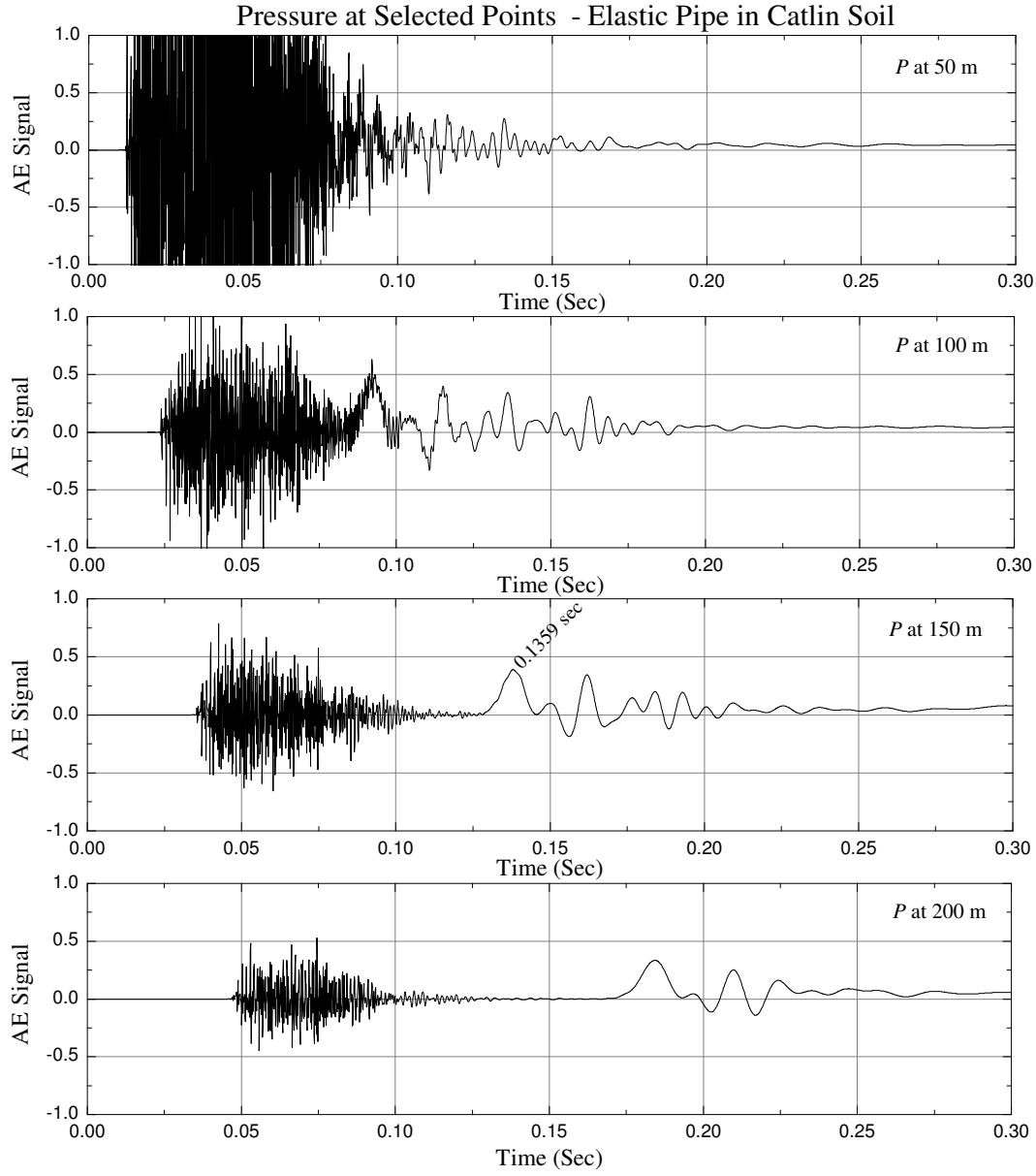

(b) Analytical $v_T = 1{,}103\,\mathrm{m\,s^{-1}}$.

Figure 6.15: Spectral response of water-filled elastic pipe surrounded by (b) Catlin soil.

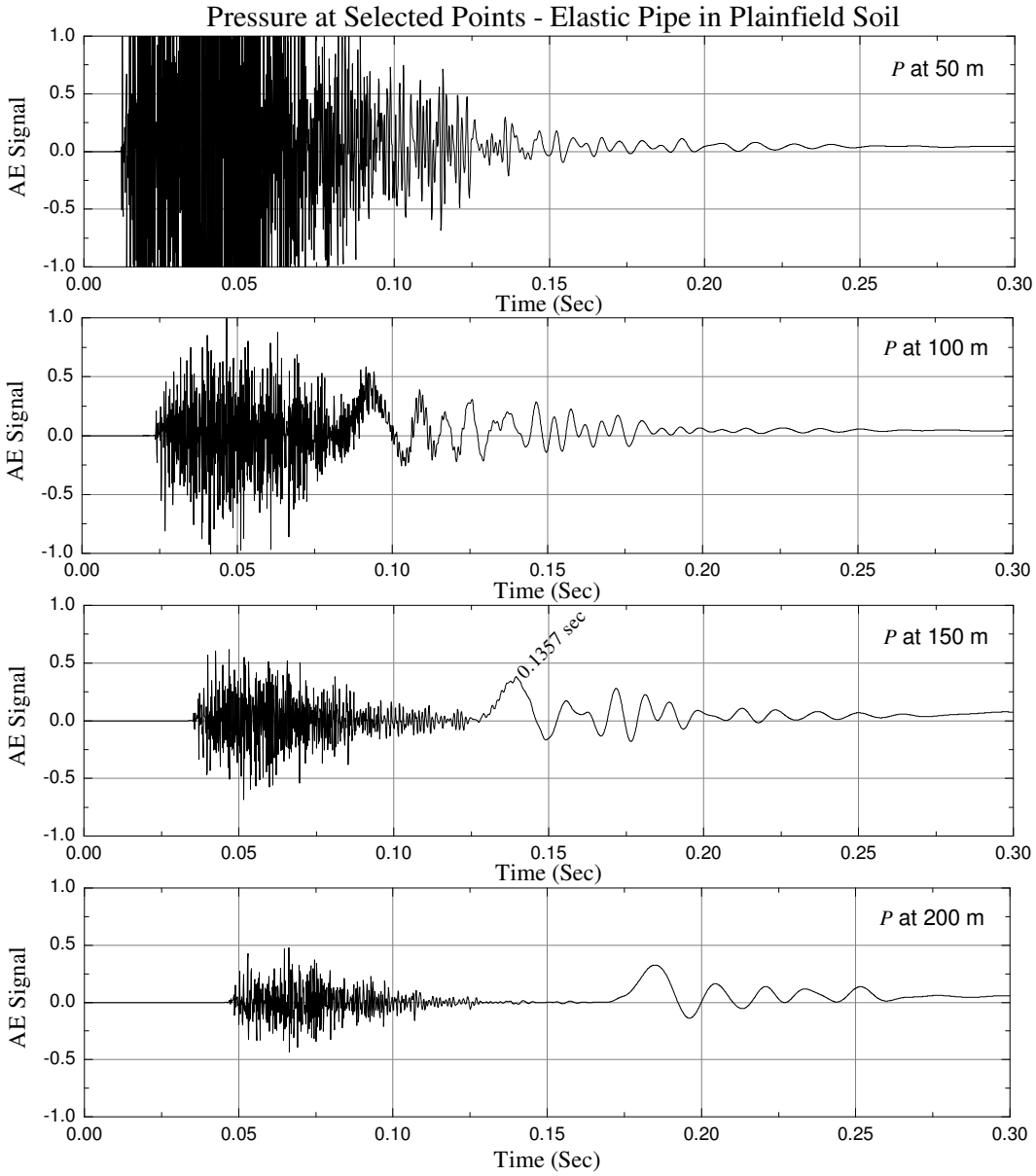

(c) Analytical $v_T = 1{,}105\,\mathrm{m\,s^{-1}}$.

Figure 6.15: Spectral response of water-filled elastic pipe surrounded by (c) Plainfield soil.

the medium. From Fig. (6.15), we can observe this effect, where higher acoustic speed of the outer formation causes more energy penetration. Moreover, higher stiffness of the outer formation causes less effect on the velocity of the acoustic wave inside the pipe.

The results has a good agreement with the result obtained in Subsection (4.6.3) of Chapter 4, for low frequency case. This type of information is important for the AE monitoring of pipeline system when the test is perform under different outer formation for high frequency AE event.

6.7 Summary

The high frequency analysis of AE signal propagation through fluid-filled PCCP is performed under different radii, thickness, and stiffness of the pipe and the outer formation. As a high frequency, we use sonic/ultrasonic frequency, with in the range of current AE signal measurement technique. The effect of pipe and outer soil formation is observed and compared the result with the available solution.

From this study it is found that, the characteristics of the propagating AE signal greatly depends on the signal and the pipe characteristics. High frequency excitation signals are not significant in the far-field measurement of long range pipe inspection. However, the high frequency analysis can provide earlier indication of incipient fault, such as, frictional rubbing of early stage of wire break or slip related event of PCCP. This kind of information can be observe by using high frequency and sensitive measuring instruments in the near-field measurement. This early warning advantage opens the way for performing following tests economically to verify the defect.

Chapter 7

Conclusions and Recommendations

7.1 Concluding Remarks

The propagation of acoustic signals provides fundamentals for non-destructive performance test of fluid-filled cylindrical pipes that are buried in the ground. Through theoretical analysis, many important mathematical features of such propagation can be revealed to help understand and interpret the testing data. In industrial applications, the acoustic signals are generated through the breakage or sliding of steel wires that are prestressed to structurally enforce the pipes. These signals feature certain frequency spectral characteristics that ranges from sonic/ultrasonic frequencies. This thesis presents numerical investigation of this problem. Insightful observations for acoustic wave in the time and frequency domain were achieved by analyzing Navier's equation of motion. The interaction between the fluid and the surrounding formations were modeled by applying Newton's laws of motion and the principle of virtual work. The model was investigated for the sonic and ultrasonic frequency excitation signal. The numerical analysis of various radius, stiffness and thickness of the pipe as well as different types of surrounding medium, was carried out by using commercial finite element code. Finally, the results were compared with available analytical solutions.

The theoretical background of current technology used in the related industry were discussed in Chapter 2. The brief overview of design details of currently used PCCP (e.g. construction, dimensions, joints) were presented according to AWWA standard and manufacturer's data sheet. The causes of corrosion, consequently, AE signal generation in the

PCCP were discussed here. Different types of AE monitoring devices, such as, hydrophones and accelerometers, were presented to get an idea about the AE signal sensors. The AET method, that is used in the related industry for the AE monitoring purpose was described here. As we described earlier, this method is based on the field data analysis. The main purpose is to detect and to locate the AE events. The testing process, localization procedures and some typical AE signals of this method were presented in this Chapter. Finally, the advantages and the limitations of the testing method were presented.

The mathematical model for the complete solution of AE signal propagation, where the signal travel through different media, such as, fluid, pipe structure, outer medium (e.g. air, water, soil) was developed in Chapter 3. The complex coupled problem of this acoustic wave propagation was modeled by using Navier's equation of motion. The interaction between the fluid and the surrounding outer layers were modeled by applying Newton's laws of motion and the principle of virtual work. The AE source was modeled based on the constant volume velocity. The Hook's law was used to model the released elastic energy of the AE events. In this chapter, the time and frequency domain models were developed for transient and time harmonic analyses of AE signal propagation.

The impact of the path on AE signal propagation was illustrated in Chapter 4 by the tube wave analysis at different pipe properties. It was observed that the speed of the wave traveling in the fluid surrounded by the finite stiffness pipe was lower than the actual speed of the wave in an unbounded fluid. The tube wave effects were observed under plane-wave propagation and verified with the calculated theoretical values. From the simulation results, it was found that, the tube wave speed depends on pipe stiffness which mainly depends on elastic properties of the pipe materials as well as dimensions of the pipe. The stiffness of the pipe increases with the increasing of elastic properties of the pipe materials and the pipe thickness. On the contrary; it decreases with the increasing pipe radius. It was also seen that the higher the stiffness, the higher the rigidity of the pipe, and that influences less on the tube waves. In contrast to the soil properties, the pipe profile depends on the pipe materials and dimensions that play an important role on the overall system stiffness. Therefore, in

case of high stiffness pipe profile, there was no need for more attention in the estimation of accurate soil parameters. Moreover, from the simulation results, it was observed that high stiffness of the pipe can reduce the signal energy penetration from inside to outside of the pipe. In this chapter, the simulation results were verified with the theoretical values and found good agreement.

In Chapter 5, the impacts of the rigid pipe radius on the stoneley and rayleigh modes, and the phase speeds of the system were studied. The results showed that the radius had significant impacts on the rayleigh modes, but not on the stoneley modes of propagation. Extra harmonic eigen waves were observed in the rayleigh modes. In the chapter, we also observed that the stiffness of the elastic pipe increased when the inner radius decreased or the pipe thickness increased, which enhanced the effective damping of the materials. Consequently, the low cut-off frequency decreased and more modes of the signals propagated, which increased the dispersion complexity at the sensors. The simulation results showed that the higher the elasticity of the pipe materials, the greater the effective damping. It was also showed that the pipes with higher rigidity had less impact on the propagation and evanescent modes. Therefore, the effect of the complicated dispersion is reduced. Regarding the effects of the surrounding formulation, the signal penetration was reduced if the phase speed of the medium was increased, resulting in lower impacts on the phase speed of the acoustic signal inside the pipe. Overall, the speed of the acoustic signals propagating through pipes was not constant and was affected by the pipe profiles and the surrounding formations.

Chapter 6 described the high frequency analysis of AE signal propagation through fluid-filled PCCP under different radii, thickness, and stiffness of the pipe and the outer formation. As a high frequency, we used sonic/ultrasonic frequency with in the range of current AE signal measurement technique. The effect of pipe and outer soil formation were performed to observe the surrounding layered medium effect. Form the results, overall it was observed that the increasing signal strength increases the system noise due to the reverberations from the pipe boundary. On the contrary, it can propagate for long distances. Moreover, increasing the excitation signal frequency increases the attenuation, which decreases the signal strength,

because the significant part of energy of the signal is carried out by the higher modes. The effect of pipe elasticity was observed by changing the stiffness, thickness and radius of the pipe. It was observed that, increasing elasticity increases the pipe stiffness, which reduces the effective cross-sectional area of the pipe. And hence, less energy is radiated from the inside to the outside. If the pipe thickness increases, it increases the effective cross-sectional area of the pipe, which decreases the pipe stiffness. As a result, more energy radiated from the inside to the outside. The effect of radius, also gave the same effect of cross-sectional area of the pipe, described in the above. The simulation results in all cases were compared with the available analytical solution and found good agreement.

Finally in the appendices, the principle of virtual work and stress, strain and displacement relationships were described. These information were used in Chapter 3 in the formulation of mathematical model.

7.2 Future Recommendations

As described in Chapter 2, the limitations of current AE monitoring method, prevents the system to get the actual AE signal. In this work, we mainly discussed some of its limitations by the theoretical analysis. This analysis is important to analyze the AE signal and to indicate the level of active distress in the observed pipeline. More precise analysis and the experimental validations are required to establish the proposed method.

The model that was developed in Chapter 3 is the fundamental mathematical model of the acoustic wave propagation through fluid-filled pipe. The proposed model is independent of sources, dimensions and medium characteristics. Therefore, it can be used for the analysis of acoustic wave propagation through any type of cylindrical shells immersed or surrounded by different types of medium. To establish this model, it is necessary to verify the numerical results with the experimental results.

The theoretical studies on tube wave analysis, presented in Chapter 4 can produces the fundamental concepts of low profile acoustic signal in the AE monitoring system. From the simulation results, it was observed that the high stiffness pipe can reduce the signal energy

penetration from the inside to the outside of the pipe. This is an important note for the AE signal when it is measured by the sensor far away from the source. The experimental validation is require to establish this comment.

The tube wave analysis of plane wave propagation in the fluid-filled pipe is also used in the measurement of acoustic properties of substance, impedance tube, and the seismic monitoring of underground fluid reservoirs, borehole coupling of dam site investigation, groundwater aquifers, etc. Therefore, the model and the knowledge obtained from the tube wave analysis can be use in many applications. The current analysis, therefore, has fundamental importance of these applications.

In Chapter 5, the eigenfrequency analysis was used to identify the system's resonance frequencies and its effect on the acoustic signal. In addition, the modal analysis was performed to identify the systems dynamic characteristics, such as, cut-off frequency, propagation constant and the number of propagating modes. This eigen and modal solutions are the fundamentals for a number of more complex wave propagation studies, such as system vibration, pulse propagation and perturbation analysis. Therefore, the study produces the fundamentals on which better non-destructive pipe performance testing technologies can be designed.

The eigenfrequency analysis of piping system is also used in thermodynamic or chemical engineering processes to observe the performance degradation of the piping system, in the design of tunable vibration absorber for noise reduction in HVAC system, aero-elastic wind tunnel and aircraft. The use of guided waves in NDT of piping system is an attractive and widely used technique. The scope of the analysis presented in this work includes the evaluation of dispersion behaviour of eigen and guided waves in hollow or liquid-filled cylinders. In long-range inspection of pipes, this will be largely reduces inspection time and costs compared to the ordinary point by point testing in large pipelines.

From the study of Chapter 6 it was found that, the characteristics of the high frequency propagating AE signal greatly depends on the signal and the pipe characteristics. High frequency excitation signals are not significant in the far-field measurement of long range

pipe inspection. However, the high frequency analysis can provide earlier indication of incipient fault, such as, frictional rubbing of early stage of wire break or slip related event of PCCP. This kind of information can be observed by using high frequency and sensitive measuring instruments in the near-field measurement. This early warning advantage opens the way for performing following tests economically to verify the defect.

Based on the research outcomes mentioned above, an intelligent AE signal sensing technology will be investigated. A number of mathematical approaches, such as neural network and fuzzy logic, will be employed in the development of a process model, on which the intelligent sensor can be built. It is anticipated that, the research will result in new knowledge and experience that will enable us to design a new AE technology that can maximize the reliability and minimize the operational cost of PCCP monitoring. Investigation into this will be reported in future publications.

Appendix A

Principle of Virtual Work

Let us consider a pipe structure with deformable body which consists of infinitesimal cubes as shown in Fig. (A). Figure (A)(a) shows external pressure forces $\mathbf{F}^P$ body forces $\mathbf{F}$ and internal stresses σ in equilibrium and Fig. (A)(b) shows continuous displacements $\mathbf{u}$ and consistent strains ε.

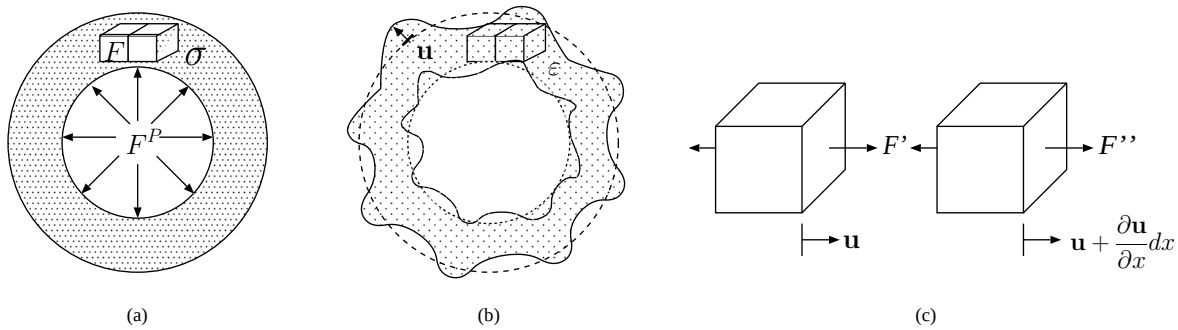

Figure A.1: Virtual work on pipe structure: (a) Surface and body forces and stresses in equilibrium, (b) Consistent deformations and displacements, and (c) Forces and displacements on cube faces.

The total virtual work (W_T) done by stresses or all forces, such as $F^{'} = \sigma dydz$ (acts on individual common faces) and $F^{''} = (\sigma + \frac{\partial \sigma}{\partial x})dydz$ (acts on other faces) as shown in Fig. (A)(c), acting on the faces of all cubes which undergo unrelated but consistent [174] displacements and deformations can be written as [175]

$$W_T = -u_j F_j^{'} + (u_j + \frac{\partial u_j}{\partial x_i} dx_i) F_j^{''} . \tag{A.1}$$

By using Newton's second law of motion ($F = m\mathbf{a}$) in equilibrium as $\frac{\partial \sigma_{ij}}{\partial x_i} + F_j = 0$, and neglecting second order term, Eq. (A.1) can be written as

$$W_T = \frac{\partial u_j}{\partial x_j}\sigma_{ij}dv + u_j\frac{\partial \sigma_{ij}}{\partial x_i}dv = (\varepsilon_{ij}\sigma_{ij} - u_j F_j)dv. \tag{A.2}$$

In Eq. (A.2), σ_{ij} and ε_{ij} are the normal and shear stress and strain distribution, respectively within the deformed body, u_j and F_j are the displacements and body forces, respectively acting in the three principal global directions as

$$u_j = \begin{bmatrix} u \\ v \\ w \end{bmatrix} \quad \text{and} \quad F_j = \begin{bmatrix} F_x \\ F_y \\ F_z \end{bmatrix}. \tag{A.3}$$

By taking the volume integral of Eq. (A.2) over the whole body, the principle of the virtual work of the surface and the body forces can be expressed as

$$\int_S u_j F_j^P ds + \int_V u_j F_j dv = \int_V \varepsilon_{ij}\sigma_{ij} dv. \tag{A.4}$$

Therefore, the principle of the virtual work states that the equilibrated stresses and body forces undergo unrelated but consistent displacements and strains only when internal virtual work is equal to the external virtual work.

Appendix B

Stress, Strain and Displacements Relations

The strain-displacement and stress-strain relations for this model can be expressed as

$$\varepsilon_{ij} = \frac{1}{2}\left(\frac{\partial u_i}{\partial x_j} + \frac{\partial u_j}{\partial x_i}\right), \tag{B.1}$$

and

$$\sigma_{ij} = C_{ijpq}\varepsilon pq. \tag{B.2}$$

Here, $\mathbf{C}$ is a 6 x 6 elastic matrix, which can be written as

$$\mathbf{C} = \begin{bmatrix} (\lambda+2\mu) & \lambda & \lambda & 0 & 0 & 0 \\ \lambda & (\lambda+2\mu) & \lambda & 0 & 0 & 0 \\ \lambda & \lambda & (\lambda+2\mu) & 0 & 0 & 0 \\ 0 & 0 & 0 & \mu & 0 & 0 \\ 0 & 0 & 0 & 0 & \mu & 0 \\ 0 & 0 & 0 & 0 & 0 & \mu \end{bmatrix}, \tag{B.3}$$

$$\Rightarrow C_{ijpq} = \delta_{ij}\delta_{pq}\lambda + (\delta_{iq}\delta_{jp})\mu, \tag{B.4}$$

where μ and λ are Lame's constants defined on the basis of the elastic modulus E and poisson's coefficient ν as

$$\mu = \frac{E}{2(1+\nu)}, \tag{B.5}$$

and

$$\lambda = \frac{\nu E}{(1+\nu)(1-2\nu)}. \tag{B.6}$$

Appendix C

List of Abbreviations

ADA	Adrian
AE	Acoustic Emission
AET	Acoustic Emission Testing
AWWA	American Water Works Association
CAB	Catlin
CBM	Condition Based Monitoring
DAS	Data Acquisition System
DU	Duration
ECP	Embedded Cylinder Pipe
FE	Finite Element
FEM	Finite Element Method
HVAC	Heating Ventilation and Air Conditioning
LCP	Lined Cylinder Pipe
MEMS	Micro Electro-Mechanical Systems
NDT	Non-Destructive Testing
NSERC	National Sciences and Engineering Research Council
OCE	Ontario Centres of Excellence
PCCP	Prestressed Concrete Cylinder Pipes
PLA	Plainfield
RCCP	Reinforced Concrete Cylinder Pipes
RT	Rise Time
TVA	Tunable Vibration Absorber
WRE	Wire-break or slip Related Events

Appendix D

List of Symbols

$\mathbf{u}$	Time harmonic displacement field vector
μ, λ	Lame's constant
ρ	Mass density of the medium
ϕ	Scalar velocity potential
$\mathbf{\Psi}$	Vector velocity potential
E	Elastic (Young's) modulus
ν	Poisson's ratio
v_L	Longitudinal wave velocities
v_S	Sear wave velocities
P	Transient (time domain) pressure distribution
p	Time harmonic (frequency domain) pressure distribution
G	Transient (time domain) source
g	Time harmonic (frequency domain) source
ρ_F	Fluid density
v_F	Speed of the signal in the fluid
F_e	Elastic forces
U_e	Elastic energy
S	Source flow strength
$\delta^{(3)}$	3D Dirac delta function
$\mathbf{x}$	3D space vector
$\mathbf{F^P}$	Pressure forces in three principal directions
$\mathbf{n}$	Outward-pointing unit normal vector
ω	Angular frequency
f	Frequency of the signal
σ_{ij}	Symmetric stress tensor

$\mathbf{C}$	Elastic matrix
$\mathbf{F^T}$	Traction forces in three principal directions
v_T	Tube wave velocity
D	Diameter of the pipe
R	Radius of the pipe
t_p	Pipe thickness
t_S	Soil thickness
E_p	Pipe elasticity
ρ_p	Pipe density
f_e	Eigenfrequency
f_c	Cut-off frequency
k_z	Wave number in z direction
ϕ_r	Radial component of velocity potential
$\triangle_T$	Laplace operator in the tangent plane

Appendix E

List of Achievements

Journal Papers

1. N.M. Alam Chowdhury, Z. Liao, L. Zhao and C.T. Yang, "Tube Wave Analysis of Buried Pipes," *Jour. Canadian Acoustics*, vol. 37, no. 2, June 2009.

2. N.M. Alam Chowdhury, Z. Liao, L. Zhao and R. Ramakrishnan, "Numerical Analysis of Acoustic Wave Propagation in Buried Fluid-filled Pipes," submitted for publication in *Applied Acoustics*, Sept. 2009.

3. N.M. Alam Chowdhury, Z. Liao and L. Zhao, "High-frequency Analysis of Acoustic Emission Signal in Buried Fluid-filled Pipes," in preparation as a *Journal paper*.

International and Domestic Conferences

1. N.M. Alam Chowdhury, Z. Liao and L. Zhao, "PCCP Profiling and Tube Wave Analysis of WRE Signal," *Proc. COMSOL Conf. 2008*, Boston, USA, Oct. 9-11, 2008.

2. N.M. Alam Chowdhury, Z. Liao and L. Zhao, "Theoretical analysis of WRE signal propagation of PCCP," *Int'l Conf. on Scientific Computation and Differential Equations 2009 (SciCADE09)*, May 25-29, 2009.

3. N.M. Alam Chowdhury, Z. Liao, L. Zhao and R. Ramakrishnan, "Eigenfrequency analysis of fluid-filled pipes," *Proc. Annual Conf. of Canadian Acoustical Assoc. 2009*, Niagara-falls, ON, Oct. 14-16, vol. 37, no. 3, pp. 118-119, 2009.

4. N.M. Alam Chowdhury, Z. Liao, L. Zhao and R. Ramakrishnan, "Modal solution of the acoustic wave propagation through fluid-filled pipes," *Proc. Annual Conf. Canadian Acoustical Assoc. 2009*, Niagara-falls, ON, Oct. 14-16, vol. 37, no. 3, pp. 120-121, 2009.

Bibliography

[1] AWWA Standard for Design of Prestressed Concrete Cylinder Pipe. American Water Works Association, ANSI/AWWA C304-99, 1999.

[2] N. Rajagopalan, *Prestressed Concrete*, 2ed., UK: Alpha Science, 2005.

[3] M. Holley and D. Buchanan, "Acoustic monitoring of prestressed concrete cylinder pipe", *Proc. ASCE Pipelines in the Const. Env. Conf.*, pp. 468-476, Aug. 1998.

[4] PCCP Evaluation Report, Nondestructive pipeline condition monitoring of the U.S. route 29 water main, The Pressure Pipe Inspection Company Ltd., Sept. 2006.

[5] M. Peacock, "Acoustic emission for detection of process related damage in pressure vessels and piping", *SPIE*, vol. 2947, 1996.

[6] R. Wu, *Time-scale Analysis and the Wavelet Application in Acoustic Emission Signal Detection of Wire Related Events in Pipeline*, Masters thesis, ELCE Dept., Ryerson University, Toronto, ON, Canada, 2008.

[7] A.W. Peabody, "Control of pipeline corrosion", *National Association of Corrosion Engineers*, Houston, 1967.

[8] R.E. Price and M.B. Brooks, "Evaluation of concrete pressure pipelines and prevention of failures", *Proc. Am. Soc. of Civil Engineers Annual Convention*, San Diego, California, 1995.

[9] F.A. Travers, "Acoustic Monitoring of Prestressed Concrete Pipe", *J. Constr. Building Mater.*, vol. 11, no. 3, pp. 175-187, 1997.

[10] J. Makar, Evaluation of acoustic monitoring for prestressed concrete cylinder pipe, NRC Report B-5103.1, National Research Council, Ottawa, Ontario, 1998.

[11] D. O'Day, "External corrosion in distribution systems", *J. Am. Water Works Assoc.*, October, pp. 45-52, 1969.

[12] R. Wirahadikusumah, D.M. Abraham, T. Iseley and R.K. Prasanth, "Assessment technologies for sewer system rehabilitation", *J. Automation in Construction*, vol. 7, no. 4, pp. 259-270, 1998.

[13] G. Phetteplace, "Infrared thermography for condition assessment of buried district heating piping", *Trans. ASHRAE*, vol. 105, part 2, pp. 776-781, 1999.

[14] B. Mergelas, Personal communication, Pressure Pipe Inspection, Mississauga, Ontario, 1998.

[15] D. Sack and L. Olson, "In site nondestructive testing of buried precast concrete pipe", *Proc. of the Am. Soc. of Civil Engineers, Mater. Engineering Conf.*, Sand Diego, Nov. 13-16, 1994.

[16] N.K. Opara, R.D. Woods and N.A. Shayea, "Nondestructive testing of concrete structures using the rayleigh wave dispersion method", *J. Am. Concrete Instit. Mater.*, vol. 93, no. 1, pp. 75-86, 1996.

[17] J.M. Makar and N. Chagnon, "Inspecting systems for leaks, pits and corrosion", *J. Am. Water Works Assoc.*, vol. 91, no. 7, pp. 36-46, 1999.

[18] R. Bernstein, M. Oristaglio, D.E. Miller and J. Haldorsen, "Imaging radar maps underground objects", *J. Computer Applications in Power*, vol. 13, no. 3, pp. 20-24, 2000.

[19] W. Worthington, "Prestressed concrete pipe inspection and monitoring methods," *Proc. Nondestructive Evaluation of Civil Structures and Mater.*, Boulder, Colo, USA, May 1992.

[20] D.C. Gazis, "Three-dimensional investigation of the propagation of waves in hollow circular cylinders: I - Analytical foundation," *J. Acoust. Soc. Am.*, vol. 31, no. 5, pp. 568-573, May 1959.

[21] D.C. Gazis, "Three-dimensional investigation of the propagation of waves in hollow circular cylinders: II-. Numerical results," *J. Acoust. Soc. Am.*, vol. 31, pp. 573-578, 1959.

[22] H.J. Shin, *Non-Axisymmetric Ultrasonic Guided Waves For Tubing Inspection*, Ph.D. thesis, Pennsylvania State University, PA, USA, May 1997.

[23] M.J. Quarry and J.L. Rose, "Multimode guided wave inspection of piping using comb transducers", *J. Mater. Eval.*, vol. 57, no. 10, pp. 1089-1090, 1999.

[24] D.N. Alleyne and P. Cawley, "Long range propagation of lamb waves in chemical plant pipework," *J. Mater. Eval.*, vol. 45, no. 4, pp. 504-508, 1997.

[25] D.E. Chimenti, A.H. Nayfeh and D.L. Butler, "Leaky waves on a layered half-space," *J. Appl. Phys.*, vol. 53, pp. 170-176, 1982.

[26] J. Ditri, J.L. Rose and G. Chen, "Mode selection guidelines for defect detection optimization using lamb waves," *Proc., 18th Annual Review of Progress in Quantitative NDE Meeting*, vol. 11, pp. 2109-2115, Brunswick, ME, 1991.

[27] R.M. Cooper and P.M. Naghdi, "Propagation of nonaxially symmetric waves in elastic cylindrical shells," *J. Acoust. Soc. Am.*, vol. 29, pp. 1365-1373, 1957.

[28] A.H. Fitch, "Observation of elastic pulse propagation in axially symmetric and nonaxially symmetric longitudinal modes of hollow cylinders," *J. Acoust. Soc. Am.*, vol. 35, pp. 706-707, 1963.

[29] J.N. Barshinger and J.L. Rose, "Ultrasonic guided wave propagation in pipes with viscoelastic coatings," *QNDE*, Brunswick, ME, July 29-Aug. 3, 2001.

[30] Y. Cho and J.L. Rose, "Guided waves in a water loaded hollow cylinder," *J. Nondestructive Testing and Eval.*, vol. 12, pp. 323-339, 1996.

[31] Y.H. Pao and R.D. Mindlin, "Dispersion of flexural waves in an elastic circular cylinder," *ASME: J. Appl. Mech.*, vol. 27, pp. 513-520, 1960

[32] I.A. Viktorov, "Rayleigh-type waves on a cylindrical surface," *Soviet Phys. Acoust.*, vol. 4, pp. 131-136, 1958.

[33] J.Jr. Zemanek, "An experimental and theoretical investigation of elastic wave propagation in a cylinder," *J. Acoust. Soc. Am.*, vol. 51, pp. 265-283, 1972.

[34] M.A. Biot, "Propagation of elastic waves in a cylindrical bore containing a fluid," *J. Appl. Phys.*, vol. 23, pp. 997-1009, 1952.

[35] P.A. Heelam, "Radiation from a cylindrical source of finite length," *Geophysics*, vol. 18, pp. 685-696, 1953.

[36] J.E. White, Underground Sound: Application of Seismic Waves, *Elsevier Science*, NY, 1983.

[37] J.E. White and R.L. Sengbush, "Shear waves from explosive sources," *Geophysics*, vol. 28, pp. 1109-1119, 1963.

[38] E.W. Peterson, "Acoustic wave propagation along a fluid-filled cylinder," *J. Appl. Phys.*, vol. 45, pp. 3340-3350, 1974.

[39] A. Abo-Zena, "Radiation from a finite cylindrical explosive source," *Geophysics*, vol. 42, pp. 1384-1393, 1977.

[40] M.W. Lee and A.H. Balch, "Theoretical seismic radiation from a fluid-filled borehole," *Geophysics*, vol. 47, pp. 1308-1314, 1982.

[41] L.D. Lafleur and F.D. Shields, "Low-frequency propagation modes in a liquid-filled elastic tube waveguide," *J. Acoust. Soc. Am.*, vol. 97, no. 3, pp. 1435-1445, 1995.

[42] W.L. Jacobi, "Propagation of sound waves along liquid cylinders," *J. Acoust. Soc. Am.*, vol. 21, pp. 120-127, 1949.

[43] V. Easwaran and M.L. Munjail, "A note on the effect of wall compliance on lowest-order mode propagation in fluid-filled/submerged impedance tubes," *J. Acoust. Soc. Am.*, vol. 97, no. 6, pp. 3494-3501, 1995.

[44] J.E. Greenspon and E.G. Singer, "Propagation in fluids inside thick viscoelastic cylinders," *J. Acoust. Soc. Am.*, vol. 97, no. 6, pp. 3502-3509, 1995.

[45] B.K. Sinha, T.J. Plona, S. Kostek and S.K. Chang, "Axisymmetric propagation in fluid-loaded cylindrical shells. I-Theory," *J. Acoust. Soc. Am.*, vol. 92, pp. 1132-1143, 1992.

[46] T.J. Plona, B.K. Sinha, S. Kostek and S. K. Chang, "Axisymmetric propagation in fluid-loaded cylindrical shells. II-Theory versus experiment," *J. Acoust. Soc. Am.*, vol. 92, pp. 1144-1155, 1992.

[47] R. Diederichs, "Nondestructive Testing," http://www.ndt.net/ndtaz/ndtaz.php, July 2007.

[48] H.L. Chen, C.T. Cheng and S.E. Chen, "Determination of Fracture Parameters of Mortar and Concrete Beams by Using Acoustic Emission," *J. Mater. Eval.*, vol. 50, no. 7, pp. 273-281, July 1992.

[49] S.W. Hearn and C.K. Shield, "Acoustic emission monitoring as a nondestructive testing technique in reinforced concrete," *ACI Mater. J.*, pp. 510-519, Nov. 1997.

[50] S. Kimura, I. Adachi, Y. Hironaka and M. Ohtsu, "AE evaluation of concrete structures," *Progress in Acoust. Emiss. IV*, The Japanese Society for NDI, pp. 350-358, 1988.

[51] M.K. Lim and T.K. Koo, "Acoustic emission from reinforced concrete beams," *Mag. of Concrete Res.*, vol. 41, pp. 229-234, 1989.

[52] S. Lovass, "Acoustic emission of offshore structures: Attenuation; Noise; Crack Monitoring," *J. Acoust. Emiss.*, p. 161, April 1985.

[53] A. Maji and S.P. Shah, "Process zone and acoustic-emission measurement in concrete," *Experimental Mechanics*, vol. 28, no. 1, pp. 27-33, Mar. 1988.

[54] P.A. Maliszkiewicz, "Acoustic emission possibilities of application to tests of concrete structures," *2nd Workshop on Bridge Engineering Research*, pp. 99-102, 1990.

[55] K. Matsuyama, T. Fujiwara, A. Ishibashi and M. Ohtsu, "Field application of acoustic emission for diagnostic of structural deterioration of concrete," *J. Acoust. Emiss.*, vol. 11, no. 4, pp. 65-73, 1993.

[56] M. Ohtsu, "Determination of crack orientation by acoustic emission," *J. Mater. Eval.*, vol. 45, no. 9, pp. 1070-1075, 1986.

[57] M. Ohtsu, "Acoustic emission characteristics in concrete and diagnostic application," *J. Acoust. Emiss.*, vol. 6, no. 2, pp. 99-108, 1987.

[58] M. Ohtsu, "Crack propagation in concrete: linear elastic fracture mechanics and boundary element method," *Theoretical and Applied Fracture Mechanics*, vol. 9, no. 1, pp. 55-60, 1988.

[59] M. Ohtsu T. Okamoto and S. Yuyama, "Moment tensor analysis of acoustic mmission for cracking mechanisms in concrete," *ACI Structural Jour.*, pp. 87-95, March 1998.

[60] R.S. Olivito, and L. Surace, "The damage assessment of concrete structures by time-frequency distributions," *Experimental Mechanics*, vol. 37, no. 3, pp. 355-359, 1997.

[61] C.S. Ouyang, E. Landis and S.P. Shah, "Damage assessment in concrete using quantitative acoustic emission," *J. Engineering Mech. Div.*, vol. 117, no. 11, pp. 2681-2698, Nov. 1991.

[62] T. Uomoto, "Application of acoustic emission to the field of concrete engineering," *J. Acoust. Emiss.*, vol. 6, no. 3, pp. 137-144, 1987.

[63] S. Yuyama, T. Imanaka and M. Ohtsu, "Quantitative evaluation of microfracture due to disbonding by waveform analysis of acoustic emission," *J. Acoust. Soc. Am.*, vol. 83, no. 3, pp. 976-983, 1994.

[64] S. Yuyama, T. Okamoto and S. Nagataki, "Acoustic emission evaluation of structural integrity in repaired reinforced concrete beams," *J. Mater. Eval.*, vol. 52, no. 1, pp. 86-90, 1994.

[65] S. Yuyama, T. Okamoto and M. Shigeishi, "Acoustic emission generated in corners of reinforced concrete rigid frame under cyclic loading," *J. Mater. Eval.*, vol. 53, no. 3, pp. 409-412, 1995.

[66] S. Yuyama, T. Okamoto and M. Shigeishi, "Quantitative evaluation and visualization of cracking process in reinforced concrete by a moment tensor analysis of acoustic emission," *J. Mater. Eval.*, vol. 53, no. 6, pp. 751-756, 1995.

[67] N.M. Hawkins, W.M. McCabe and Y. Nobuta, "Use of acoustic emission to detect debonding of reinforcing bars in concrete," *Progress in Acoust. Emiss. IV*, The Japanese Society for NDT, pp. 342-349, 1988.

[68] Z.F. Li, A. Zdunek, E. Landis and S.P. Shah, "Application of acoustic emission technique to detection of reinforcing steel corrosion in concrete," *ACI Material J.*, pp. 68-76, Jan. 1998.

[69] D.J. Yoon, W.J. Weiss and S. Shah, "Assessing damage in corroded reinforced concrete using acoustic emission," *J. Engineering Mechanics*, vol. 126, no. 3, p. 273, March 2000.

[70] G. Lackner, G. Schauritsch and P. Tsheliesnig, "Acoustic emission: a modern and common NDT method to estimate industrial facilities," *ECNDT* 2006, 2006.

[71] K. Wissawapaisal, *Nondestructive Testing of Reinforced and Prestressed Concrete Structures Using Acoustic Waveguides*, PhD thesis, CEE Dept., West Virginia University, Morgantown, West Virginia, 2001.

[72] F.B. Stulen and J. F. Kiefner, "Evaluation of acoustic emission monitoring of buried pipelines," *IEEE Trans. Ultronics Symp.*, vol. 90, pp. 898-903, 1982.

[73] C.U. Grosse, "Editorial: Special issue on acoustic emission," *NDT.net*, vol. 7, no. 9, Sept. 2002.

[74] What is acoustic emission, http://www.ndt.net/article/az/ae/index.htm.

[75] H. Vallen, "AE testing fundamentals, equipment, applications," *NDT.net*, vol. 7, no. 9, Sept. 2002.

[76] J.R. Smith, G.V. Rao and R. Gopal, "Acoustic monitoring for leak detection in pressurized water reactors," ASTM. Special Technical Publications, pp. 177-204, Jan. 1979.

[77] K. Yoshida, H. Kawano, Y. Akematsu and H. Nishino, "Frequency characteristics of acoustic emission waveforms during gas leak," *The European Working Group on Acoust. Emiss.*, 2004.

[78] V.V. Muravev, M.V. Muravev and S.A. Bekher, "A novel technique of AE signal processing for upgrading the accuracy of localization," *Acoust. Methods, Russian J. of NDT*, vol. 38, no. 8, pp. 600-610, Aug. 2002.

[79] W. Worthington, Perspective on Prestresses Concrete Cylinder Pipe, Pipeline Technologies, Inc., Scottsdale, AZ.

[80] The Design Concept of PCCP. (2008, Feb. 21). [Online]. Available: http://www.pipesite.com/pbpccp.html

[81] Report, AMERON Prestressed Concrete Cylinder Pipe, AMERON Int'l., USA, 2002.

[82] M. Dingus, J. Haven and R. Austin, Nondestructive, Noninvasive Assessment of Underground Pipelines, Denver: Amer. Water Works Assn., 2002.

[83] American Society for the Testing of Materials. Standard definitions of terms relating to acoustic emission, STM E610-82, 1982.

[84] M. Weaver, "Fundamentals in acoustic emission," *Proc. 22nd European Conf. on Acous. Emission Testing*, Aberdeen, UK, 1996.

[85] O. Tozser and J. Elliott, "Continuous Acoustic Monitoring of Prestressed Structures," *Proc. CSCE Structural Specialty Conf.*, 2000.

[86] Acoustic Emission Testing Service. (2009, Feb. 11). [Online]. Available: http://enerisq.com/EnerisQ_Recap_AET.pdf

[87] M. Peacock, "Acoustic emission for detection of process related damage in pressure vessels and piping," *SPIE*, vol. 2947, 1996.

[88] J. N. Barshinger and J. L. Rose, "Guided wave propagation in an elastic hollow cylinder coated with a viscoelastic material", *IEEE Trans. Ultrason., Ferroelect., Freq. Contr.*, vol. 51, no. 11, pp. 1547-1556, 2004.

[89] K. F. Graff, *Wave Motion in Elastic Solids*, NY: Dover, 1991.

[90] J. D. Achenbach, *Wave Propagation in Elastic Materials*, NHPC, 1973.

[91] M. S. Howe, *Acoustic of Fluid-Structure Interaction*, Cambridge Univ. Press, UK, 1998.

[92] A.E. Lord, J.N. Deisher and R.M. Koerner, "Attenuation of elastic waves in pipelines as applied to acoustic emission leak detection", *J. Mater. Eval.*, vol. 35, no. 11, pp. 49-54, Nov. 1977.

[93] R.J. Urick, *Principles of Underwater Sound*, McGraw-Hill, 1975.

[94] V.N. Rama Rao and J.K. Vandiver, "Acoustics of fluid-filled boreholes with pipe: Guided propagation and radiation," *J. Acoust. Soc. Am.*, vol. 105, no. 6, pp. 3057-3066, 1999.

[95] H.Y. Lee, *Drillstring Axial Vibration and Wave Propagation in Boreholes*, Ph.D. thesis, MIT, Cambridge, MA, USA, May 1991.

[96] K. Seo and M. Morita, "Guidelines for LTS magnet design based on transient stability," *Proc. 2nd Asian Conf. on Applied Superconductivity and Cryogenics (ACASC 2004)*, Elsevier, vol. 46, no. 5, pp. 354-361, 2006. P.A.A. Laura, "Acoustic detection of structural failure of mechanical cables," J. Acous. Soc. America, vol. 45, pp. 791-793, 1969.

[97] P.A.A. Laura, "Mechanical behaviour of stranded wire rope and feasibility of detection of cable failure," *J. Marine Tech. Soc.*, vol. 4, pp. 19-32, 1970.

[98] D.O. Harris and H.L. Dunegan, "Acoustic emission testing of wire rope," *J. Mater. Eval.*, vol. 15, pp. 79-82, 1974.

[99] N.F. Casey and J.L. Taylor, "Evaluation of wire ropes by AE techniques," *J. Non-Destr. Test.*, vol. 27, no. 6, pp. 351-356, 1985.

[100] N.F. Casey, D. Wedlake, J.L. Taylor and K.M. Holford, "Acoustic detection of wire rope failure," *Wire Ind.*, vol. 52, no. 617, pp. 307-309, 1985.

[101] K.M. Holford, '*The non-destructive testing of wire rope by acoustic emission*, Ph.D. thesis, University College, Cardiff, 1987.

[102] N.F. Casey, H. White and J.L. Taylor, "Frequency analysis of the signals generated by the failure of constitutent wires of a wire rope," *Elsevier: NDT Int.*, vol. 56, no. 669, pp. 583-586, 1989.

[103] N.F. Casey and P.A.A. Laura, "A review of the acoustic-emission monitoring of wire rope," Elsevier: Ocean Engng., vol. 24, no. 10, pp. 935-947, 1997.

[104] G. Drummond, J.F. Watson and P.P. Acarnley, "Acoustic emission from wire ropes during proof load and fatigue testing," *Elsevier: NDT & E Int.*, vol. 40, pp. 94-101, 2007.

[105] P.A. Martin and J.R. Berger, "On mechanical waves along aluminum conductor steel reinforced (ACSR) power lines," *ASME J. Appl. Mech.*, vol. 69, no. 6, pp. 740-48, 2002.

[106] Y.Z. Pappas, A. Kontsos, T.H. Loutas and V. Kostopoulos, "On the characterization of continuous fibres fracture by quantifying acoustic emission and acousto-ultrasonics waveforms," *Elsevier: NDT & E. Int.*, vol. 37, no. 5, pp. 389-401, 2004.

[107] COMSOL 3.4: *Acoustics Module - User's Guide*, Comsol User Doc., COMSOL AB, Stockholm, 2007.

[108] B.J. Tester, "The propagation and attenuation of sound in lined ducts containing uniform or plug flow," *Journal of Sound and Vibration*, vol. 28, no. 2, pp. 151-203, 1973.

[109] M.K. Myers, "On the acoustic boundary condition in the presence of flow" *Journal of Sound and Vibration*, vol. 71, no. 3, pp. 429-434, 1980.

[110] T.L. Parrott, W.R. Watson and M.G. Jones, *Experimental Validation of a Two-Dimensional Shear-Flow Model for Determining Acoustic Impedance*, Technical report TP-2679, NASA, Washington, DC, 1987.

[111] T.L. Parrott, A.L. Abrahamson and M.G. Jones, *Measured and Calculated Acoustic Attenuation Rates of Tuned Resonator Arrays for Two Surface Impedance Distribution Models with Flow*, Technical report TP-2766, NASA, Washington, DC, 1988.

[112] W.R. Watson, M.G. Jones, S.E. Tanner and T.L. Parrott, *A finite element propagation model for extracting normal incidence impedance in nonprogressive acoustic wave fields*, Technical report TP-110160, NASA, Washington, DC, 1995.

[113] Y. Ozyoruk and L.N. Long, A time-domain implementation of surface acoustic impedance condition with and without flow, *J. Comput. Acoustics*, vol. 5, no. 3, pp. 277, 1997.

[114] H. Bolton-Seed and I.M. Idriss, *Soil Moduli and Damping Factors for Dynamic Response Analyses*, Earthquake Engineering Research Center, Report no. 70-10, Univ. of California, Berkeley, USA, 1970.

[115] E.L. Hamilton, "Shear wave velocity versus depth in marine sediments: A review," *Geophysics*, vol. 41, pp. 985-996, 1976.

[116] B.A. Hardage, "An examination of tube wave noise in vertical seismic profiling data," *Geophysics*, vol. 46, pp. 892-903, 1981.

[117] J.P. Henriet, J. Schittekat and P. Heldens, "Borehole seismic profiling and tube wave applications in a dam site investigation," *Geophysics*, vol. 31, pp. 72-86, 1983.

[118] J.E. White and E. Welsh, "Borehole coupling of seismic waves in a permeable solid," *Geophysics*, vol. 36, pp. 417-429, 1988.

[119] M.L. Batzle and Z. Wang, "Seismic properties of pore fluids," *Geophysics*, vol. 57, pp. 1396-1408, 1992.

[120] J.M. Harris, R.C. Nolen-Hoeksema, R.T. Langan,M. Schaack, S.K. Lazaratos and J.W. Rector, "High-resolution crosswell imaging of a West Texas carbonate reservoir: Part 1-Project summary and interpretation," *Geophysics*, vol. 60, pp. 667-681, 1995.

[121] R.C. Nolen-Hoeksema, Z. Wang, J.M. Harris and R.T. Langan, "High-resolution crosswell imaging of a West Texas carbonate reservoir," *Part 5-Core analysis: Geophysics*, vol. 60, pp. 712-726, 1995.

[122] S.K. Lazaratos and B.P. Marion, "Crosswell seismic imaging of reservoir changes caused by CO2 injection," *66-th Ann. Internat. Mtg., Soc. Expl. Geophys.*, Expanded Abstracts, pp. 1871-1879, 1996.

[123] R.D. Fay, R.L. Brown and O.V. Fortier, "Measurement of acoustic impedances of surfaces in water," *J. Acoust. Soc. Am.*, vol. 19, pp. 850-856, 1947.

[124] M.P. Home and R.J. Hansen, "Sound propagation in a pipe containing a liquid of comparable acoustic impedance," *J. Acoust. Soc. Am.*, vol. 71, pp. 1400-1405, 1982.

[125] P. M. Morse and H. Feshbach, *Methods of Theoretical Physics-II*, McGraw-Hill, NY, 1953.

[126] D. Givoli, B. Neta, "High-order Non-reflecting Boundary Scheme for Time-dependent Waves", *Journal of Computational Physics*, vol. 186, pp. 24-46, 2004.

[127] A. Bayliss, M. Gunzburger, E. Turkel, "Boundary Conditions for the Numerical Solution of Elliptic Equations in Exterior Regions", *SIAM Journal of Applied Mathematics*, vol. 42, no. 2, pp. 430-451, 1982.

[128] F. Adamo, G. Andria, F. Attivissimo, N. Giaquinto, "An acoustic method for soil moisture measurement", *IEEE Transaction on Instrumentation and Measurements*, vol. 53, no. 4, pp. 891-898, 2004.

[129] M.L. Oelze, W.D. O'Brien and R.G. Darmody, "Measurement of attenuation and speed of sound in soils," J. Soil Sci. Soc. Am., vol. 66, pp. 788-796, 2002.

[130] E.E. Zajac, *Propagation of Elastic Waves*, Handbook of engineering mechanics. 1st ed., McGraw-Hill, New York, 1962.

[131] C.R. Fuller, F.J. Fahy, "Characteristics of wave propagation and energy distributions in cylindrical elastic shells filled with fluid", *Journal of Sound and Vibration*, vol. 81, no. 4, 1982.

[132] Y.P. Guo, "Approximate solutions of the dispersion equation for fluid-loaded cylindrical shells", *Journal of the Acoustical Society of America*, vol. 95, no. 3, pp. 1435-1445, 1994.

[133] P. Klosowski, et al., "Dynamics of elasto-viscoplastic plates and shells", *Archive of Applied Mechanics*, vol. 65, no. 5, pp. 326-345, 1995.

[134] F.J.Q. Melo, J.P. Noronha, E.A. Fernandes, "The propagation of axisymetric transverse waves along a thin-walled cylindrical pipe", *International Journal of Pressure Piping*, vol. 65, pp. 109-16, 1996.

[135] S.I. Lee, J. Chung, "New non-linear modeling for vibration analysis of s straight pipe conveying fluid", *Journal of Sound Vibration*, vol. 254, no. 2, pp. 313-25, 2002.

[136] M.S. Qatu, "Recent research advances in the dynamic behavior of shells", 1989-2000 Part 2: Homogeneous Shells, *Applied Mechanics Reviews*, vol. 55, no. 5, pp. 415-434, 2002.

[137] S. Finnveden, C.M. Nilsson, "Waveguide finite elements for fluid-shell coupling", *Eleventh International Congress on Sound and Vibration*, Stockholm, pp.501-518, 2003.

[138] G. Pavic, "Acoustical analysis of pipes with flow using invariant field functions", *Journal of Sound and Vibration*, vol. 263, pp. 153-174, 2003.

[139] B.R. Mace, D. Duhamel, M.J. Brennan, L. Hinke, "Wave number prediction using finite element analysis", *Eleventh International Congress on Sound and Vibration*, St. Petersburg, pp.3241-3248, 2004.

[140] J.O. Carneiro, F.J.Q. Melo, J.F.D. Rodrigues, H. Lopes, V. Teixeira, "The modal analysis of a pipe elbow with realistic boundary conditions", *Journal of Pressure Vessels and Piping*, vol. 82, pp. 539-601, 2005.

[141] B.R. Mace, D. Duhamel, M.J. Brennan, L. Hinke, "Wave number prediction using finite element analysis", *Journal of the Acoustical Society of America*, vol. 117, pp. 2835-3843, 2005.

[142] M. Maess, N. Wagner, L. Gaul, "Dispersion curves of fluid-filled elastic pipes by standard FE models and eigenpath analysis", *Journal of Sound and Vibration*, vol. 296, pp. 264-276, 2006.

[143] R.E.D. Bishop and D.B. Welbourn, "The problem of the dynamic vibration absorber," *J. Engineering*, vol. 174, pp. 796, 1952.

[144] G.B. Warburton, "On the theory of the acceleration damper," *J. Appl. Mech.*, vol. 24, pp. 322324, 1957.

[145] J.B. Hunt and J.C. Nissen, "The broadband dynamic vibration absorber," *J. Sound and Vibration*, vol. 83, pp. 573578, 1982.

[146] J.C. Snowdon, A.A. Wolf and R.L. Kerlin, "The cruciform dynamic vibration absorber," *Journal of Acoustical Society of America*, vol. 75, pp. 17921799, 1984.

[147] N. Olgac and B. Holm-Hansen, "Tunable active vibration absorber; the delayed resonator," *ASME: Journal of Dynamic Systems, Measurement and Control*, vol. 117, pp. 513519, 1995.

[148] K. Nagaya and L. Li, "Control of sound noise radiated from a plate using dynamic absorbers under the optimization by neural network," "*Journal of Sound and Vibration*, vol. 208, pp. 289298, 1997.

[149] G. Lee, J. Gina, G. Ahmad and G.H. Lucas, "Integrated passive/active vibration absorber for multistory buildings," *Journal of Structural Engineering*, vol. 123, pp. 499504, 1997.

[150] K. Nagaya and Y. Li, "Method for reducing sound radiated from structures using vibration absorbers optimized with a neural network," *Journal of Acoustical Society of America*, vol. 104, pp. 14661473, 1998.

[151] K. Nagaya, A. Kurusu, S. Ikai and Y. Shitani, "Vibration control of a structure by using a tunable absorber and an optimal vibration absorber under auto-tunning control," *Journal of Sound and Vibration*, vol. 228, no. 4, pp. 773-792, 1999.

[152] S. Keyea, R. Keimerb and S. Homann, "A vibration absorber with variable eigenfrequency for turboprop aircraft," *Elsevier: Aerospace Science and Technology*, (in press).

[153] R.D. Mindlin, *Waves and vibrations in isotropic, elastic plates*, In: J.N. Goodir and N. Hoff, Editors, Structural Mechanics, Pergamon Press, Oxford, pp. 199232, 1959.

[154] M. Onoe, "Contour vibrations of thin rectangular plates," *J. Acoust. Soc. Am.*, vol. 30, no. 12, pp. 1159, 1962.

[155] I.A. Victorov, *Rayleigh and Lamb Waves*, Plenum Press, New York, 1967.

[156] J.L. Rose, *Ultrasonic Waves in Solid Media*, Cambridge University Press, 1999.

[157] T. Hayashi, C. Tamayama and M. Murase, "Wave structure analysis of guided waves in a bar with an arbitrary cross-section," *Ultrasonics*, vol. 44, no. 1, pp. 17-24, 2006.

[158] D.N. Alleyne and P. Cawley, "Long range propagation of Lamb waves in chemical plant pipework," *J. Mater. Eval.*, vol. 55, pp. 504-508, 1997.

[159] P.J. Mudge, "Field application of the teletest (R) long-range ultrasonic testing technique," *J. Insight*, vol. 43, pp. 74-77, 2001.

[160] D.N. Alleyne, B. Pavlakovic, M.J.S. Lowe and P. Cawley, "Rapid long-range inspection of chemical plant pipework using guided waves," *J. Insight*, vol. 43, pp. 93-96, 2001.

[161] P. Cawley, M.J.S. Lowe, D.N. Alleyne, B. Pavlakovic and P. Wilcox, "Practical long range guided wave testing: application to pipes and rails," *J. Mater. Eval.*, vol. 61, no. 1, pp. 66-74, 2003.

[162] H. Kwun, S.Y. Kim and G.M. Light, "The magnetostrictive sensor technology for long range guided wave testing and monitoring of structures," *J. Mater. Eval.*, vol. 61, no. 1, pp. 80-84, 2003.

[163] H. Lamb, "On the velocity of sound, as affected by the elasticity of the wall", *Manchester Memoirs*, vol. 17, no. 9, pp. 1-16, 1898.

[164] L.E. Kinsler, A.R. Frey, A.B. Coopens and J.V. Sanders, *Fundamental of Acoustics.* 4th ed., John Wiley and Sons, Inc., NY, 2000.

[165] R. E. Collin, *Field Theory of Guided Waves*, 2nd ed. New York: IEEE Press, 1991.

[166] T. D. Rossing, N. H. Fletcher, *Principles of Vibration and Sound*, New York, Springer-Verlag, 1995.

[167] I. Sato, "Rotating machinery diagnosis with acoustic emission techniques, *Electrical Eng. Japan*, vol. 110, no. 2, pp. 115-127, 1990.

[168] T. Holroyd and N. Randall, "The use of acoustic emission for machine condition monitoring, *British Journal of Non-Destructive Testing*, vol. 35, no. 2, pp. 75, 1992.

[169] M.A. Hamstad and J.D. McColskey, "Wideband and narrowband acoustic emission waveforms from extraneous sources during fatigue of steel samples," *Journal of Acoustic Emission*, vol. 15 no. 1-4, pp. 1-18, 1997.

[170] D. Mba and R.H. Bannister, "Condition monitoring of low-speed rotating machinery using stress waves: Part 1 and Part 2, *Proc. Inst. Mech. Engrs.*, vol. 213, Part E, pp. 153-185, 1999.

[171] M.A. Hamstad and J.D. McColskey, "Detectability of slow crack growth in bridge steels by acoustic emission," *Jour. of Materials Evaluation*, vol. 57, no. 11, pp. 1165-1174, 1999.

[172] A. Choudhury and N. Tandon, "Application of acoustic emission techniques for the detection of defects in rolling element bearings, *Tribology International*, vol. 33, no. 1, pp. 39-45, 2000.

[173] L.D. Hall, D. Mba and R.H. Bannister, "Acoustic emission signal classification in condition monitoring using the kolmogorov-smirnov statistic," *Jour. of Acoustic Emission*, vol. 19, pp. 209-228, 2001.

[174] B. Torby, *Energy Methods, Advanced Dynamics for Engineers*, HRW Series in Mechanical Engineering, CBS College Publishing, USA, 1984.

[175] C. Jong, Teaching students work and virtual work method in statics: A guiding strategy with illustrative examples, *Proceedings American Society for Engineering Education Annual Conference and Exposition (ASEE)*, 2005.